Understanding of geochemical partitioning and surface complexation modeling of heavy metals during treatment of mine drainage for green mining: Case study of the Zambian Copperbelt

グリーンマイニングのための廃水処理中の重金属分配の理解と

表面錯体モデリング

－ザンビア国カッパーベルト地帯を例に－

A dissertation submitted in partial fulfillment
of the requirements for the degree of
Doctor of Philosophy in Engineering

by

PHIRI Cryton

HOKKAIDO UNIVERSITY

Division of Sustainable Resources Engineering
Graduate School of Engineering, Hokkaido University, Japan

March 2021

Abstract

The metalliferous Zambian Copperbelt mining district which straddles along the frontier with the Democratic Republic of Congo (DRC), is famous for hosting large deposits of copper (Cu) and cobalt (Co) sulphide ore mineralisation of Central Africa. As a result of ore beneficiation, volumes of sludge effluents are generated and later stored as sludge deposits at large sectional areas of ponds and impoundments after the sedimentation process. During periods of heavy rainfall, surface erosion at storage facilities causes stream and river siltation resulting in subsequent non-compliance metal concentration discharges into the nearby surrounding environments. This condition, therefore, suggests that the sludges exhibit high potential to be of negative legacy in Zambia. In order to (i) minimise the generation of sludge volumes, (ii) reduce or minimise on the environmental contamination and (iii) to promote their recycling and reuse, understanding of geochemical partitioning and surface binding of heavy metals during treatment of mine drainage is unambiguously important for green mining.

Chapter 1 introduces the research background and problem statements. The targeted objectives were to: (i) investigate the physio-chemical and geochemical factors influencing metal partitioning onto sludge at solid-liquid interface, (ii) predict the geochemical behaviours of the contaminants with the host mineral surfaces and (iii) discover ways that the Zambian Copperbelt mining industry can reduce environmental impacts from sludge and make its practices more sustainable.

Chapter 2 reviews the literatures of surface complexation modeling (SCM) prediction of Cu and Co metals with the mineral surfaces such as kaolinite and hydrous ferric oxide (HFO) present in the sludges during treatment. These minerals are reportedly responsible for controlling the mobility of metals in natural systems and in the studied sludges. Based on the use of the available diffuse

double layer modeling database and of previous literature, metal behaviours with the complex natural materials are easily predicted and understood.

Chapter 3 gives a brief background of the geology of the Zambian Copperbelt including the host minerals and dominant mineable ores. Site characteristics, target sampling points such as the drainages and storage ponds are described. The sampled materials in drainages were sludge effluents along the drainage course and solid sludge both along the drainage course and at storage ponds. The sampling protocols, onsite data collection, kinds and types of onsite field samples at each sampling site are described.

Chapter 4 discusses the physical and chemical partitioning of the metals (i.e., Cu and Co) with the host minerals in effluents and with the solid deposits. The differences in metal concentrations between the dissolved and suspended solid particles were envisaged including the effects of lime treatment to drainage effluent. The chemical partitioning of metal onto sludge was generated by the eight steps chemical extraction sequence, with results showing the metals to be mostly partitioned in the labile fractions associated with anthropogenic mining related activities.

Chapter 5 focusses on the outcomes of batch adsorption experiments and metal binding behaviours at solid-liquid interface. Batch experiments revealed adsorption to be the main metal retention mechanism. Through SCM simulations, the effects of metal competition and the resultant concentrations of the metal binding sites onto kaolinite and HFO surfaces were revealed. Simulations by model predictions indicated that the metal binding surfaces were of loose and weak binding behaviours suggesting that the metals are potentially easily releasable and susceptible to high mobility conditions, thus indicating that the metal stability conditions in sludge is probably of a short-term condition especially under decreasing pH and changes in the reduction-oxidation conditions.

Chapter 6 discusses ways of making the Zambian Copperbelt mining activities more sustainable through the green mining concepts based on the studied sites and sludge characteristics. In this chapter, discussion on the lower impact mining techniques (i.e., heap/dump leaching), reusing mining waste (i.e., for backfilling surface mining open pits, for reconstructing mined terrain in a way that prevents soil erosion) and for making aggregates (e.g. sand) in construction engineering and rehabilitating mining sites (i.e., use of waste for land reclamation or fill in excavated areas) are emphasised

Chapter 7 highlights the research contributions, conclusion and recommendation. Although the study discussed and recommended the sustainable mining research technologies that might seem economically viable, however, the onus is on the mining industry as a whole to implements them, and so far, does seem to be moving in the direction of sustainability.

Acknowledgement

It is my great pleasure and privilege to express my deepest appreciation to my principal supervisor Prof. Tsutomu Sato for the invaluable supervision, guidance and continuous encouragements throughout this study. He was truly instrumental in bringing about the hidden potential in me to achieve certain things that I personally could not envision during the commencement of this research project. My future career progression will not be complete without acknowledging Prof. Sato, and to him, I wish the very best of his professional career. I wish to further extend my appreciation to Associate Prof. Tsubasa Otake and Assistant Prof. Ryosuke Kikuchi for the professional and academic discussions throughout my study period.

I wish to acknowledge the generous financial support provided by the Japan International Corporation Agency (JICA) under the KIZUNA program during field excursions and the entire study duration. Particularly, Prof. Dr Hosoi, the mineral resources technical advisor of JICA for been behind the brainchild of the KIZUNA program that has and is greatly supporting human resources training and capacity development throughout the globe. Many to also Japan International Cooperation Center (JICE) technical staffs for organizing and supporting the student's welfare throughout their study program.

Konkola Copper Mines (KCM) management are thanked for their reservedly allowing access to the Mine premises to conduct this research, and not forgetting Mr. Isaac Chintu from the Environment and Safety department for tirelessly coordinated the mine permit entry proceedings.

Finally, my sincere thanks to everyone in the laboratory of environmental geology for their support rendered either directly or indirectly.

Dedication

To my LATE MOTHER who passed on **(2020. June)** at a time that I needed her most. Her attributes and my memories will forever remain.

Table of Contents

List of Tables

List of Figures

Chapter 1: General Introduction

1.1 Background

Generally, the Zambian Copperbelt province is famous for copper (Cu) and cobalt (Co) sulphide ore deposits of Central Africa. And these ores include chalcocite (Cu_2S), bornite (Cu_5FeS_4), chalcopyrite ($CuFeS_2$) and carrolite ($Cu(Co)_2S_4$). Ore beneficiation processing is by both hydrometallurgical and pyrometallurgical processes, however, hydrometallurgical processing generates metal-laden sludge effluents that are often discharged/spill-over into nearby drainages (Fig. 1.1a) prior to their sedimentation and settling at ponds and impoundments (Fig. 1.1b). After sedimentation process, the metal-laden sludge solids are hydro sloughed and pumped back to the source (i.e., initial treatment site) located 2 – 2.5 km away from storage sites because of: (a) limited availability of storage space and (b) high metal concentrations that might cause environmental hazardous conditions. The whole process of sludge handling from treatment site to storage ponds and impoundments has been observed to have the following major concerns:

- Environmental pollution"

  - **Along the drainages**, discharge of metal-laden sludge effluents causes stream and river siltation (Fig. 1.1c) resulting in subsequent non-compliance metal concentration discharges (Pettersson and Ingri 2001; Sracek et al., 2012). Siltation by mine activities increases the pollution of heavy metals in water courses which in-turn significantly affects aquatic life such as benthic communities, invertebrates, fish, as well as humans at large that are entirely dependent on agricultural activities along the rivers and streams.
  - **At storage sites** (i.e., ponds & impoundments), surface erosion of sludges by rainfall and winnowing by wind (Fig. 1.1d) causes both land and water pollution which adversely affects

both agricultural activities and human habitation. Sracek et al., 2012 also indicated that erosion of sludges and tailings has led to some high metal concentration in streams and river of the Zambian Copperbelt. Apart from winnowing, the other sources and effects of air pollution has previously been reported on the Zambian Copperbelt by Ettler et al. (2014) through pyrometallurgical processes with results indicating that Cu^{2+} and Co^{2+} are the most important pollutant through the direct pathways of dust particles in the industrial parts of the Zambian Copperbelt. Pyrometallurgical process has been reported to contribute over 98% of the country's SO_2 emissions through smelters (Environmental Council of Zambia 2008) and this condition is expected to increase due to the recent investments in the mining activities because of several new copper smelters.

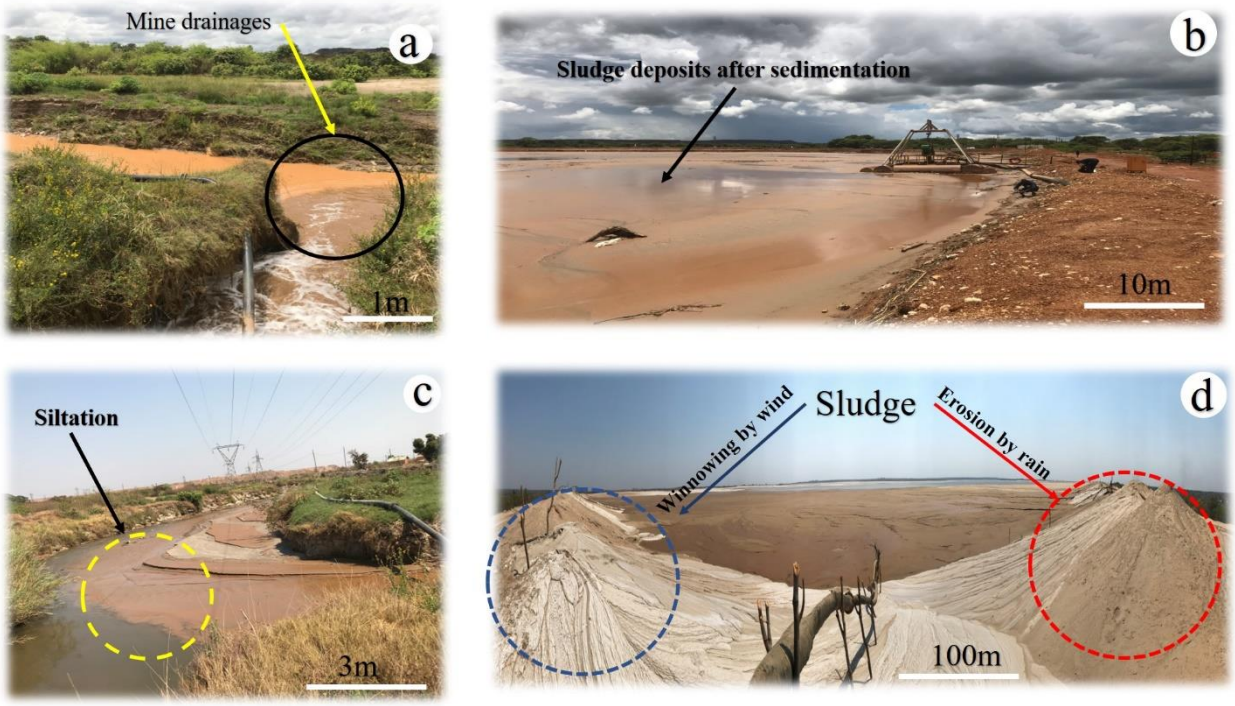

Fig.1.1. a) Mine drainage; b) sludge storage site; c) drainage siltation by sludge effluents from mining sources; c) sludge solid surface erosion by rainfall or winnowing by wind

❑ Lack of optimisation of mining operations

- Un-mechanised lime treatment of effluents is commonly been practiced along the mine drainage course (Fig. 1.2a). This practice has however been found to have poor monitoring and control of pH (i.e., $pH_{neutral}$) conditions. The pH is one of the most important parameters in study of natural environments. For instance, high lime dosages during the treatment optimisation of wastewater generates voluminous sludges through large dosages that are costly to handle. During the rainy season, storage sites become overwhelmed with large volumes of sludge, and with limited available storage spaces, metal-laden sludge spillages into pristine environmental tends to become of common place (Fig. 1.2b) which also affects the natural ecosystem.

Fig.1.2. a) Un-mechanised lime treatment of mine drainage; b) sludge spillages at storage site

Therefore, the Zambian Copperbelt sludges seems to have a high potential of been of negative legacy to Zambia. To optimize effluent treatment, minimize sludge generation and avoid secondary contamination from the sludges, the understanding of both the physio-chemical and geochemical characteristics, geochemical processes influencing metal partitioning, adsorption mechanisms, specific binding surfaces and stability conditions are unambiguously important.

Previous studies on the Zambian Copperbelt by Sracek et al. (2010; 2012) reported on partitioning and concentrations of metals in stream sediments and sludge by sequential extraction method with their results showing Cu^{2+} and Co^{2+} ions above the regulated standards associated with the exchangeable/acid-soluble fraction. But their works did not fully envisage the host minerals in exchangeable/acid-soluble fractions except for the metals partitioned to hydrous ferric oxide (HFO). Furthermore, Sracek et al. (2010); Sracek (2015) illustrated the geochemical and mineralogical capacities of sludges and tailings, the formation of iron ochre and secondary hematite and attenuation of contaminants through the oxidative dissolution of pyrite and chalcopyrite (Fig. 1.3). However, at some of the mine sites on the Copperbelt, no iron ochre has been reported or observed in the vicinity of the drainages and storage sites. This geochemical condition is completely different from the ordinary acid mine drainage (AMD) treatment sites in which secondary minerals play important roles in the metal removal. Therefore, there is still limited information regarding the metal behaviours and stability conditions in sludge effluents and solid deposits.

Fig. 1.3. Fe-ochre at sludge and/or tailing storage site on Copperbelt (After Sracek et al., 2011)

1.2. Problem statement

It is clear that despite previous studies having researched on the sources, partitioning and consequences of environmental contaminations by sludge effluents and solid deposits, there has been little work investigating on the:

- Host minerals of Cu^{2+} and Co^{2+} metals in sludge
- Metal (i.e., $Cu^{2+}$and Co^{2+}) stability conditions in sludge
- Potential sustainable (Green) mining practices that promote optimisation of mining operations

1.3 Aims and objectives

1.3.1 Aims

1. Metal geochemical partitioning, host minerals and retention mechanisms of the metals in sludge
2. Potential green mining practices (i.e., metal recoveries and reuse of sludges) on the Zambian Copperbelt

1.3.2 Objectives

- Geochemical characterisation of effluents and solid deposits through hydrogeochemical and mineralogical analysis
- Metal partitioning through sequential extractions
- Metal retention mechanisms and stability conditions through batch experiments and surface complexation modeling

Chapter 2: Definition of terms and Surface Complexation Modeling

2.1 Sludge effluents and solid deposits

Effluents are a liquid waste, that are discharged from an industrial source such as metallurgical or wastewater treatment processing plant. Effluents are more viscous in texture (Fig. 2.1), often discharged or pumped into storage ponds and impoundments. After sedimentations and settling of effluents, solid deposits form. Generally, sludge deposits are regarded to have of little economic value, hence essentially handled as waste. But this material can be a resource if it contains significant extractable metal concentration when economic demand arises. Such waste if improperly stored can easily release weakly or loosely adsorbed heavy metals and become mobile in the environment, and if that happens, then sludge may be classified as hazardous waste requiring special handling and disposal methods.

Figure 2. 1. Sludge effluents in mine drainages undergoing sedimentation and settling

2.2 Ponds and impoundments

These are storage sites where the solid particles settle through gravity (Fig. 2.2a), and the supernatant (wastewater) (Fig. 2.2b) can be collected as a separate entity. Depending on the heavy metal composition in sludge, the material can either be pumped back to the treatment plant to recover the metals or stored as waste heaps (Fig. 2.2c). The wastewater is mostly treated by lime at neutral pH (i.e., pH 7-7.5) prior to discharge into nearby drainages or pumped back to the water treatment plants for further treatment and purifications.

Figure 2. 2. (a) Sedimentation pond; (b) supernatant after sedimentation process; (c) waste heaps

2.3 Cation exchange capacity (CEC)

The dissolved and adsorbed cations may easily exchange with other cations at soli-liquid interface, hence the term "cation exchange. CEC is a measure of the total negative charges within the soil that adsorb cations. CEC is calculated based on the sum of extractable cations expressed in terms of milliequivalents per100 grams of soil. Soils, sediments and sludges having a low CEC hold fewer cations. The following steps are adopted for calculating CEC (https://ohioline.osu.edu/factsheet/anr-81). The formula is as shown below:

$$CEC = [Basic\ cation(i.e. Ca^{2+} + Mg^{2+} + K^{+} + Na^{+}) + Acid\ cations(i.e. H^{+} + Al^{3+} + NH_4^{+})]$$

Table 1. Determination of CEC.

Cation	(ppm)	Gram equivalent weight (mwt./charge)	Milliequivalent/ 100 g (Gram eq. * 10)	meq/100 g
Calcium	2000	20	200	10
Magnesium	240	12	120	2
Potassium	100	39	390	0.26
Sodium	20	23	230	0.09
Subtotal				12.4
Acidic Cation (H^+, Al^{3+}, NH^{4+})		Buffer pH	Conversion Eqn.	
Exchangeable acidity		6.6	12 (7-6.6)	4.8
If buffer pH is 7 or above, then you have no exchangeable acidity (CEC = sum of base cations). CEC is just the sum of base cations.				

Table 2. CEC of clay minerals in cmol (+)/kg (= meq/100 g) (Grim,1968)

Kaolinite	3–15
Halloysite · $2H_2O$	5–10
Halloysite · $4H_2O$	40–50
Montmorillonite	70–120
Vermiculite	130–210
Illite	10–40
Micas (biotite, muscovite)	up to 5
Chlorite	10–40
Sepiolite, palygorskite	20–30

2.4 Loss on ignition (LOI)

LOI estimates the volatiles such as carbonates and organic matter (Heiri et al., 2001). The method is based on gravimetric weight change associated with high temperature oxidation of organic matter and carbonate minerals. LOI is calculated as follows:

$$\%\ LOI = \left[\frac{(Weight\ before\ heating)_{25^oC} - (Weight\ after\ heating)_{1000^oC}}{(Weight\ before\ heating)}\right] \times 100$$

2.5 Adsorption

Adsorption is a two (2)-dimension accumulation of matter at solid-liquid interface understood in terms of intermolecular interactions between solutes and solid phases (Sposito 1984). According to Bradl (2004), these interactions comprise of: (i) electrostatic interactions where metals form outer sphere complexes at a certain distance from the surface; (ii) surface complexation reactions which are basically inner sphere complexes of the metal ions and their respective surface functional groups; and (iii) hydrophobic expulsion of metal complexes containing highly nonpolar organic solutes. Furthermore, adsorption is described in terms of 2-basic mechanisms; (1) nonspecific adsorption (ion exchange) which involves weak and less selective outer sphere complexes and (2)

specific adsorption characterized by more selective and less reversible reaction including chemisorbed inner sphere complexes.

2.5.1 Types of adsorption

- Non-specific adsorption (outer sphere complexation)

Outer sphere complexation involves one or more water molecules separating the adsorbed ion and the surface (Fig. 2.3). These ions accumulate at the interface of the charged surfaces in response to electrostatic forces. The reactions are rapid and reversible with only a weak dependence on the electron configuration of the surface group and the adsorbed ion. Adsorption occurs at permanent negatively charged sites on planar surfaces of silicate layers (i.e., silanol (SiOH)) sites.

- Specific adsorption (inner sphere complexation)

Inner sphere complexes involve some degree of covalent bonding between the adsorbed species and atoms on the surface (Fig. 2.3). It is distinguished from the exchangeable state by having covalent character between the metal and the surface. Metals such as Cu, Pb display strong adsorption in the presence of high concentrations of exchangeable base cations. Under specific adsorption, pH-dependent sites (i.e., aluminol (AlOH) sites and iron oxides (FeOH) sites) are the main adsorption sites (Sposito, 1984).

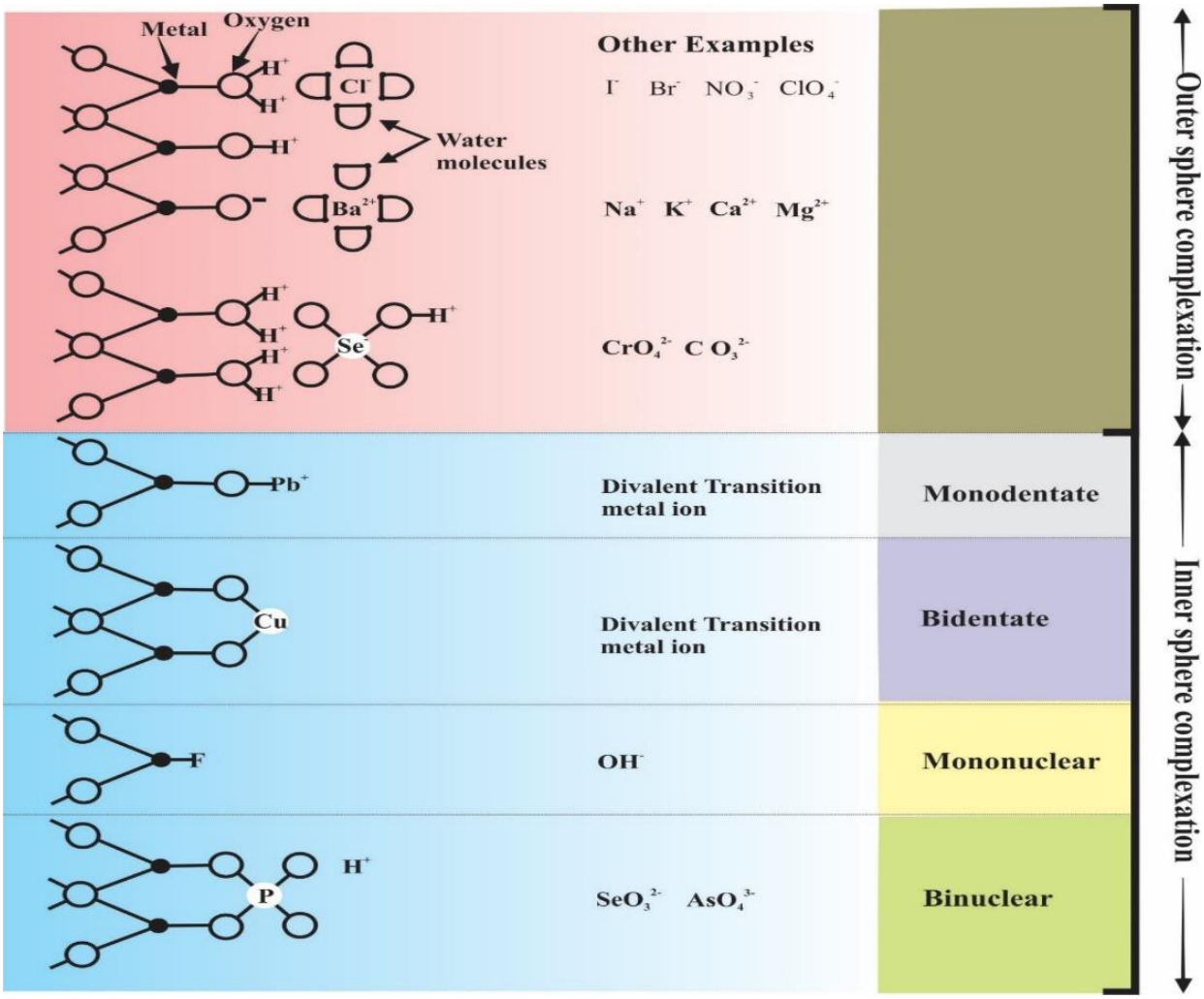

Figure 2. 3. Adsorption mechanisms and types of binding species (modified after Hayes, 1987)

2.5.2 Adsorption edge

A sigmoidal plot of cation adsorption to surface against pH over a narrow pH range is referred to as adsorption edge (Hayes and Leckie, 1986). The shape is influenced by the sorbate/solid ratio. At high solid ratio, the adsorption edge is skewed towards a lower pH condition. At high sorbate concentration, the adsorption edge either; (i) shows no significant shift at very low coverage or (ii) shows some slight shift to higher pH values and becoming less steep with increasing coverage (Hayes and Katz, 1996).

2.5.3 Complexes

Metal ion in solution do not exist in isolation, but in combination with complexes (such as solvent molecules or simple ions) giving rise to complex ions or coordination compounds (Dzombak and Morel, 1990). Complexes are ions or neutral molecules that bond to a central metal atom or ion such as anions, cations, or neutral molecules. Complexes can be further characterized as monodentate and bidentate.

2.5.3.1 Monodentate ligands

The term "monodentate" can be translated as "one tooth," referring to the ligand binding to the center through only one atom (Fig. 2.3). Some examples of monodentate ligands are chloride ions, hydroxide ions (referred to as hydroxo), and ammonia (referred to as ammine).

2.5.3.2 Bidentate ligands

Bidentate means "two-toothed. Bi(multi)dentate surface complexes form through binding of an adsorbate to two or more adjacent functional groups (Fig. 2.3). Bidentate ligands could also involve one sorbate molecule reacting with two sites of different types (Wang and Giammar, 2013).

2.5.4 Adsorption capacity (AC)

Adsorption capacity is defined as the amount of adsorbate needed to occupy all adsorption (Sheng-Fong Lo, 2012). It can be described by the following equation:

$$\boldsymbol{AC} = (\frac{\boldsymbol{C_i} - \boldsymbol{C_f}}{\boldsymbol{W_g}}) * \boldsymbol{V}$$

where C_i = initial concentration; C_f = final concentrations; V = volume and W_g = weight (dosage) of analysed sample

2.5.5 Surface coverage

Surface coverage is defined as the amount of adsorbed substance to the adsorption capacity

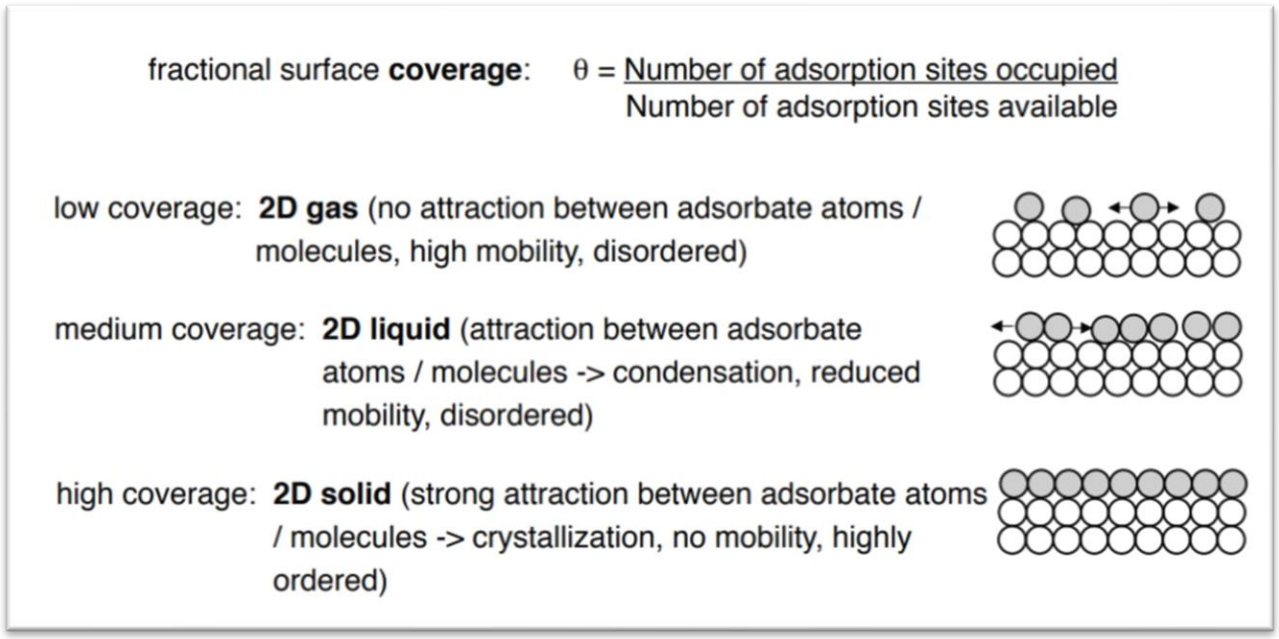

Figure 2. 4. Description of adsorption properties of metal adsorption. Courtesy of Prof. Dr Ulrich Jonas; Macromolecular chemistry- University of Siegen

2.6 Surface complexation modeling (SCM)

SCM represent one type of mechanistic approach that has been used to model contaminant sorption on (hydro)oxide surfaces over a wide range of physio-chemical and geochemical conditions such as pH, ionic strength and total concentration of adsorbate (Sanchez et al., 1985; Girvin et al., 1991; Payne et al., 1992; Turner, 1993). These models rely on the assumption that the formation of surface complexes with functional binding sites at the mineral-water interface is analogous to aqueous speciation reactions occurring in the bulk solution.

2.6.1 Component additivity (CA)

The CA approach assumes that the solid surface can be considered as a mineral assemblage composed of a mixture of reference minerals whose surface reactions/constants are known from independent studies of each mineral or from the literature (Dong and Wan, 2014). The CA-SCM approach attempts to predict adsorption on a complex natural material by treating it as an assemblage of minerals. If the reactive surface area of each mineral component present in the sediment can be estimated, adsorption by the sediment can be predicted by a simple sum of adsorption from each component, without any fitting of experimental data for the sediment. The advantages of the CA-SCM are that (i) the surface adsorption models and parameters can be developed from reference minerals or obtained from the literature (Davis et al., 2004), (ii) the model parameters are transferable from one field site to another (Davis et al., 2004), and (iii) the modeling results can be useful for understanding the relative contributions of each mineral components for the overall adsorption (Dong and Wan, 2014).

2.6.2 General adsorption surfaces

The pH dependence is mostly widely utilized SCM by assuming surface sites comprising of hydroxyl groups >SOH (Schindler et al., 1987). The potential determining ion at the mineral-water interface is assumed to be hydrogen. By adding a hydrogen ion (protonation), a positively charged surface site, > SOH^{2+}, is developed (Schindler et al., 1987). Conversely, losing a proton (deprotonation) leads to the development of a negatively charged surface > SO^-. At low pH, the > SOH^{2+} sites outnumber the >SO^- sites, and the surface is positively charged (Schindler et al., 1987). At higher pH, the > SO^- sites are more numerous, and the net surface charge is negative. At some intermediate pH, referred to as the zero point of charge (pHzpc), the sites will balance, and the surface will not exhibit any net charge (Schindler et al., 1987). Therefore, depending on the pH, the electrostatic attraction from these sites can lead to the specific adsorption of cations and anions from solution. By assuming an analogy to aqueous speciation reactions, surface adsorption is then described using a combination of equilibrium protonation/deprotonation and complexation reactions

2.6.2.1 Surface Reactions

SCM models assumes all reactions to be at equilibrium. SCMs share at least three common characteristics. First, it is assumed that mineral surfaces can be described as flat planes of surface hydroxyl sites and that equations can be written to describe reactions at these specific sites (Koretsky, 2000). The second assumption common to all SCMs is that reactions at mineral surfaces may be described using mass law equations. For instance, a surface protonation reaction might be written as,

$$> SOH + H^+ \leftrightarrow > SOH^{2+}\ ;\ K_1^{app} = \frac{[> SOH^{2+}]}{[> SOH][H^+]} \quad \ldots\ldots\ldots\ldots\ldots\ldots\ldots\ldots\ldots\ldots\ldots\ldots 1$$

$$> SOH \leftrightarrow > SO^- + H^+ ; K_2^{app} = \frac{[> SO^-]H^+}{[> SOH]} \quad \text{.....2}$$

Here the SOH represents a species or functional group on solid surface. In the first reaction, SOH gains an H+ and becomes positively charged. In the second reaction, >SOH loses an H+ and becomes negatively charged. The apparent equilibrium constants K^{app} describe the relationship between activities of different species, written in the same format as we do for aqueous complexations except now, we include activities of solid species.

Similarly, for a metal ion M with a positive charge m, the reactions are represented by:

$$> SOH + M^{m+} \leftrightarrow > SOH^{(m-1)} + H^+ ; K_{M1}^{app} = \frac{\left[> SOH^{(m-1)}\right][H^+]}{[> SOH][M^{m+}]} \quad \text{.....3}$$

$$2 > SOH + M^{m+} \leftrightarrow (> SO)_2 M^{(m-2)} + 2H^+ ; K_{M2}^{app} = \frac{\left[(> SO)_2 M^{(m-2)}\right][H^+]^2}{[> SOH]^2[M^{m+}]} \quad \text{.....4}$$

The third assumption adopted in all SCMs is that variable charge at the mineral surface is the direct result of chemical reactions at the surface. According to Koretsky (2000), minerals have zero surface charge at a particular pH, termed the pH of the pristine point of zero charge (pH_{PPZC}) which is a predictable function of mineral structure (Sverjensky, 1994). For all pH dependent charged surfaces, whether organic or inorganic, as the pH decreases, the number of negatively charged sites diminishes. Under more acidic conditions, most pH dependent surfaces are positively charged and in alkaline to more alkaline conditions, with the majority site becoming negatively charged.

2.6.2.2 Surface area (SA)

The specific surface area of a fine particles (powder) is determined by physical adsorption of a gas on the surface of the solid and by calculating the amount of adsorbate gas corresponding to a monomolecular layer on the surface (Brame and Griggs, 2016). Physical adsorption results from

relatively weak forces (van der Waals forces) between the adsorbate gas molecules and the adsorbent surface of the test powder. The determination is usually carried out at the temperature of liquid nitrogen. The amount of gas adsorbed can be measured by a volumetric or continuous flow procedures suggested by Brame and Griggs (2016).

2.6.2.3 Site density

The total surface site density, Ns is related to the total number of reactive surface sites (i.e. hydroxyl groups) per unit amount of solid or surface area expressed as sites/nm^2 or mol/mol Al. Surface site density can be calculated by experimental data through crystal dimensions or optimized to fit the experimental data (Davis and Kent, 1990). Experimental methods include the potentiometric titration, maximum ion adsorption and infrared spectroscopy. Davis and Kent (1990) recommended surface site density of $2.31nm^{-2}$ for natural materials. The total concentration of sites, N_t (mol/l) for a solid concentration, Cs (g/l) is related to the site density Ns (sites/nm^2) as:

$$N_T = N_s \times A \times C_s \times \frac{1}{N_A} \times \frac{10^{18} nm^2}{m^2}$$

Where A is the specific surface area (m^2/g) of the solid and NA the Avogadro's number (6.02 X 10^{23} sites/mol). Dzombak and Morel (1990) used 2.31 sites/nm^2 for HFO. For hematite, gibbsite and titanium oxide (TiO_2), Hayes et al. (1991) suggested 10 sites/nm^2.

2.7 Surface complexation modeling of Cu (II) and Co (II) adsorption on kaolinite and hydrous ferric oxide (HFO)

2.7.1 Cu adsorption on kaolinite

SCMs have been proposed to describe Cu adsorption on kaolinite. Most of these follow the lead author such as Schindler et al. (1987). Gu and Evan (2008) described the two major adsorption sites on kaolinite surfaces. The permanent negatively charged sites on the basal surfaces which

undergo on-specific ion exchange reactions, which occur at lower pH values and are strongly influenced by ionic strength (Fig. 2.5a, b). Inner sphere complexes are common at high pH, hence are pH dependent (Fig. 2.5a, b). The pH dependent adsorption takes place at the hydroxyl groups on the mineral edges (Gu and Evan, 2008). Adsorption of Cu onto kaolinite was conducted by Ikhsan et al. (1999); Peacock and Sherman (2005); Jung et al. (1998) and Hizal and Apak (2006).

The general agreement between the predicted edges from the model derived data from four independent studies using different ionic strength, background electrolyte, sorbate/sorbent ratio and kaolinite specimens is encouraging (Fig. 2.6) and the discrepancies between model predictions and the experimental data could be due to differences in experimental conditions.

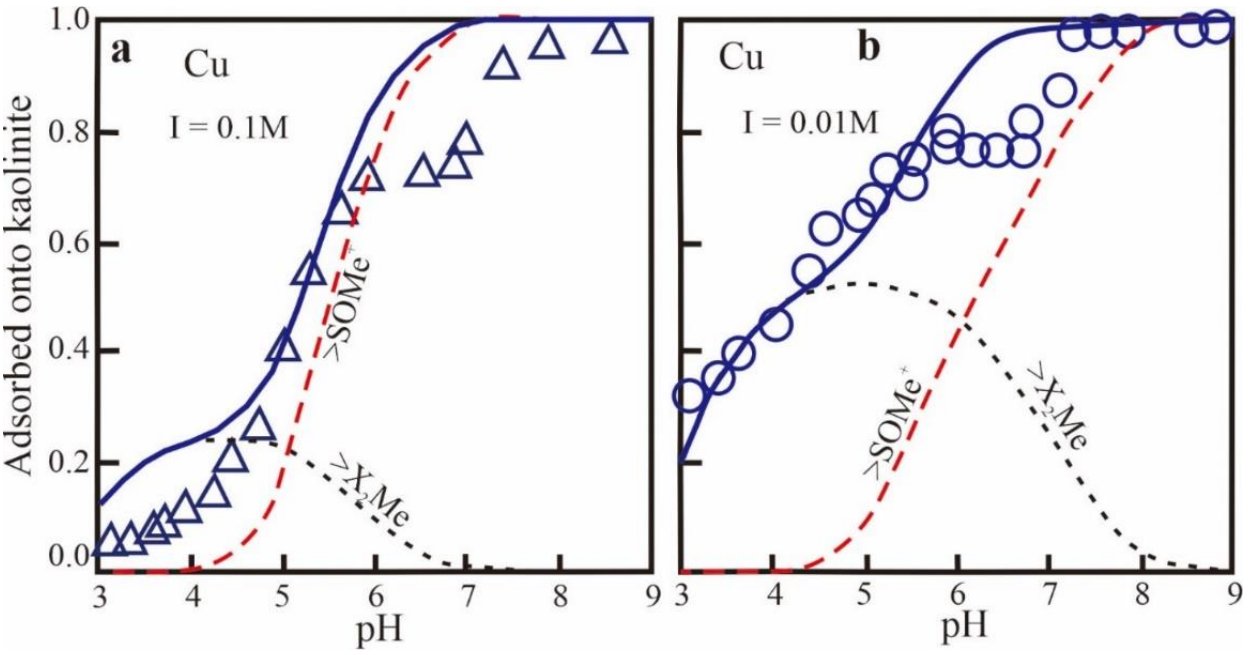

Figure 2. 5. The distribution of modeled surface complexation species of Cu (II) onto kaolinite at different ionic strengths (Modified from Gu and Evan, 2008).

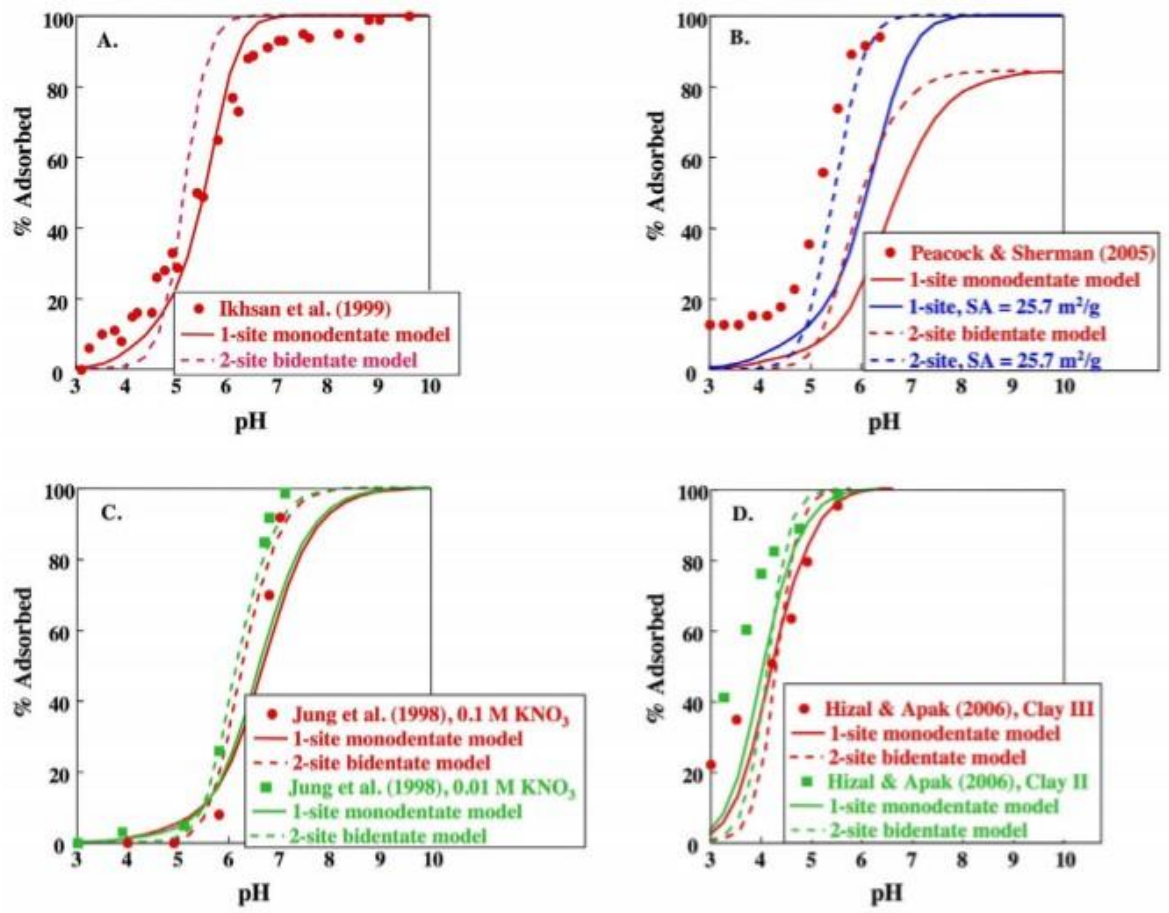

Figure 2. 6. Comparisons 1-site and 2-site kaolinite models with previously reported data. The 1-site model includes a monodentate Cu complex on a variable charge site. The 2-site model includes a bidentate cu complex on a variable charge site and an ion exchange site that does not bid Cu (Lund et al., 2008)

Table 2: Reaction stoichiometries and stability constants used in DLM calculations for kaolinite (Lund et al., 2008)

Reaction	Log Stability Constant	V(Y) ($V_{min}(Y)$, $V_{max}(Y)$)
>KaoliniteOH + $H^+_{(aq)}$ = >KaoliniteOH$_2^+$	2.1[38]	
>KaoliniteOH = >KaoliniteO$^-$ + $H^+_{(aq)}$	-8.1[38]	
Monodentate variable charge site:		23.3
>KaoliniteOH + $Cu^{+2}_{(aq)}$ = >KaoliniteOCu$^+$ + $H^+_{(aq)}$	-1.7 (this study)	(20.2, 27.1)
Bidentate variable charge site:		28.5
2 > KaoliniteOH + $Cu^{+2}_{(aq)}$ = >KaoliniteO$_2$Cu + 2$H^+_{(aq)}$	-4.6 (this study)	(24.8, 33.2)
Monodentate variable charge + ion exchange site (all log K's fit in this study):		
>KaoliniteOH + $Cu^{+2}_{(aq)}$ = >KaoliniteOCu$^+$ + $H^+_{(aq)}$	-1.9 (this study)	
X(Na) + $H^+_{(aq)}$ = X(H) + $Na^+_{(aq)}$	4.1 (this study)	44.9
2X(Na) + $Cu^{+2}_{(aq)}$ = X$_2$(Cu) + 2$Na^+_{(aq)}$	0.72 (this study)	(38.9, 52.2)
Monodentate variable charge + ion exchange site model (fixed Na-H exchange stability constant):		
>KaoliniteOH + $Cu^{+2}_{(aq)}$ = >KaoliniteOCu$^+$ + $H^+_{(aq)}$	-2.3 (this study)	
X(Na) + $H^+_{(aq)}$ = X(H) + $Na^+_{(aq)}$	4.3 (this study)	108
2X(Na) + $Cu^{+2}_{(aq)}$ = X$_2$(Cu) + 2$Na^+_{(aq)}$	2.5[7]	(93.6, 126)
Bidentate variable charge + ion exchange site model (fixed Na-H exchange stability constant):	-5.3 (this study)	
2>KaoliniteOH + $Cu^{+2}_{(aq)}$ = >KaoliniteO$_2$Cu + 2$H^+_{(aq)}$	4.6 (this study)	62.6
X(Na) + $H^+_{(aq)}$ = X(H) + $Na^+_{(aq)}$	2.5[7]	(54.4, 72.9)
2X(Na) + $Cu^{+2}_{(aq)}$ = X$_2$(Cu) + 2$Na^+_{(aq)}$		
Monodentate variable charge + ion exchange site model, no Cu sorption on ion exchange site (fixed Na-H exchange stability constant):	-1.8 (this study)	190
>KaoliniteOH + $Cu^{+2}_{(aq)}$ = >KaoliniteOCu$^+$ + $H^+_{(aq)}$	2.5[7]	(165, 221)
X(Na) + $H^+_{(aq)}$ = X(H) + $Na^+_{(aq)}$		
Bidentate variable charge + ion exchange site model, no Cu sorption on ion exchange site (fixed Na-H exchange stability constant):	-4.6 (this study)	33.8
2 > KaoliniteOH + $Cu^{+2}_{(aq)}$ = >KaoliniteO$_2$Cu + 2$H^+_{(aq)}$	2.5[7]	(29.4, 39.3)
X(Na) + $H^+_{(aq)}$ = X(H) + $Na^+_{(aq)}$		

38- Sverjensky and Sahai (1996)

2.7.2 Co adsorption onto kaolinite

Several SCM models have been proposed previously to describe Co adsorption on kaolinite by Angove et al. (1998) and Ikhsan et al. (1999). Similar to the adsorption behavior of Cu, Co adsorption at low pH is also pH independent at permanent negative charge site and is a much greater dependent on the ionic strength (Fig. 2.7). At low ionic strengths the edges have a relatively shallow slope, with significant adsorption even at low pH, whereas at higher ionic strengths the edges are much sharper (Landry et al., 2009). With increasing pH conditions, Ikhsan et al. (1999) concluded that Co adsorption forms a bidentate complex on the variable charge sites of kaolinite. Thus, the formation of a bidentate Co complex (Table 3) on the variable charge site is used to model Co adsorption on kaolinite surfaces and other solid mixtures (Landry et al., 2009).

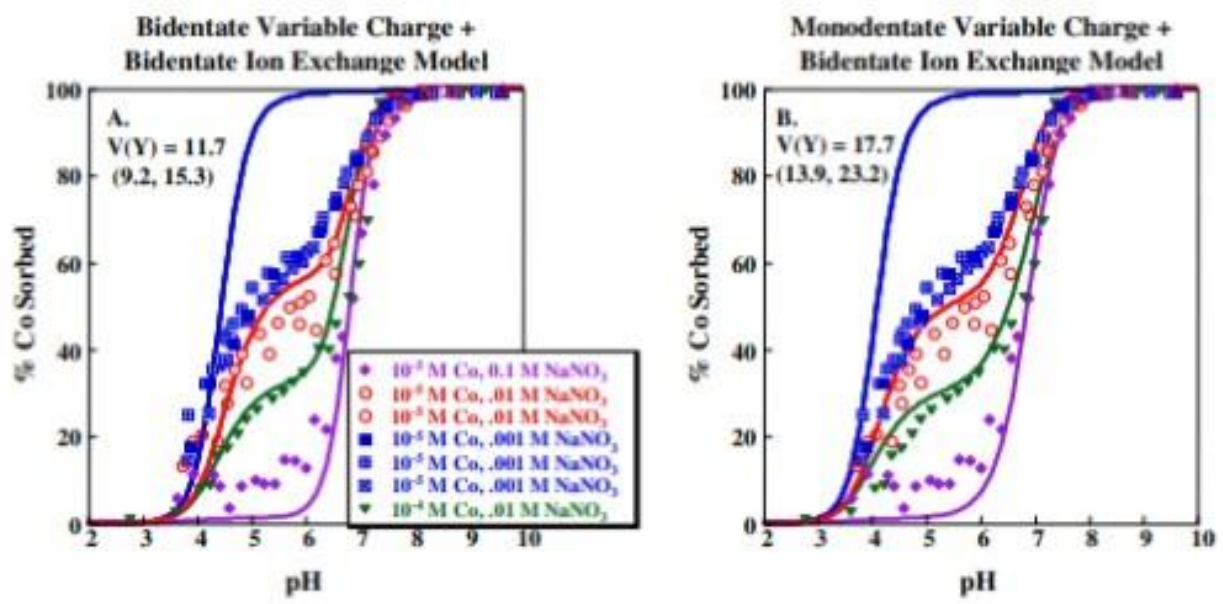

Figure 2. 7. Co sorption as a function of pH on 5 g/L Wards kaolinite with 104 or 105 M Co and 0.1–0.001 M NaNO3. Lines indicate fits predicted for models calibrated using KGa-1b data with an ion exchange site and (A) a bidentate Co complex on the variable charge site or (B) a monodentate Co complex on the variable charge site (Landry et al., 2009)

Table 3: Reaction stoichiometries and stability constants used in DLM calculations for kaolinite (Landry et al., 2009)

Reaction	Log stability constant	KGa-1b $V(Y)$ ($V_{min}(Y)$, $V_{max}(Y)$)	Wards $V(Y)$ ($V_{min}(Y)$, $V_{max}(Y)$)
$>KaoliniteOH + H^{+}_{(aq)} = >KaoliniteOH_2^{+}$	2.1[a]		
$>KaoliniteOH = >KaoliniteO^{-} + H^{+}_{(aq)}$	−8.1[a]		
Monodentate variable charge site		16.9	24.0
$>KaoliniteOH + Co^{+2}_{(aq)} = >KaoliniteOCo^{+} + H^{+}_{(aq)}$	−3.9 (this study)	(14.4, 20.1)	(18.9, 31.5)
Bidentate variable charge site		23.8	31.9
$2>KaoliniteOH + Co^{+2}_{(aq)} = >KaoliniteO_2Co + 2H^{+}_{(aq)}$	−7.3 (this study)	(20.3, 28.3)	(25.2, 41.9)
Monodentate variable charge + ion exchange site			
$>KaoliniteOH + Co^{+2}_{(aq)} = >KaoliniteOCo^{+} + H^{+}_{(aq)}$	−4.3 (this study)		
$X(Na) + H^{+}_{(aq)} = X(H) + Na^{+}_{(aq)}$	2.1 (this study)	6.6	17.7
$2X(Na) + Co^{+2}_{(aq)} = X_2(Co) + 2Na^{+}_{(aq)}$	3.8 (this study)	(5.6, 7.9)	(13.9, 23.2)
Bidentate variable charge + ion exchange site			
$2>KaoliniteOH + Co^{+2}_{(aq)} = >KaoliniteO_2Co + 2H^{+}_{(aq)}$	−7.9 (this study)		
$X(Na) + H^{+}_{(aq)} = X(H) + Na^{+}_{(aq)}$	2.5 (this study)	6.8	11.7
$2X(Na) + Co^{+2}_{(aq)} = X_2(Co) + 2Na^{+}_{(aq)}$	3.9 (this study)	(5.8, 8.1)	(9.2, 15.3)

[a] Sverjensky and Sahai (1996).

2.7.3 Cu adsorption on hydrous ferric oxide (HFO)

Cu adsorption on HFO was measured as a function of pH (Fig. 2.8) (Lund et al., 2008). Cu adsorption on HFO has been described by Dzombak and Morel (1990) using double layer surface complexation model (DLM) with the parameters shown in Tables 4 and 5. Cu adsorption at HFO sites is pH dependent and adsorption showed increases at increasing pH conditions (Fig. 2.8). Cu (II) adsorption reveals the sigmoid adsorption edge for HFO in good agreement with several previous studies of Cu adsorption onto HFO (Dzombak and Morel, 1990).

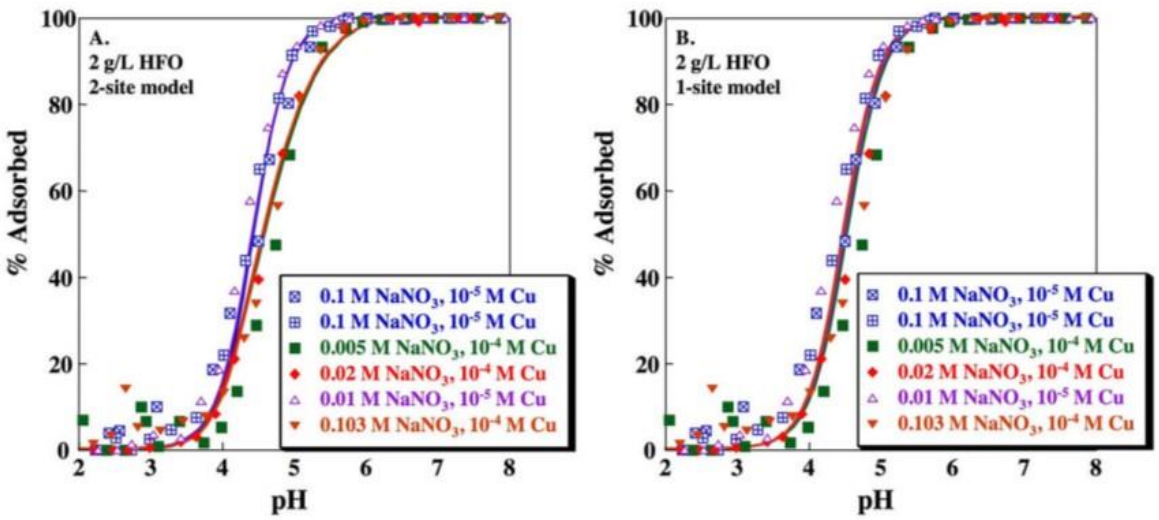

Figure 2. 8. Cu adsorption as a function of pH on HFO. Solid concentration is 2 g/L. Lines indicate fits for (A) Dzombak and Morel (1990), 2-site HFO model and (B) Sverjensky and Sahai (1996), 1-site HFO model calculated using parameters shown in Tables 4 and 5

Table 4: Surface areas, surface site types and site densities used in DLM calculations (Lund et al., 2008)

Solid	Surface Area (m^2/g)	Site Types	Site Density ($\mu mol/m^2$)
HFO (2-site model)	600[4]	$>Fe_{(s)}OH$	0.094[4]
		$>Fe_{(w)}OH$	3.74[4]
HFO (1-site model)	600[4]	>FeOH	16.6[38]
Kaolinite (KGa)	13.6 (this study)	>SOH	16.6[38]
		X	2.2[a]
Kaolinite (Wards)	25.7 (this study)	>SOH	16.6[38]
		X	1.2[a]

4- Dzombak and Morel (1990); 38- Sverjensky and Sahai (1996)

Table 5: Reaction stoichiometries and stability constants used in DLM calculations for HFO (Lund et al., 2008)

Reaction	Log Stability Constant	V(Y) ($V(Y)_{min}$, $V(Y)_{max}$)
HFO (2-site model):		
$>Fe_{(s)}OH + H^{+}_{(aq)} = >Fe_{(s)}OH_2^{+}$	7.29[4]	
$>Fe_{(w)}OH + H^{+}_{(aq)} = >Fe_{(w)}OH_2^{+}$	7.29[4]	
$>Fe_{(s)}OH = >Fe_{(s)}O^{-} + H^{+}_{(aq)}$	-8.93[4]	
$>Fe_{(w)}OH = >Fe_{(w)}O^{-} + H^{+}_{(aq)}$	-8.93[4]	14.0
$>Fe_{(s)}OH + Cu^{+2}_{(aq)} = >Fe_{(s)}OCu^{+} + H^{+}_{(aq)}$	2.89[4]	(10.9, 18.5)
HFO (1-site model):		
$>FeOH + H^{+}_{(aq)} = >FeOH_2^{+}$	7.5[38]	
$>FeOH = >FeO^{-} + H^{+}_{(aq)}$	-10.2[38]	12.2
$>FeOH + Cu^{+2}_{(aq)} = >FeOCu^{+} + H^{+}_{(aq)}$	0.98 (this study)	(9.5, 16.1)

4- Dzombak and Morel (1990); 38- Sverjensky and Sahai (1996)

2.7.4 Co adsorption on hydrous ferric oxide (HFO)

Adsorption of Co on HFO has been described by Dzombak and Morel (1990) using a DLM with the parameters shown in Tables 4 and 6. The Dzombak and Morel (1990) model, predicts increasing adsorption at higher pH condition (Fig. 2.9). There is very good agreement between the experimental data and the predicted adsorption edge indicating that at least for the conditions considered in their study, the influence of mineral–mineral interactions on Co adsorption is within the uncertainty of the fits derived for the pure solid systems

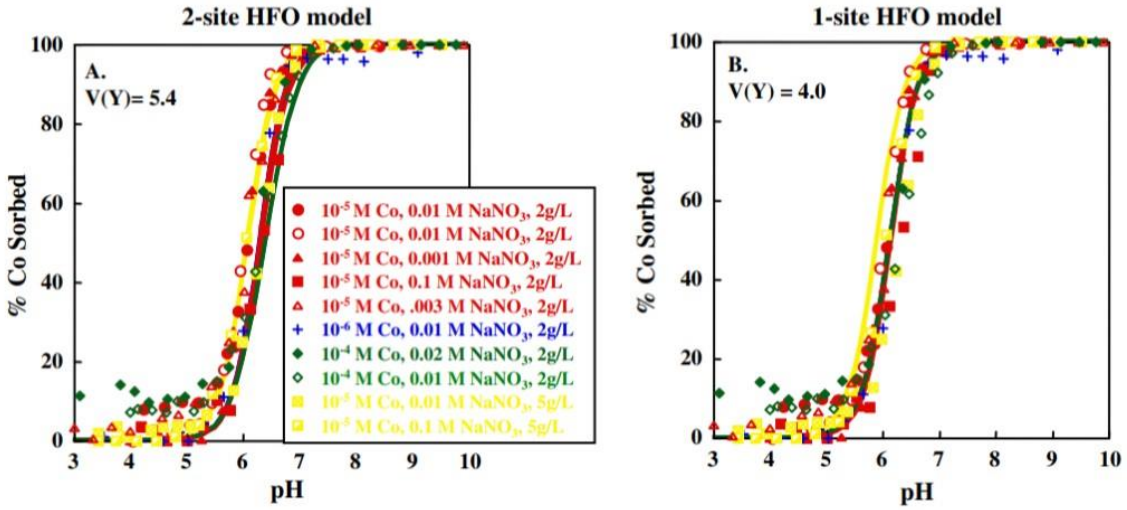

Figure 2. 9. Co sorption on HFO. Points indicate data measured in this study using 2 g/L HFO. (A) Lines indicate fits calculated using 2-site model DLM parameters derived by Dzombak and Morel (1990). (B) Lines indicate fits calculated using best-fit stability constants for a 1-site DLM. Parameters for the models are shown in Tables 1and 2.

Table 6: Reaction stoichiometries and stability constants used in DLM calculations for HFO (Landry et al., 2008)

Reaction	Log stability constant	$V(Y)$ ($V(Y)_{min}$, $V(Y)_{max}$)
HFO (D&M 2-site model)		
$>Fe_{(s)}OH + H^{+}_{(aq)} = >Fe_{(s)}OH_2^{+}$	7.29[a]	
$>Fe_{(w)}OH + H^{+}_{(aq)} = >Fe_{(w)}OH_2^{+}$	7.29[a]	
$>Fe_{(s)}OH = >Fe_{(s)}O^{-} + H^{+}_{(aq)}$	−8.93[a]	
$>Fe_{(w)}OH = >Fe_{(w)}O^{-} + H^{+}_{(aq)}$	−8.93[a]	
$>Fe_{(s)}OH + Co^{+2}_{(aq)} = >Fe_{(s)}OCo^{+} + H^{+}_{(aq)}$	−0.46[a]	5.4
$>Fe_{(w)}OH + Co^{+2}_{(aq)} = >Fe_{(w)}OCo^{+} + H^{+}_{(aq)}$	−3.01[a]	(4.2, 7.2)
HFO (1-site model)		
$>FeOH + H^{+}_{(aq)} = >FeOH_2^{+}$	−7.5[b]	4.0
$>FeOH = >FeO^{-} + H^{+}_{(aq)}$	−10.2[b]	(3.1, 5.4)
$>FeOH + Co^{+2}_{(aq)} = >FeOCo^{+} + H^{+}_{(aq)}$	−1.8 (this study)	

[a] Dzombak and Morel (1990).
[b] Sverjensky and Sahai (1996).

Chapter 3: Geological setting, site description and sampling

3.1 Geological setting of the Zambian Copperbelt

The Zambian Copperbelt (Fig. 3.1a) lies within the convex orogenic belt known as the Lufilian Arc formed by the Lufilian orogeny of the Neoproterozoic time (Wilderode et al., 2014). Regionally, the area is underlain by basement rocks comprising of granitic intrusion and metamorphic assemblages (Fig. 3.2), which formed during the Neoproterozoic age (600–544 Ma) and overlain by the thick sedimentary sequence of the Katangan Supergroup (McGowan et al., 2006). Mining is generally concentrated in the Lower Roan Formation (Fig. 3.2), where ore sulphides are dominated by chalcopyrite ($CuFeS_2$), bornite (Cu_5FeS_4), chalcocite (Cu_2S), digenite (Cu_9S_5), linnaeite (Co_3S_4), and carrolite ($Cu(Co)_2S_4$), embedded in carbonate-rich shale, argillite or in sandstone (McGowan et al., 2006). Specific to the studied site, chalcocite (Cu_2S), and carrolite ($Cu(Co)_2S_4$) are quite dominant.

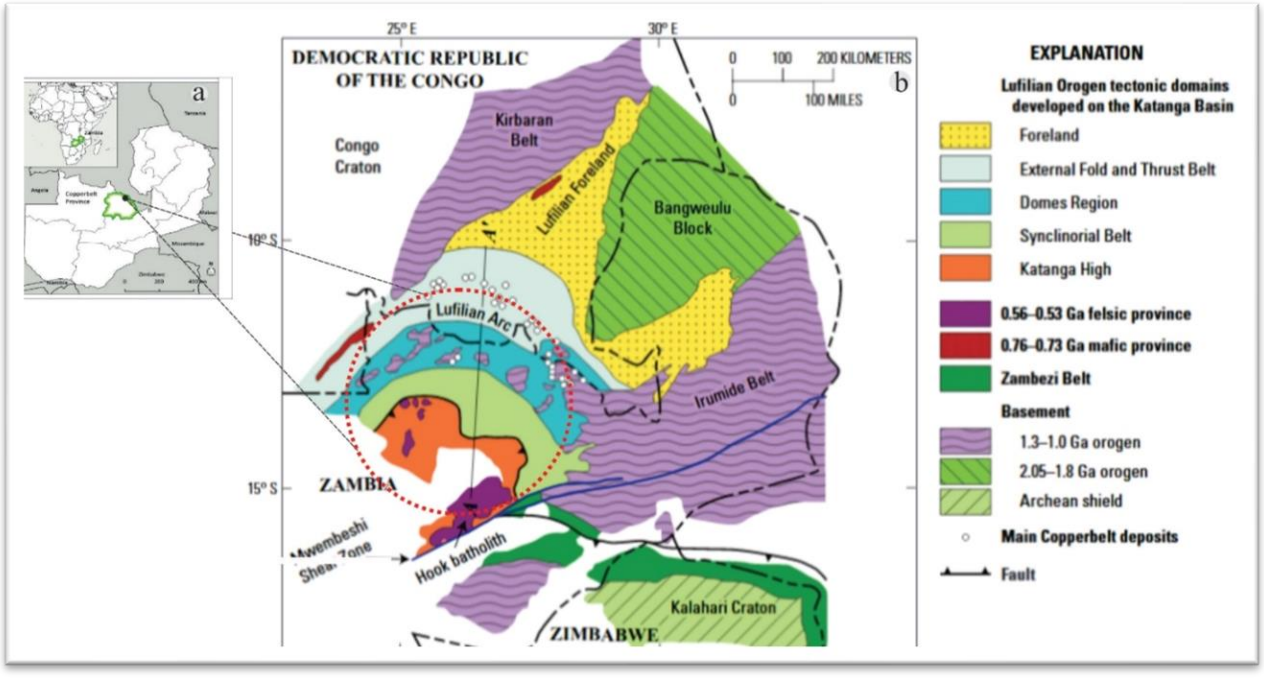

Figure 3.1. Regional setting of the Zambian Copperbelt (McGowan et al., 2006)

3.2 Site geological characteristics

At the studied site, the exposed bedrock is the feldspathic granite (Fig. 3.2) quite distinguishable from several of the overburden characteristic waste rock types that have been found on surfaces of the studied site so far. The formation shows little variations at the regional scale, which supports the idea that areas where the Formation is exposed today is all part of a much larger basement complex system of the entire Zambian Copperbelt mining district. At the studied site, the feldspathic granitic bedrock is exposed along the eroded drainage courses (Fig. 3.2) and it is possible to follow the exposures for more than hundreds to a kilometer along the drainages. The exposed bedrock (i.e., feldspathic granites) are highly weathered and are possibly the main sources of dominant component minerals that are common to sludges.

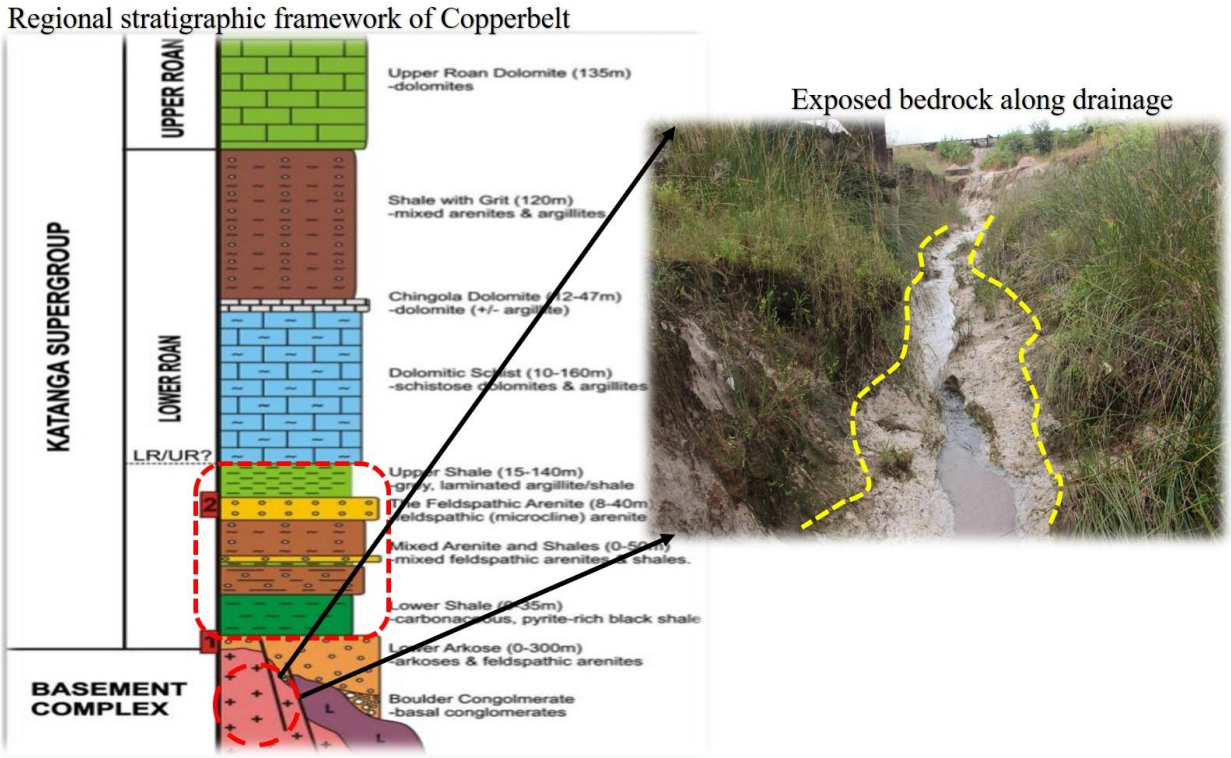

Figure 3.2. Regional stratigraphy of the Zambian Copperbelt (modified after Rainaud et al., 2005)

3.3 Site description

Two (2) studied sites belong to the Konkola Copper Mines (KCM), Nchanga mine Division license.

A) Site 1 is situated approximately 2 – 3 km north of Chingola town centre (Fig. 3.3b) and characterized mostly by drainages and sludge storage sites. The main drainage in this site is the Chingola Stream labelled S0 – S11 (Fig. 3.3b) which stretches from the township side to far beyond the mining license site, and then meanders through the mine site collecting and transporting mine effluent spillages containing high Cu^{2+} and Co^{2+} concentrations and waste heap rocks during surface erosion by rainfall. S0 represents the background water from catchment sources unaffected by anthropogenic mining-related activities whereas S1 represents the anthropogenic source from the metal processing at the concentrator prior to mixing with the nearby receiving drainage. After mixing, the diluted effluents (i.e., S2 – S6) are transported downstream to the storage ponds. Because of some intermittent low pH conditions along the drainage, lime is added to increase the pH of the drainage wastewater.

B) Site 2 is situated approximately 15 km south of Chingola town (Fig. 3.3c). Sludge is transported and deposited at storage sites through piping and drainage channels. At this site, there is relatively a continuous deposition of young (new) sludge on top of the old sludge. It is not, however clear whether this kind of sludge deposition causes anaerobic conditions beneath at depth but considering the physical characteristics of sludge, which is sandier in texture, aeration and oxic condition could also be taking place.

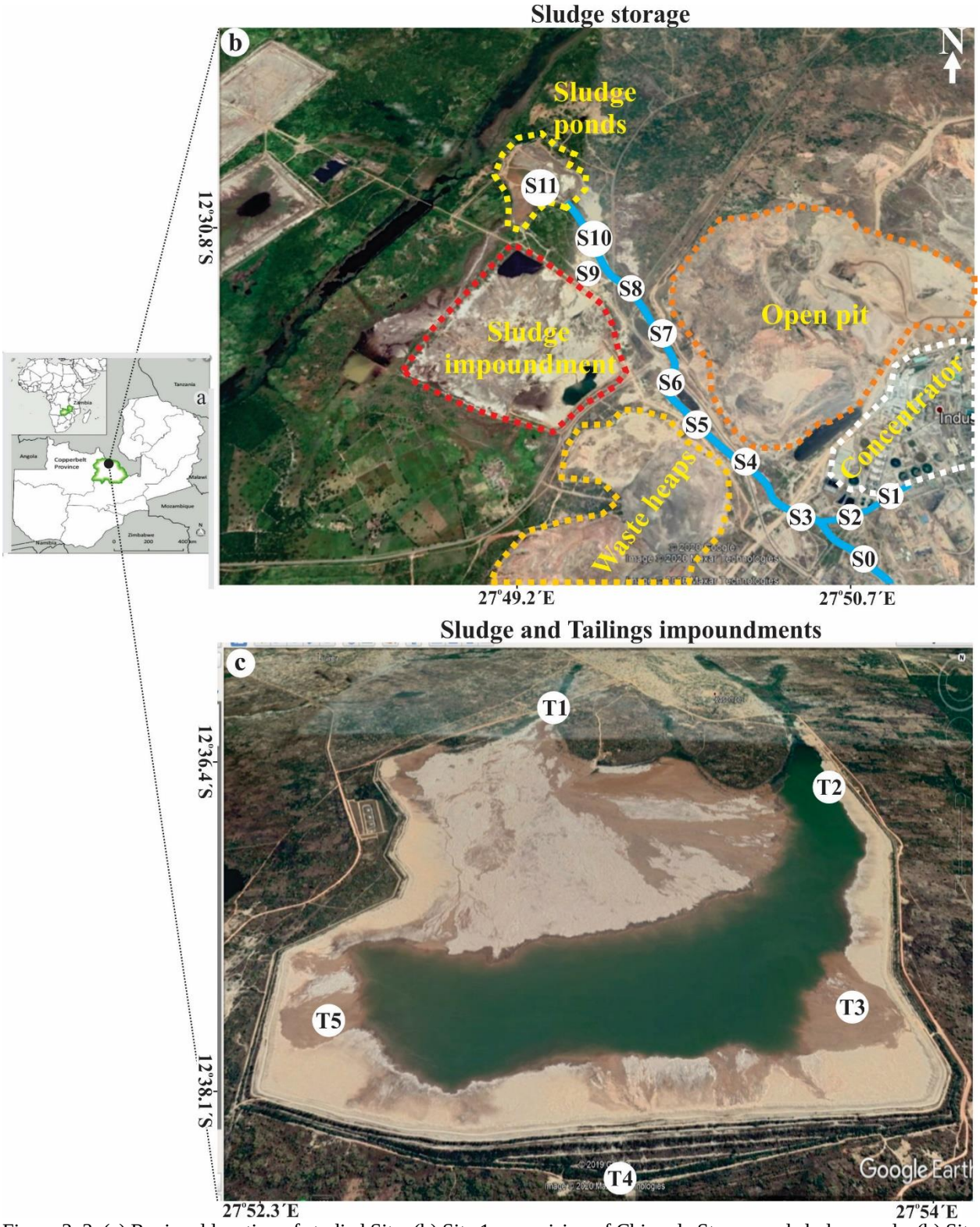

Figure 3. 3. (a) Regional location of studied Site; (b) Site 1 comprising of Chingola Stream and sludge ponds; (b) Site 2 predominantly as the tailings impoundments. Abbreviations: S and T are sample locations

3.4 Sampling of drainage effluents

Three (3) sampling periods were conducted between dry (D) and wet (W) season in the year 2018 and 2019. The drainage effluents were sampled and measured at site (Fig. 3.4a) for their pH, electrical conductivity (EC) and oxidation-reduction potential (ORP) at each sampled location by placing the probe directly into the flowing stream water using a multi-probe (model W-22XD, Horiba Ltd. Kyoto, Japan). The collected effluent samples were filtered with 0.2 and 0.45µm (ADVANTEC-cellulose-acetate) disposable membrane filters. The 0.2µm filtrates were split into two subsample sets, one acidified with 100µl of analytical grade nitric acid (HNO_3) for analyses of dissolved major and minor cations and another set of the non-acidified sample was analysed for the major anions. The 0.45µm filtrate was measured for the alkalinity conditions through titration with 100µl of 1% HNO_3.

Figure 3. 4. (a) Field measurements of pH, EC and ORP in drainage effluents

3.5 Sampling of sludge solids

Solid sampling took place during the similar sampling dates as reported in section 3.3. Solid materials were collected as; (1) residues after settling of effluents, and (2) sampled directly with the steel shovel (Fig. 3.4b). Besides, sludge solids and during the dry season, white precipitates (i.e., efflorescent salts) were also collected on sludge surfaces (Fig. 3.4b). Sampling occurred at the top 10 centimeters (cm) using the steel shovel and stored in Ziploc® plastic bags at ambient temperature prior to shipment for laboratory analyses.

Figure 3.5. Field sampling of solid material at storage sites

3.6 Results and Discussion

During the reconnaissance surveys, no carbonate rocks were envisaged in the studied site. The only carbonate mineral observed especially along the drainage was in the form of surface precipitate perceived to be malachite (Fig. 3.6a). Its formation may be linked to drying up or evaporation of aqueous $CuCO_3$ bearing solutions due to lime addition and reactions of lime with the atmospheric conditions in the presence of high Cu concentrations in effluents. From the results of some previous studies by Bourg (1988); Prusty et al. (1994); Solomons (1995), detrital and non-detrital carbonate minerals were reported to enhance heavy metal complex formation on surfaces of primary minerals, a condition which parallels the studied site. Thus, the observed malachite is possibly authigenic in origin due to the abundant Cu concentration adsorbed by the detrital and non-detrital carbonate and primary minerals. The presence of malachite precipitates is also evidence that its formation acts as a sink and hosts the Cu in dry seasons, but not during rainy seasons.

During the dry season, white precipitates of efflorescent salts were common along the drainage (Fig. 3.6b) and storage ponds (Fig. 3.6c). Efflorescence salts, usually form on a surface and substance having emerged in solution and subsequently precipitated by evaporation of water (Sghaier and Prat, 2009) or interaction with carbon dioxide in the atmosphere These minerals are generally sulfates and carbonates of sodium, potassium, or calcium with the major component being calcium carbonate. The presence of efflorescence salts means that the sludges:

- contains soluble mineral salts
- contains enough moisture to dissolve those salts and
- is porous enough for the salt solution to make its way to the surface.

Due to their high solubility, the salts dissolve during the rainy season and mix with river water during the flow. The significance of understanding efflorescent salts in this studied site are that the

identification of both their physiochemical and geochemical characteristics is important due to high solubility and their potential to hosts heavy metals by isomorphic substitution (Nordstrom, 2011). Mud cracks were observed at sedimentation ponds (Fig. 3.6d). These form when a shallow body of water (e.g., pond), into which muddy sediments have been deposited, dries up and cracks. They normally happen because the clay in the upper mud layer tends to shrink on drying, and so it cracks because it occupies less space when it is dry. The significance in the presence of mud cracks in this study is that they reveal the presence of clay mineralogy, the depositional environment of the sediments and the climate at the time of deposition including estimates of the depth of the water; detect the existence of currents; and estimate average temperature and precipitation.

Fig. 3.6. a) Malachite precipitates along drainage; b-c) efflorescent salts precipitates along drainage and ponds; d) mud cracks formation at storage ponds

3.7 Chapter 3-Summary

1. The mappable lithology in the studied site is the exposed bedrock along the drainage comprising of the feldspathic granites that are low to moderately weathered. Pristine drainages meandering through the mining license receive lime treated mine wastewater. The chemical reaction of lime treated water with atmospheric conditions with the accompanying high Cu concentration is observed to facilitate the precipitation of greenish malachite through evaporation in the dry season. Both malachite and efflorescent salts were only observable during the dry season through evaporation suggesting that precipitation is one potential mechanism taking place in the effluents.

2. The physical characteristic of sludge effluents in the high density (>2μm) particle sizes and as a result, low turbidity in effluents. This condition therefore suggest that sludge effluents are mainly comprised of high-density sludges (HDS). The HDS indicates that lime treatment and neutralization is effective. Factors influencing the HDS process is the result of the formation of a precipitate of calcium sulfate (gypsum) and a co-precipitate (metal hydroxide) with iron on the surfaces of recycled sludge particles (SGS, 2013)

3. The presence of mud cracks is a better indication of the presence of clay minerals in sludge. Clay minerals are important in the study of natural environments because of their potential to host heavy metals.

Overall, chapter 3 concentrated on providing the physical background framework of the effluents. The geochemical characteristics including the metal partitioning in sludge is however provided in the next chapter 4.

Chapter 4: Geochemical characteristics, metal partitioning in effluents and sludge solid deposits

4.1 Overview

The geochemical characterization and metal partitioning within contaminated area has widely been recognized as a strong tool to identify the influence of anthropogenic related activities upon which heavy metals distribution in natural materials and systems takes place (Salomons and Fösrtner 1984). So far, factors such as the physio-chemical and geochemical characteristics that control the mobility of metals in the drainage effluents and solid deposits have been revealed by Shuman (1991) and geochemical processes by O'Connor, 1988, McBride, 1989 and Evans (1989). However, mechanisms (specific) processes controlling the mobilities with the solid materials at solid-liquid interface are not always evident and that the above factors have not fully considered the mechanisms at solid-liquid interface (Zhang et al., 2014). Previous studies by Shuman (1991); McLean and Bledsoe, (1992) have indicated that metal concentrations at the solid-liquid interface are mostly associated with the solid material particles such as clay minerals and metal oxides than in the dissolved phase. Clay minerals and metal oxides can coexist as heterogeneous mineral assemblages whose relative abundance depends on pH, redox conditions, hydrological regime and the depositional environment (Windom et al., 1991; Stumm and Morgan, 1996). Clay minerals and hydrous ferric oxides (HFO) are abundant in nature and tend to reduce the concentrations of metals in natural systems by both precipitation and specific adsorption reactions (Zimdahl and Skogerboe, 1977; Kinniburgh and Jackson, 1981; Stumm and Morgan, 1995). For instance:

1. Clay minerals are thought to adsorb metal ions through both ion exchange and specific adsorption (Schindler et al., 1987; Stumm and Morgan, 1995). According to these authors, the process of metal adsorption occurs at hydroxyl ions or to sites created by proton removal. The

metals may be bound to the surface hydroxyl groups along edges of solid particles as well as being directly bound to the clay surface. And where clay minerals are dominant, a large proportion of the adsorption capacity is partitioned at both exchange sites (Kinniburgh and Jackson, 1981) and pH-dependent sites (Dzombak and Morel, 1990). In natural systems, and in most cases, clay minerals may not exist individually, instead they might be coated by hydrous ferric oxides (HFO) as free gels and crystals (Kinniburgh and Jackson, 1981).

2. HFO are the dominant solid particles controlling metal mobility in natural environments. Sources of HFO are variable ranging mostly from the weathering of various mineral species and precipitation (Jenne, 1968, 1998; Lee, 1975). There have been numerous studies which point to the potential significance of HFO in influencing chemical contaminants in the environment. Jenne (1968) proposed that HFOs are the principal control mechanisms of heavy metals in soils and freshwater sediments. The author stated that their common occurrence is in the form of surface coatings which allows them to exert a chemical activity far in excess of their total concentrations. Furthermore, their adsorption or desorption is a function of such factors as increased metal ion concentration, the concentrations of other heavy metals, pH, and the amount and types of complex in solution. Due to high affinity surfaces of HFO, their partitioning determines the metal behaviours in the environment. It is evident from the above discussion that while there is no doubt that clay minerals and HFOs are important sinks and modes of transport for heavy metals in the environment, the quantitative magnitude of this role is not known for a variety of natural materials such as sludges. Thus, a much better understanding of the interactions between heavy metals and the solid materials (i.e., sludges) from wastewater treatment must be addressed to provide insight onto the treatment and metal stability conditions.

This chapter addresses the hydrogeochemical and geochemical characteristics of effluents and sludge solid deposits at solid-liquid interface through laboratory experimental methods.

4.2 Materials and methods

4.2.1 Water sample

The acidified water samples were analysed for the major and minor cations using the standard stock solution, Certipur® ICP multi-element, part No. 1.11355.0100 (for Ag, Al, B, Bi, Ca, Cd, Co, Cr, Cu, Fe, Ga, In, Li, Mg, Mn, Ni, Pb, Sr, Tl and Zn) at stock solution concentrations of 1000 mg/l from Merck-chemicals of Germany. Stock solution was diluted to 10 mg/l for the purpose of the standard calibration curve. Water samples were measured between 10 – 1000 dilutions, filled in the 10 ml plastic autosampler test tubes and analysed using inductively coupled plasma-atomic emission spectroscopy (ICP-AES; ICPE-9000, Shimadzu). The non-acidified water samples were analysed for major anions using ion chromatography (IC; IC861, Metrohm) with standard solution (FUJIFILM Kanto analytical grade). The measured major anions are chloride (Cl^-) and sulphate (SO_4^{2-}) at stock solution concentrations of 20 mg/l and 100 mg/l respectively. Bicarbonate (HCO_3^-) ion concentration was estimated from the alkalinity measurement data using the Gran function plot method suggested by Rounds (2015). Limit of detection (LOD) was calculated by average and standard deviations from 5 blank water (18 MΩ) samples acidified with 1% ultrapure HNO_3. In the calculation of the LOD, the 3 s/b equation was taken into consideration, where s is the standard deviation of absorbance of the blank samples and b is the slope of the calibration curve for each element. The correlation coefficients (r) of the calibration curves were greater than 0.998 for all elements studied. The LOD values for cations varied from 0.01 – 0.09 mg/l and for anions from 0.01- 0.5 mg/l.

4.2.2 Sludge solids

Sludge solids were air-dried at room temperature, homogenised and sieved to bulk (i.e., < 53μm) particle sizes. To obtain the clay (i.e., < 2μm) particle size, a series of continuous shaking and centrifugation in polyethylene bottles with deionized water were conducted following procedures outlined by Arroyo et al. (2005). This process involved adding bulk solid materials (i.e., sludge) in 100 ml plastic bottle filled with deionized water and mixed with an end-to-end shaker for 24 hours, and after which placed in the ultrasonic diffuser. Ultrasonic diffuser uses ultrasonic vibrations to aggregate fine and coarse samples with polar solvents in an ultrasonic bath, and then subjected to low-speed centrifugation as before to recover additional clay-sized particles. The supernatant suspension was siphoned and added to the previously collected suspension of clay-sized materials. The >2μm particles (sediment) were quick frozen and freeze dried.

Samples for X-ray diffraction (XRD) analyses were manually prepared through grinding of the < 2μm sizes using mortar and pestle (the so called "grinding bowl"). The sample is initially mounted on the sample holder and its surface pressed (flattened) with a glass plate. The prepared sample was analysed by XRD; RINT 1200, Rigaku equipped with CuKα at fixed working conditions of 30kV and 20mA and 2Θ-scanning rate of 0.02º/min. Quantitative estimation of mineral composition from XRD patterns was achieved by PANalytical X'pert HighScore Plus software (Malvern Panalytical, UK). Scanning electron microscopes (SEM) equipped with an energy dispersive X-ray spectrometry (JSM-6500F; JSM-IT200, JEOL) were used to analyse the morphology and chemical compositions of solids. SEM sample preparations involved adding sample particle on a carbon tape attached to aluminum specimen tub, coated with graphite and analysed at 15 - 20 keV conditions. Optical microscope (Olympus, U-LH100) was used to analyse both thin and polished sections of solid phase samples. A transmission electron microscope (TEM-

JEM-2010, JEOL) was used to observe the surface morphology and check the chemical composition of the mineral particles in the sludges. White precipitates were dissolved in deionised water, pH measured, filtered with 0.2µm membranes and split into acidified and non-acidified samples prior to ICP-AES and IC analyses. Cation exchange capacity (CEC) measurements were performed using protocols described in section 2.1.3 of Chapter 2.

4.2.3 Whole rock geochemistry

Solid samples were dried at room temperature and pulverized using a Multi-Beads Shocker (PV1001(S), Yasui Kikai) and sieved through a < 53 µm stainless steel sieve. A sample weight of 2g was placed in the individual weighed crucibles and total weight measured (i.e., weight of crucible + sample) prior to sample heating at 1000^{o}C for 24hrs. After heating, LOI was measured using equation described in section 2.1.4 of chapter 2. The heated samples were analysed for bulk chemical compositions using glass-bead X-ray fluorescence (XRF; MagiX PRO, Spectris) spectrometer following the protocols outlined. A solid sample of 0.4000 g was weighed. Then, a flux equal to 10 times the sample was weighed with precisely three decimal digits, e.g., 4.007 g. The 2 samples were thoroughly mixed with a spatula. Alternatively, sample and flux powder can also be transferred to an agate mortar and mixed thoroughly. The mixed powder is transferred into a platinum (95%) and gold (5%) alloy crucible. Before melting with the TK-4100, little or small grains of releasing agent, a lithium bromide (LiBr) was added equivalent to 3.74 wt.% in the sample. The crucible was placed in the fusion unit of the TK4100 and covered with a platinum lid (Pt-Au alloy). The heating parameters of the TK4100 was controlled in three steps. Although the temperature of each step can be set separately, the temperature settings of the present protocol are fixed to 1150 ºC for all steps. The duration of the initial heating stage is 120 seconds and that of the main fusion stage is 180 seconds. This is followed by 180 seconds of fusion with agitation to

make the melt homogeneous without any bubbles. After the third step, an initial cooling cycle of approximately 20 seconds is started. The crucible is then transferred from the heating unit to the quenching station until complete cooling, which requires approximately 3 minutes on the quenching station. After the transferring the crucible from the heating unit to the quenching station, the next sample can be placed in the heating unit for fusion. Thus, the total cycle time, excluding the quenching phase, is approximately 8.5 minutes. The parameters were selected so as to maximize the efficiency of sample preparation and the complete digestion of typical geological samples. The glass beads can be kept in a plastic bag with a seal and are stored in a desiccator until measurement (Ogasawara et al., 2018).

4.2.4 Sequential extraction

The study adopted the modified eight (8) operationally defined procedures and protocols suggested by Horowitz (1985); Filgueiras et al. (2002) shown in Table 1. The protocol defines clearly (i) the exchangeable and acid-soluble fractions and (ii) the three (3) leaching stages (i.e. easily, moderately and strongly) of the reducible fraction. Trace metals partitioned in the exchangeable fraction are associated with clay minerals (Stumm and Morgan, 1995), in acid-soluble fraction with carbonates (Tessier et al., 1979) and in reducible fraction with HFO (Tessier et al., 1979; Rauret et al., 1999), thus the behaviours of the metals with the host mineral in each fraction can easily be studied. The choice of the leaching reagent was based on the reagent chemical properties and leaching efficacy as recommended by the cited literature. For example, in step 1 and 2 (Table 1), ammonium acetate (NH_4OAc) inhibits the possible precipitation of metals after leaching (Hass and Fine, 2010; Leermakers et al., 2019) especially that the studied sludge samples contained some considerable number of metals that might easily precipitate with other anionic complexes in solution. Acidified hydroxylammonium chloride ($NH_2OH{\cdot}HCl$) is effective in dissolving the easily

or weakly adsorbed metals associated with amorphous Fe oxides (Qin et al., 2020). Similarly, $NH_2OH{\cdot}HCl$ cannot liberate metals that are moderately bound to Fe oxides (Hass and Fine, 2010). Instead, acidified ammonium oxalate ($NH_4Ox.HOx$) liberates metals moderately adsorbed or incorporated with Fe oxides (Chao and Zhou (1983). Therefore, the 3 leaching stages involving $NH_2OH{\cdot}HCl$ and $NH_4Ox.HOx$ of the reducible fraction provides a better understanding of metal partitioning in reducible fraction.

Table 7: Sequential extraction protocols (Modified after Horowitz (1985) and Filgueiras et al. (2002)

	1g of sludge sample	
Fraction	Procedure and Conditions	Reference
Exchangeable (1)	1M ammonium acetate (NH_4OAc; Wako Pure Chemicals) at pH = 7, shake at room temperature and pressure (RTP) in darkness for 10hours at 200rpm	1
Acid soluble (2)	1M NH_4OAc/acetic acid (HOAc) at pH = 5, shake at RTP in darkness for 10hours	2
Weakly reducible (3)	0.25M Hydroxylamine hydrochloride (NH_4OHCl) + 0.25M hydrochloric acid (HCl) at pH = 2.5, water bath heating at 80^oC for 2hrs and shaking for 2hours at 25^oC	3
Moderate reducible (4)	0.1M ammonium oxalate (NH_4Ox; Wako Pure Chemicals) + 0.1M oxalic acid (HOx) at pH 3, water bath heating at 80^oC for 2hrs and shaking for 2hours at 25^oC	3
Strongly (Crystalline) reducible (5)	1M Sodium dithionite ($Na_2S_2O_4$; Wako Pure Chemicals) + Trisodium citrate ($Na_3C_6H_5O_7$; Wako Pure Chemicals) +sodium bicarbonate ($NaHCO_3$; Wako Pure Chemicals) shake overnight at RTP	4
Organic Matter (6)	35% hydrogen peroxide (H_2O_2) water bath heating for 1hr	5
Sulphide (7)	7mg Potassium chlorate ($KClO_3$; Wako Pure Chemical) + HCl + HNO_3, water bath heating for 1hr	1
Residual (8)	Microwave digestion (Ethos Advance microwave Lab station, milestone Inc, Sorisole, Italy) in Teflon beakers at 200oC for 55 min, HNO_3 + HCl + Perchloric acid ($HClO_4$) at (6:3:1) acid ratios	3

4.2.5 Metal speciation and solubility calculation

Speciation-solubility models are used to define the distribution of stable species in the system and to determine the saturation states of minerals (Zhu and Anderson, 2002). Most models assume local equilibria in order to solve the equations involved in determining the species spectrum. This assumption is often valid as the reactions which affect the bulk chemistry of natural water bodies occur relatively fast with reference to the time scale of interest (van der Lee and De Windt, 2001). Chemical equilibrium can be solved in two ways, either by minimising the Gibbs' free energy of

a system or by using mass action equations combined with equilibrium constants. The second method is used by the majority of programming software because of a lack of consistent Gibbs' free energy data (Crawford, 1999). Geochemist's Workbench® (GWB ver.14, Bethke, 2008) with the Lawrence Livermore National Laboratory database (thermo.tdat) and ACT2 module was used to obtain metal solubility diagrams using laboratory measurement analyses of water chemistry data for checking the saturation state of secondary precipitates.

4.3 Results and discussion

4.3.1 Chemistry of effluents

Trends in the hydrogeochemical characteristics of the drainage effluents are given in Fig. 4.1 and Table 8. Generally, the overall pH (Fig. 4.1) ranges from acidic (pH 4.66) to neutral (pH 7.50) conditions. In background water (S0), pH was consistently neutral, and at S1, low pH values were often recorded. For instance, at S1, the low pH values recorded in 2018W (pH 4.66) and 2018D (pH 5.14) were probably caused by acidic effluents emanating from the metal processing concentrator (Fig. 3.3b) during the ore beneficiation process. Reasons for the neutral pH recorded in 2019D (pH 7.09) are unclear, though this may be due to either the absence of low pH effluent or lime treatment at the time of sampling. The observed variations in the pH values at S1 suggest that there is a high potential for metal remobilisation along the drainage as evidenced by the decrease in pH at S2 in 2018W (pH 5.49). The increasing trends in EC values towards the downstream (Fig. 4.1b) are positively correlated with the increase in dissolved major ions concentrations such as calcium (Ca^{2+}), HCO_3^- and SO_4^{2-} (Fig. 4.1c, d, e). The increase in Ca^{2+} and HCO_3^- concentrations is a presumably good indication for the activity of continuous dissolution of lime. The SO_4^{2-} ion concentrations also showed increasing trends towards the downstream flow path (Fig. 4.1c), suggesting the possibilities of other drainage effluent inputs, especially between

S3 – S5. The dissolved concentrations of trace elements (i.e. Cu^{2+} and Co^{2+}) were high at S1 (Fig. 4.1f, g) owing to the prevailing acidic condition. Cu has had the highest concentration of 70 mg/l which is above the maximum contamination levels (MCL) of 1.3 mg/l recommended by the environmental protection agency (EPA, 2017). The highest Co concentration was 6.75 mg/l, 10 times lower than Cu but above the standard guideline of 5 – 50 μg/l recommended by the world health organization (WHO, 2006). The highest dissolved iron (Fe) (probably Fe^{2+}) concentration measured at S1 (i.e., 15 mg/l) (Fig. 4.1 h) is much lower compared to areas affected by Fe-sulphide oxidations (Sanchez Espana, 2008) indicating that ordinary acid mine drainage (AMD) conditions are not the ultimate source of Fe in sludge effluents. Although other contaminant sources are expected between S3 - S5 from external drainage sources according to SO_4^{2-}concentration, the dissolved metals kept their decreasing concentrations, probably due to the lime neutralisation of the effluents. Therefore, the decrease in the dissolved metal concentrations from S2 – S6 shows that lime treatment is effective, though the geochemical processes responsible for decreasing trends and keeping low concentrations still needed to be addressed.

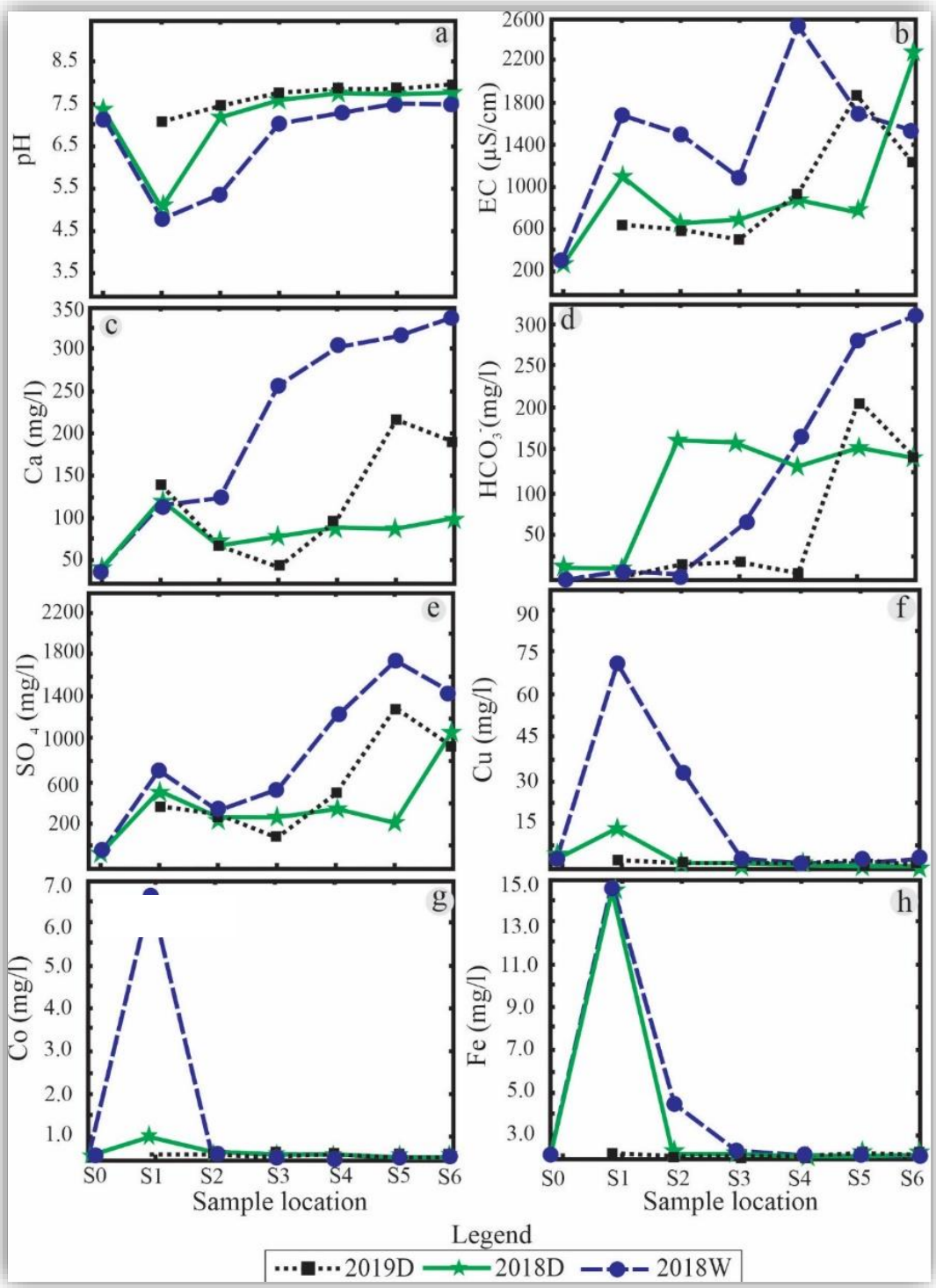

Figure 4. 1. Hydrogeochemical data of sludge effluents; (a) pH; (b) EC; (c) Ca^{2+}; (d) HCO_3^-; (e) SO_4^{2-} (f) Cu^{2+}; (g) Co^{2+}; (h) Fe^{2+}. Abbreviations: 2018D, 2019D, 2018W are sampling dates (i.e., in Years) and seasons (W-wet season) and (D-dry season). S1 – S6 are drainage sample location (refer to Fig. 1b).

In lime treatment systems, the reaction of lime with the atmospheric conditions (i.e., atmospheric carbon dioxide) is reported to promote the precipitation of carbonate minerals (Shin-Min Shih et al., 1999). To check the possibility of metal precipitation by carbonates at the studied site, metal solubility diagrams were constructed through geochemical modeling and results are as shown in Fig. 4.2. In Fig. 4.2a, Cu showed undersaturation to near saturation with respect to malachite whereas Co metal (Fig. 4.2b) showed under-saturation with respect to Co carbonate complex. Both metals exhibited the lowest metal solubility characteristics and based on the thermodynamic modeling results, the removal of metals in effluents may not be expected by the metal carbonate precipitation process. Instead, the major solute compositions of effluents are consistent with several processes occurring within the drainages including the dissolution of lime and possible weathering of the component minerals.

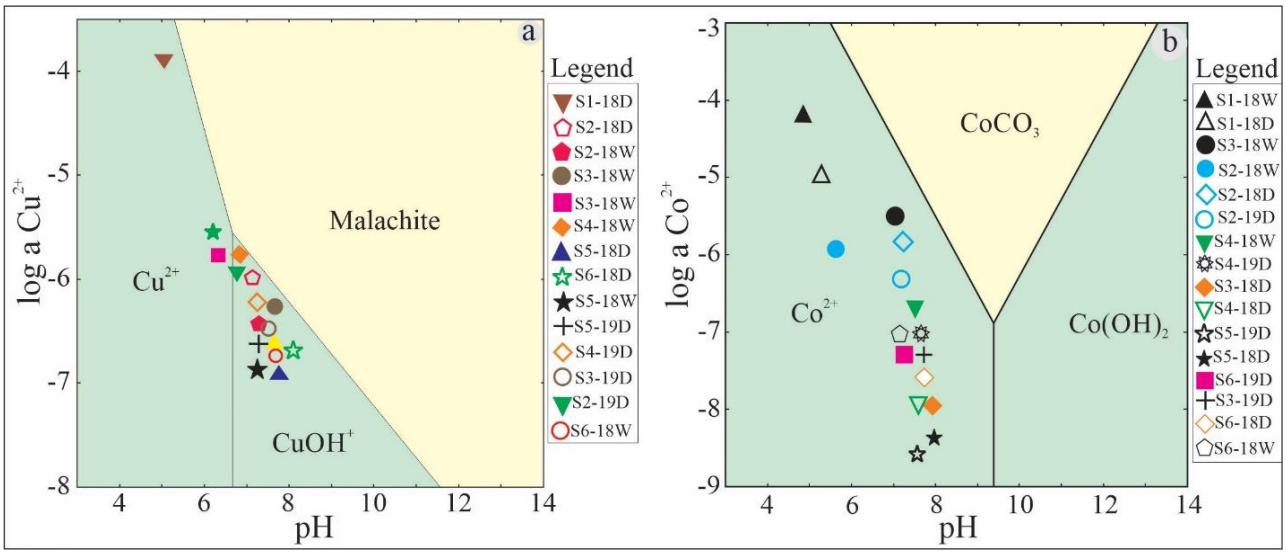

Figure 4. 2. Metals solubility diagrams plotted as a function of pH at 25ºC of: (a) Cu and (b) Co. Abbreviation of symbols; S1 – S6 are sampled location (refer to Fig. 1b); 18W, D and 19D are sampling dates (i.e., in Years) and seasons (e.g., - wet season) and (e.g., D-dry season).

Table 8: Chemical characteristics of sludge effluents

Sample	Background water (S0)		Mine Drainage (S1)			Stream drainage (S2 to S6)														
Sample Date	2018W	2018D	2018W	2018D	2019D	2018W	2018D	2019D	2018W	2018D	2019D	2018W	2018D	2019D	2018W	2018D	2019D	2018W	2018D	2019D
Sample	S0	S0	S1	S1	S1	S2	S2	S2	S3	S3	S3	S4	S4	S4	S5	S5	S5	S6	S6	S6
pH	7.38	7.42	4.66	5.14	7.09	5.49	7.31	7.51	6.88	7.69	7.62	7.18	7.82	7.65	7.32	7.9	7.66	7.5	7.77	7.67
Temp. (°C)	25.4	26.1	23.8	26.5	26.3	26	26.1	26	25.1	26.4	26.2	26.7	25.8	26.3	26.4	26.8	26	26.1	26.5	26.2
EC (µs/cm)	276	215	1650	1189	624	1497	640	651	1141	663	492	2510	860	962	1680	700	1889	1590	2240	1290
Eh (mV)	420	425	490	479	475	491	372	443	413	433	420	408	438	424	426	435	430	428	442	461
Major Cation																				
mg/l																				
Ca	35.07 (0.2)	39.62 (0.6)	113 (0.6)	122 (0.1)	140 (0.5)	113 (0.2)	62.12 (0.2)	65.92 (0.2)	252(3)	66.56 (0.3)	39.62 (0.6)	296 (0.8)	74.33 (0.6)	109 (0.9)	317 (0.8)	69.88 (0.4)	210 (0.9)	336 (0.9)	107 (0.3)	193 (0.7)
Mg	28.23 (0.1)	18.97 (0.3)	115 (0.4)	95.67 (0.4)	69.07 (1)	120 (1.5)	31.96 (0.3)	35.81 (0.1)	98.09 (0.2)	32.71 (0.2)	18.97 (0.7)	91.38 (0.9)	40.06 (0.4)	42.47 (0.3)	104 (0.9)	34.14 (0.3)	59.07 (0.2)	100 (0.7)	44.81 (0.7)	51.3 (0.6)
Na	15.13 (0.3)	10 (0.3)	18.18 (0.2)	0.55 (0.1)	bdl	11.04 (0.4)	0.6 (0.1)	bdl	5.34 (0.2)	0.6 (0.1)	bdl	4.5 (0.6)	0.51 (0.2)	bdl	5.34 (1)	bdl	bdl	18.04 (2)	bdl	0.6 (0.1)
K	32.11 (0.2)	29.64 (0.7)	50.66 (0.3)	29 (0.1)	29.60 (0.2)	21.37 (0.3)	28.92 (0.2)	28.95 (0.2)	33.51 (0.1)	28.89 (0.2)	29.64 (0.2)	25.2 (0.5)	29 (0.4)	29.58 (0.5)	27.39 (0.2)	29.08 (0.5)	29.6 (0.4)	41.7 (0.2)	22.94 (0.3)	42.56 (0.2)
Major Anions																				
mg/l																				
SO_4^{2-}	94 (3.4)	80 (6.2)	737 (15)	523 (21)	370 (34)	426 (22)	262 (45)	300 (12)	523 (21)	208 (32)	150 (11)	1356 (18)	284 (20)	468 (22)	1692 (33)	209 (10)	1370 (12)	1413 (22)	1083 (23)	812 (12)
HCO_3^-	5.1	19	13.3	13.2	9	12.5	160	16.8	61.6	159	19	161	135	12.9	282	159	209	303	135	135
Cl^-	20.22 (0.3)	20.18 (0.2)	16.7 (0.11)	14.29 (0.3)	9.5 (0.8)	18.25 (0.4)	16.53 (0.1)	10.38 (0.2)	31.73 (0.3)	15.85 (0.1)	20.18 (0.6)	20.54 (0.4)	15.02 (0.1)	14.41 (0.2)	20.28 (0.3)	15.91 (0.7)	9.58 (0.1)	17.09 (0.2)	10.93 (3)	11.09 (0.1)
Minor Cations																				
mg/l																				
Cu	1.57 (0.03)	0.18 (0.01)	70.21 (0.3)	14.52 (0.03)	0.61 (0.07)	38.4 (0.8)	0.4 (0.02)	0.75 (0.03)	3.59 (0.03)	0.15 (0.05)	0.18 (0.04)	1.74 (0.03)	0.18 (0.01)	0.38 (0.01)	0.08 (0.01)	0.17 (0.01)	0.19 (0.01)	2.73 (0.05)	0.58 (0.02)	0.16 (0.01)
Co	bdl	0.05 (0.01)	6.75 (1)	0.95 (0.05)	0.19 (0.03)	0.11 (0.02)	0.22 (0.06)	0.25 (0.05)	0.35 (0.03)	0.06 (0.01)	0.05 (0.02)	0.04 (0.02)	0.1 (0.01)	0.17 (0.01)	0.05 (0.01)	0.06 (0.01)	0.01 (0.01)	0.1 (0.01)	0.13 (0.01)	0.12 (0.1)
Fe	bdl	bdl	15.02 (1)	15.38 (2)	bdl	4.62 (0.1)	0.05 (0.01)	bdl	bdl	bdl	bdl	bdl	bdl	bdl	bdl	bdl	bdl	bdl	bdl	bdl

bdl- below detection limit

4.3.2 Whole rock geochemistry

Results of whole rock geochemistry are shown in Table 9. According to the results, the following range of mineral abundance is revealed: Q (63 - 72%), Al (11 – 18%) and K (5 – 8%) suggesting that aluminosilicate and phyllosilicate minerals are relatively dominant. The common aluminosilicates such as feldspar was found to be mostly orthoclase and microcline ($KAlSi_3O_8$) and minor plagioclase ($(Ca,Na)AlSi_3O_8$). The dominance of ($KAlSi_3O_8$) indicates that the weathering of silica-rich igneous rocks such as granites are the major protoliths and that the weathering of aluminosilicate minerals rich in feldspar commonly usually form kaolinite. Ions such as Na, K, Ca, Mg, and Fe are a bye-product of the weathering or alteration process of the aluminosilicates and phyllosilicate minerals.

The Fe concentration in the form of Fe_2O_3 ranges between 3 – 6% which is lower than the iron-rich rocks that are generally reported to be greater than 10 -15% or more such as goethite and hematite and pyrite (Blowes et al., 2003). This low Fe concentrations suggests that weathering of either phyllosilicates (i.e., micas; biotite) or sedimentary Fe- containing sediments are the likely sources of Fe in both sludges and sediments (Everett et al., 2019). Calcium concentrations expressed as calcium oxide (CaO) range between 0.1 – 5%. This low value strongly reflects the absence in the underlying carbonate rich bedrock or the low to absence in the distribution of Ca-bearing minerals. The low CaO content is also a valid evidence of sedimentary rock such as mudstones, siltstones and sandstones. Locally elevated CaO concentrations (i.e., 4.1%) (Table 9) may reflect the anthropogenic activities, particularly the practice of lime addition to drainage effluents during wastewater treatment (Everett et al., 2019). The magnesium (Mg) content measured in the form of magnesium oxide (% MgO) ranges between 3 – 7% in composition. No dolomitic rocks were envisaged in the underlying bedrock or in the vicinity of the sample locations.

Therefore, the possible sources of Mg are the weathering of ferromagnesium minerals and Mg-rich micas. Additionally, the Mg concentrations spikes were observed in effluents associated with low pH conditions such as at sample point S1 (Table 8) suggesting that dissolution and weathering of Mg-rich metasedimentary rock are among the major sources. The organic matter concentrations measured through LOI in the sediments are of considerably low values (< 10%) indicating that the effects of organic matter are relatively low.

The Cu and Co concentrations in sludge as measured by XRF is as shown in (Table 9). The high Cu concentration at S1 (i.e., 7100ppm) and S2 (i.e., >12265ppm) and of Co; (i.e., 397.6ppm) and (i.e., 401.5ppm) are associated with the pH and proximity to the sources of the metals (i.e. concentrator). The high metal concentrations in solid materials reflects that anthropogenic activities associated with the mining operations.

Table 9: Whole rock geochemistry of sludge

Sample #	**(%)**	**SiO_2**	**TiO_2**	**Al_2O_3**	**Fe_2O_3**	**MnO**	**MgO**	**CaO**	**Na_2O**	**K_2O**	**P_2O_5**	**LOI**	**Co**	**Cu**
		Si	Ti	Al	Fe	Mn	Mg	Ca	Na	K	P		Co	Cu
		(%)	(%)	(%)	(%)	(%)	(%)	(%)	(%)	(%)	(%)	%	(ppm)	(ppm)
S0	93.40	71.89	0.74	18.00	1.48	0.01	0.14	0.05	0.24	0.78	0.04	9.56	13.89	142.46
S1	102.10	66.98	1.55	12.61	5.13	0.13	6.77	1.76	0.34	5.85	0.18	5.13	397.65	7103.13
S2	101.95	64.12	1.31	12.07	6.10	0.15	6.67	4.07	0.05	5.86	0.27	4.65	401.48	12265.92
S3	95.24	63.34	1.87	11.42	5.70	0.10	4.82	1.34	0.47	5.27	0.20	5.63	270.33	6502.69
S4	96.40	68.44	1.28	11.03	3.88	0.07	3.37	1.61	0.21	5.84	0.15	3.24	188.06	4828.47
S5	98.13	67.40	1.02	13.10	3.88	0.08	4.09	1.26	0.21	6.38	0.13	4.03	234.26	5529.69
S6	99.50	63.24	0.95	16.94	4.66	0.13	4.24	0.95	0.21	7.25	0.23	6.12	284.68	6464.22

4.3.3 Mineralogical composition of sludge solids

The XRD patterns of sludge are shown in Fig. 4.4. From the XRD patterns, it is clear that no significant variations in mineral compositions exists between different sampling dates (i.e., S3-2018D; S3-2018W) suggesting that the supply sources may be uniform (i.e., weathered feldspathic granites). The dominant mineral components are micas (i.e., biotite and muscovite), kaolinite, quartz and k-feldspar. Mineral quantification by XRD shows that mica constitutes about 40 -70% of the total mineral composition in sludge. The presence of micas is an important indicator of the presence of metamorphic assemblages and their accompanying mineral weathering conditions (Fanning et al., 1989).

The second most common mineral as revealed by XRD is kaolinites. The mud cracks (Fig. 3.6d) are therefore a product of the presence of kaolinite associated with the tropical climates and with high rainfall conditions due to weathering of primary minerals such as aluminosilicates and phyllosilicates (White and Dixon, 2002). Quantification by XRD shows that its abundant ranges between 25 – 40% (Fig. 4.4). It is not clear the type of kaolinite is present in sludge, however because the source is the highly weathered soils and sediments, the disordered type of kaolinite seems likely (Hughes and Brown, 1979). Evidence of disordered type of kaolinite are highly disordered XRD patterns (Hughes and Brown, 1979).

Quartz is another common mineral in sludge especially in coarse grained particle sizes (i.e., >53μm). Weathering of granites that are reportedly commonly exposed in the drainage accounts for its dominance. Another potential source is suggested to be by crystallization out of the dissolution products of feldspars (Estoule-Choux et al., 1995).

The amount of feldspar is of lowly quantity in sludge. As indicated in Section 4.2.2, the estimated amount is less 2% of the total mineral composition in sludge and linked to the weathering of a

wide range of component minerals (Hughes and Brown, 1979; White and Dixon, 2002) consistent with the weathering of mineral components around the Zambian Copperbelt (McGowan et al., 2006).

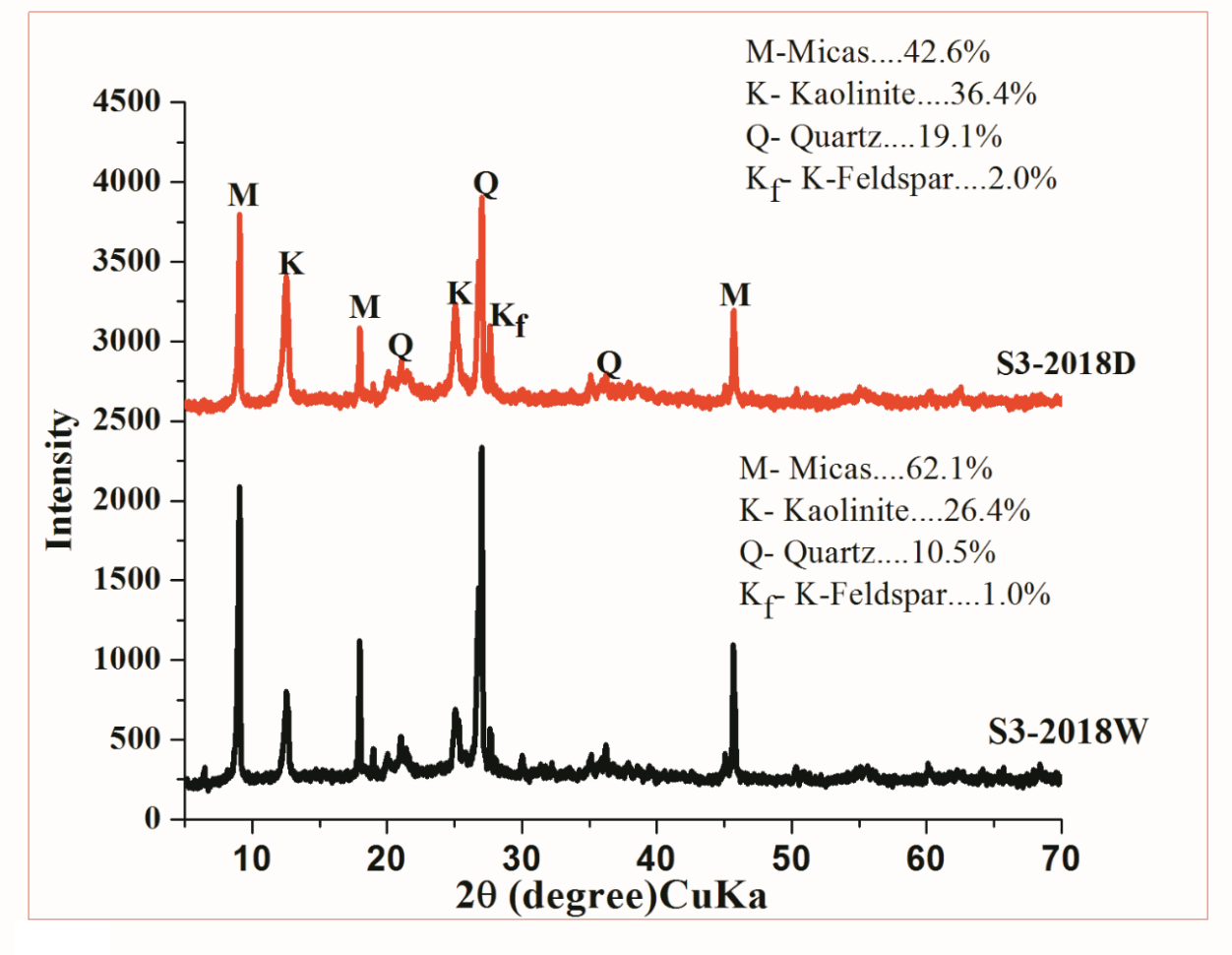

Figure 4. 3. XRD patterns of sludge

4.3.4 Formation of secondary mineral in sludge

The commonly and much susceptible minerals to weathering conditions are biotite and feldspar (Fig. 4.4). Weathering of biotite involves more complex process such as exfoliation process as revealed by Gilkes and Suddhiprakarn (1979) in Fig. 4.5 and evidenced by microscopic analyses (Fig. 4.6).

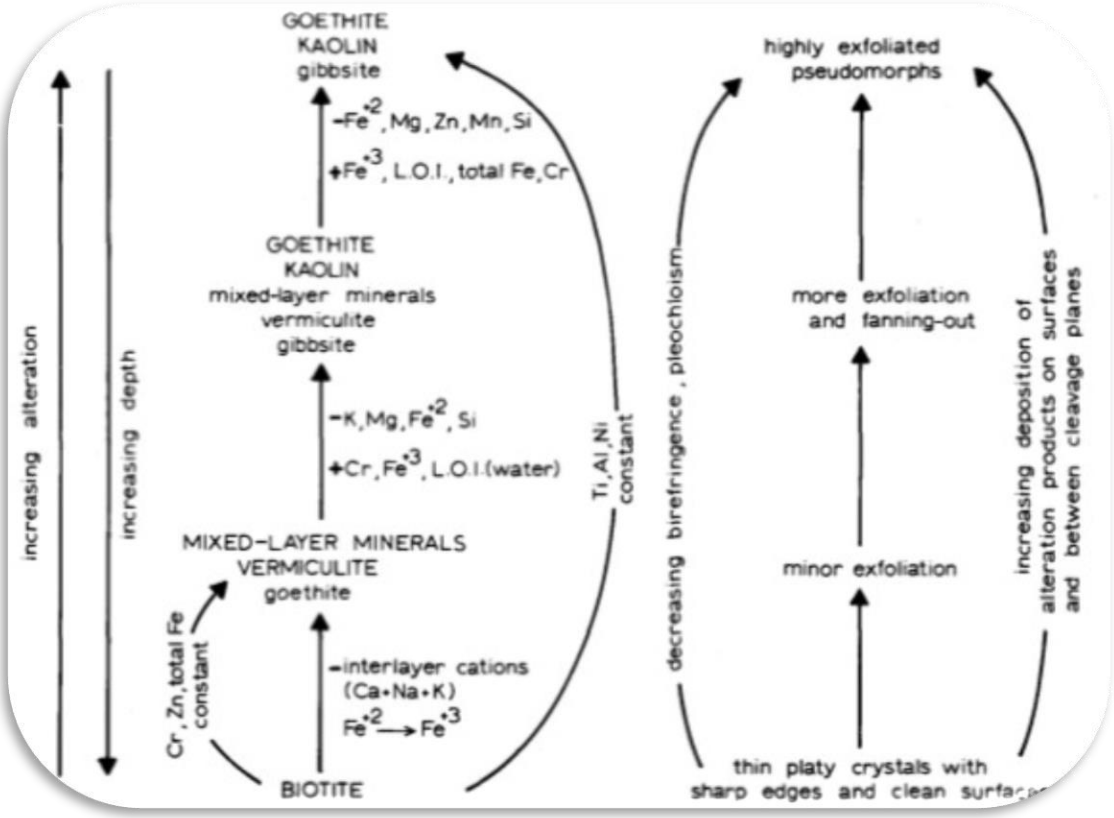

Figure 4. 4. Pathways for biotite alteration deduced from morphological, mineralogical, and chemical studies of specimens from deeply weathered profiles (From Gilkes and Suddhiprakarn, 1979)

Exfoliations were evidenced in SEM analyses in form of (i) the layer weathering and rugged erosion surfaces (Fig. 4.6a) and (ii) the etched pits (Fig. 4.6b). Both these features indicate the tendency of biotite to undergo layered and edge weathering mechanisms consistent with the studies conducted by Ghabru et al. (1987): Wilson (2004). Edge weathering (i.e., etched pits) are reported by Wilson (2004) to cause mineral deformations, easy disintegration and rapid fracturing of minerals along certain crystallographic orientations. Specific to biotite, Davis and Hayes (1986) indicated that such structural deformations tend to cause the release of the octahedral ferrous (Fe^{2+}) ion which oxidises to ferric (Fe^{3+}) ion forming Fe oxides (i.e., HFO). The evidence of Fe^{2+} to Fe^{3+} oxidation is bleaching and opacity of biotite surface grains (Fig. 4.6c) consistent with the earlier findings by Bisdon et al. (1982). With ageing, more discrete forms of HFO are evidenced by SEM (Fig. 4.6d). According to Chakraborty et al. (2011), Fe (III) oxyhydroxides are a potential sink of heavy metals and are expected to control the mobility of metals in oxidising conditions.

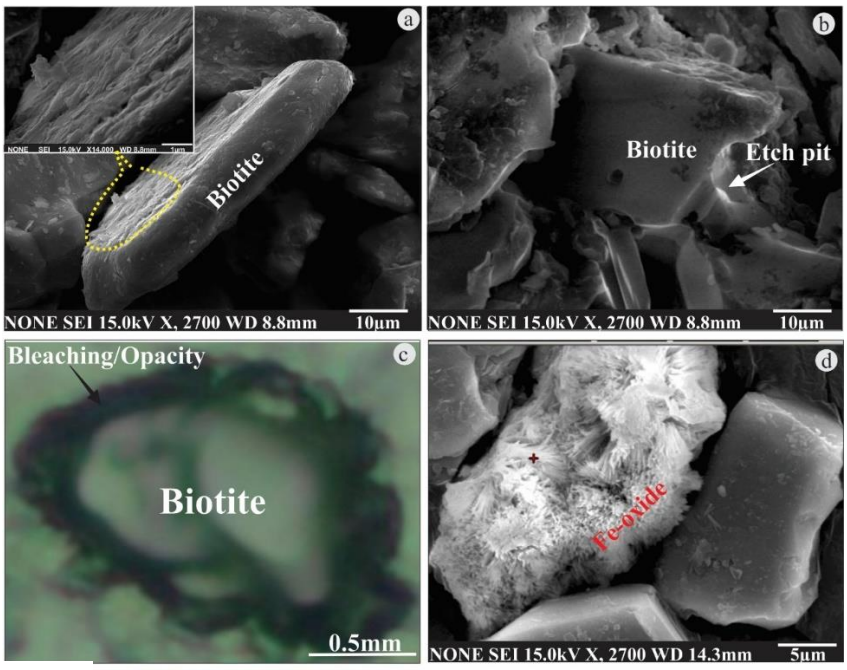

Figure 4. 5. (a) Exfoliation layers formed by the layered weathering of biotite grains, (b) Etched pits formed by edge weathering of biotite grains, (c) Bleaching and opacity of biotite grain surfaces due to coatings with non-crystalline material (i.e., HFO) during and after biotite weathering, (d) HFO precipitate formation from oxidations of Fe^{2+}/Fe^{3+} ions released from biotite weathering. Abbreviations: HFO-hydrous ferric oxide

4.3.5 Grain surface coating

Freshly precipitated HFO has been found to occur as a surface coating on suspended sediments, carrying several adsorbed metals during transport (Singh et al.,1984). In the studied sludge, the existence of HFO coating was indirectly recognized by XRD pattern (Fig.4.7). Before chemical treatment, low peak intensities of micas, kaolinite and quartz were determined. After treatment with NH_4Ox solution, the signal/noise ratio of the peak increased suggesting that the X-ray amorphous materials are removed. The estimated amount of chemically extracted HFO coating is in the ranges of 5 – 10 g/kg (Table 10). The measured amount of HFO is low and consistent with the limited proportion of the released Fe ion from biotite weathering rather than from the known Fe-rich sulphide oxidations common in AMD conditions (Blowes et al., 2003).

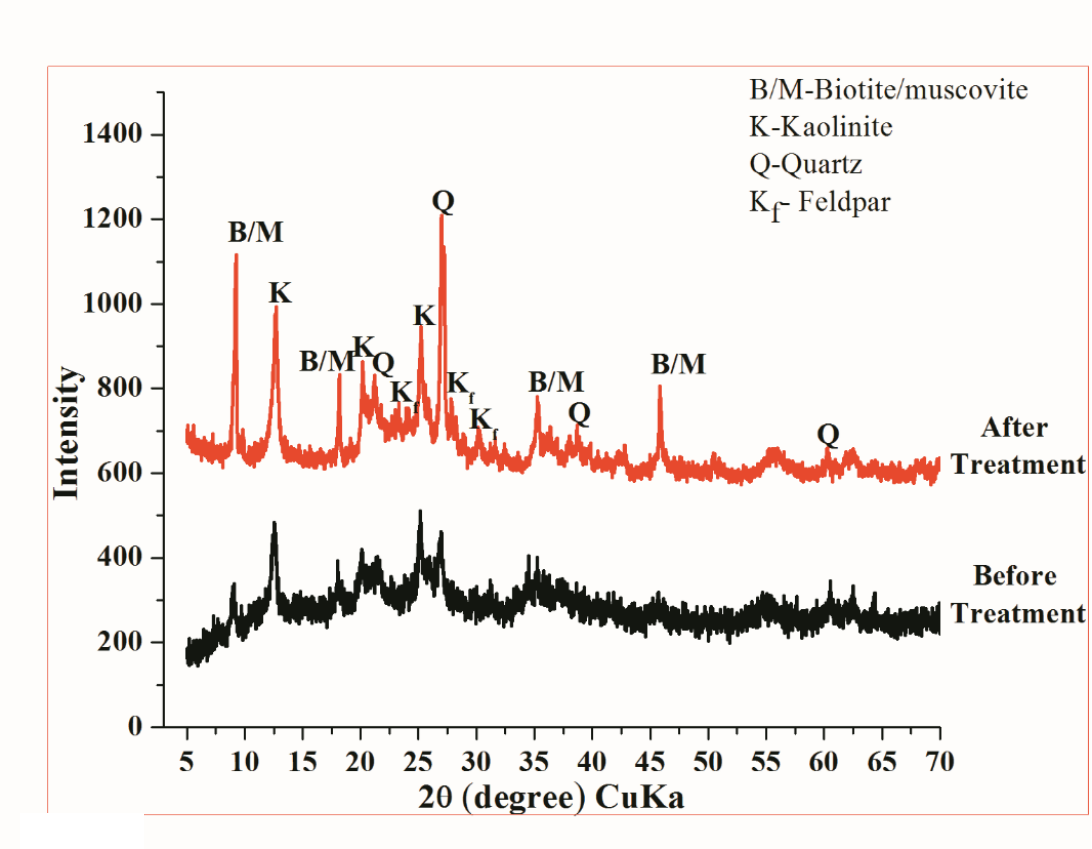

Figure 4. 6. XRD pattern of surface coated sludge before and after treatment. The coating material is HFO precipitate from the weathering of biotite

The interactions of HFO with other component minerals were commonly observed with the kaolinite surface by SEM-EDS (Fig. 4.8a). HFO – kaolinite association has been reported by Carroll (1959); Jenne (1998) to especially modify the metal adsorption behaviour and affinity characteristics of kaolinite surface. Such modification has been studied with models by Lund et al. (2008); Landry et al. (2009) and their results confirm that both minerals display capacities to control heavy metal mobilities. It is, therefore, to be expected that kaolinite – HFO associations in the studied sludge are to a greater extent controlling the retention and transport of the heavy metals. In TEM-EDS analyses (Fig. 4.8b), another type of surface coating resembling "microencapsulation" was observed around a micaceous grain which according to Quispe et al. (2013) is attributed to the rapid precipitation of HFO under neutral to alkaline conditions. Microencapsulation is likened to the formations of hardpans and cemented layers commonly observed in tailings surfaces (Graupner et al., 2007) and widely investigated especially for their potential in minimizing the discharge of metal contaminants (McGregor and Blowes, 2002; Gilbert et al., 2003) either by adsorption or precipitation (Jenne, 1998). The processes (i.e., dissolution of primary mineral phases, transport processes, and precipitation of secondary phases) leading to the formation of hardpans have been reported by Graupner et al. (2007) and appear to parallel the conditions under study. The significance of these layers in environmental studies is that they can temporarily act as a potential sink of metal thereby limiting the metal mobility. In the studied sludge, this condition has the ability to enhance metal-stability conditions, though maybe in a short-term condition due to the observed variations in the low pHs in drainage effluents (Fig. 4.1: Table 8). Under SEM-EDS elemental surface mapping (Fig. 4.8c), HFO coating was observed onto the surface of sand grains. Quartz sands are relatively abundant in sludge and their capacities to adsorb metals are relatively unclear. However, based on these results, the grains are seemingly potential transporting

mediums of heavy through grain surface coating. Quartz surface coating is reportedly similar to iron oxide-coated sands (IOCS) that are currently studied and applied in the pretreatment of wastewater (Hansen et al., 2001).

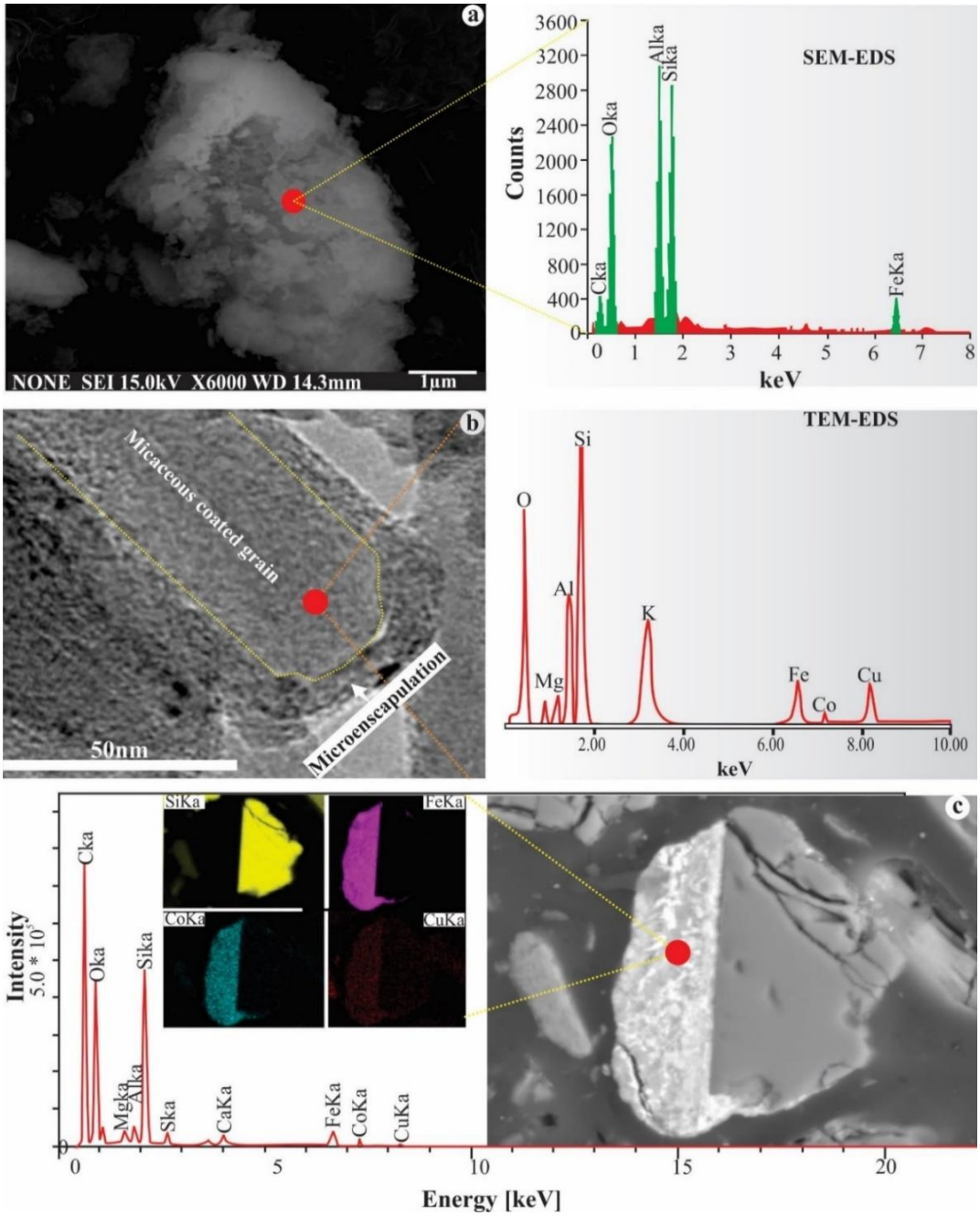

Figure 4. 7. Freshly HFO precipitates adhering and coatings kaolinite surfaces, (b) Layered (cemented) surface coating onto micaceous grains resembling microencapsulation or hardpans (c) SEM elemental mapping of grain surfaces showing HFO coating onto silica/quartz grain and their subsequent adsorbed metals (i.e. Co adsorption onto HFO)

4.3.6 Mineral composition of efflorescent salts precipitates

XRD analyses revealed that salt composition comprised mainly of gypsum ($CaSO_4.2H_2O$) and hexahydrite ($MgSO_4.6H_2O$) (Fig. 4.10). The two (2) salts are linked to the presence of high Ca^{2+}, Mg^{2+} and SO_4^{2-} observed in effluents (Table 8). Ca^{2+} is likely sourced from lime, Mg^{2+} from weathering of component minerals and SO_4^{2-} from sulphuric acid. At the laboratory scale, dissolving the salts in deionized water and analysing their elemental concentrations showed Cu and Co concentrations to be below the detection limit (Table 10). The absence of Cu and Co in the efflorescent salts indicates that the salts are not the potential hosts or sinks of metals in both short-term and long-term conditions. This condition is unique because heavy metals (i.e. Cu, Zn, Mn) are commonly found to undergo isomorphic substitution with AMD salts such melanterite ($FeSO_4 \cdot 7H_2O$) forming alpersite (Cu, Zn, Mn, Mg, Fe) $SO_4 \cdot 7H_2O$ in typical AMD conditions (Nordstrom and Alpers, 1999; Peterson et al., 2006). This observation suggest that some metal retention mechanisms are likely to be taking place in sludge.

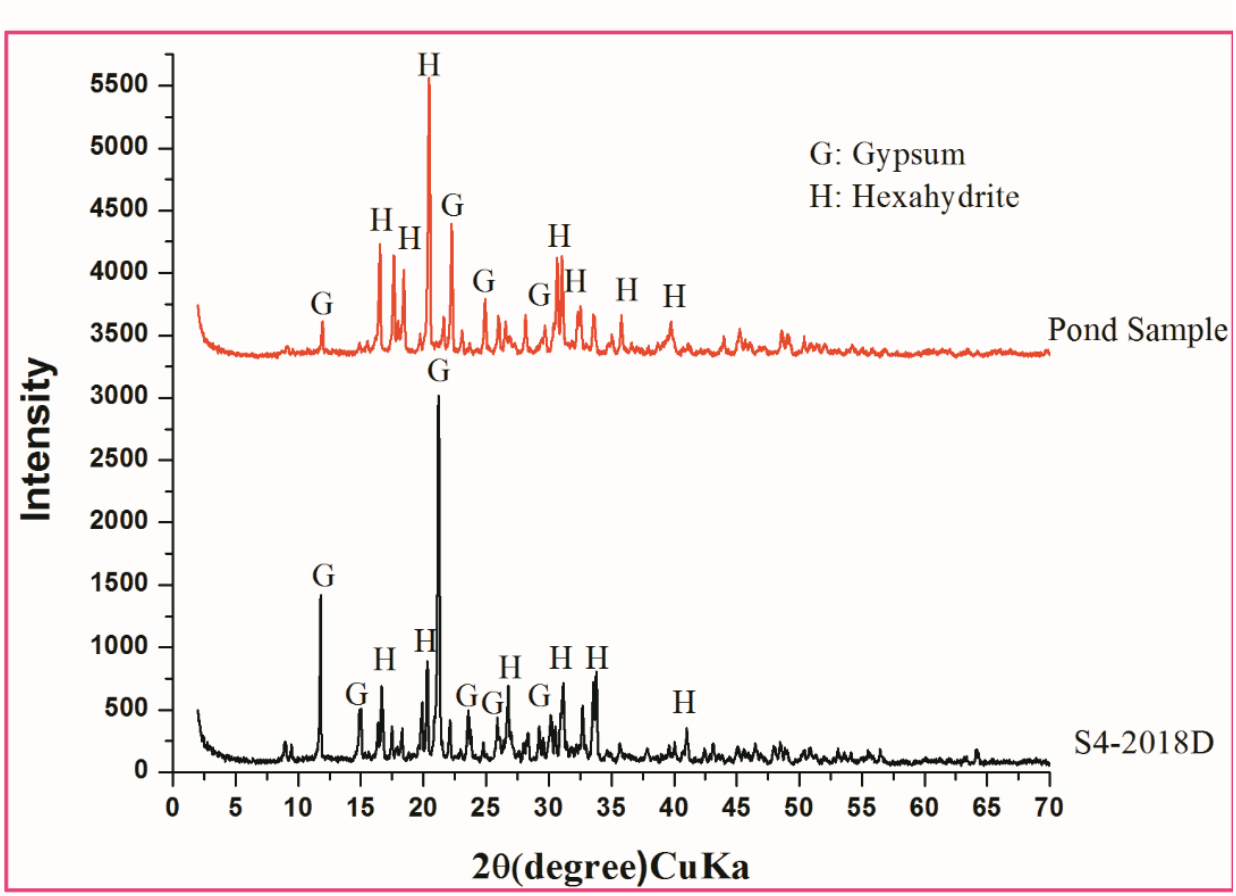

Figure 4. 8. XRD patterns of gypsum and hexahydrite formed during dry season and devoid of metals due to adsorption processes in sludge associated with the host minerals such as HFO and kaolinite which bind the metals making them not easily releasable during salt precipitations

Table 10: Physiochemical characteristics of sludge and effluents

Sludge				
Sample location	S1	S4	S5	S6
Clay (g/kg)	85.43	105.1	115.26	148.34
HFO (g/kg)	10.2	8.32	9.53	4.89
CEC (cmol/kg)	6.7	7.71	15.17	18.88
Efflorescent Salts				
Sample location	S4	S6	P3	P4
pH	8.62	7.28	7.62	7.68
Major Cations				
Ca (g/kg)	24.17(0.15)	24.32(0.14)	20.82(0.13)	23.87(0.12)
Mg (g/kg)	159.07(21)	176.86(0.12)	110.46(0.13)	160.62(0.25)
Na (g/kg)	9.24(0.2)	10.48(0.23)	4.92(2.1)	4.54(0.33)
K (g/kg)	5.76(0.26)	6.17(0.15)	5.18(2.1)	5.15(2.1)
Major Anions				
SO_4^{2-} (mg/l)	16837(0.92)	19117(0.85)	10774(0.91)	18620(0.92)
bdl- below detection limit; CEC- cation exchange capacity; HFO-hydrous ferric oxide; cmol/kg- centimole per kilogram				
Cl^- (mg/l)	47.09(0.6)	25.36 (0.52)	21.73 (0.11)	20.56(0.9)
Minor Cations				
Cu ppm	bdl	bdl	bdl	bdl
Co ppm	bdl	bdl	bdl	bdl

4.3.7 Metal partitioning by sequential extraction

Figure 4.11 shows the results of metal partitioning analysed in the bulk-sized and clay-sized particles. In both particle sizes, metals are partitioned into; exchangeable (F1), acid soluble (F2) and reducible (F3) fractions. Overall, the differences in the metal concentration between bulk and clay-sized particle is largely a function of surface area. For instance, in F1, Cu and Co concentrations in the bulk-sized and clay-sized particles were in the ranges of; 50 – 350 mg/kg Cu; 20 – 30 mg/kg Co and 200 – 1000 mg/kg Cu ;30 – 100 mg/kg Co respectively. As earlier indicated (section 2.2.3), clay minerals (Stumm and Morgan 1995) are the host minerals in F1, hence kaolinite present in sludge based on the mineralogical composition analyses by XRD (Fig. 4) is the potential host of metals. Furthermore, the observed variations in Cu and Co concentration in F1 according to Appel and Ma (2002) commonly occur as a result of the presence of high concentrations and selectivity adsorption characteristics of the metals. This condition reflects the (i) relatively affinity of the metal to the host minerals and (ii) competition for adsorption sites.

In F2 fraction, metals are associated with carbonate minerals (Tessier et al., 1979). However, XRD and SEM analyses revealed that the carbonates are absent in the studied sludge. The measured concentrations in bulk and clay-sized particles for each metal were in the ranges of 600 – 1500 mg/kg Cu ;100 – 200 mg/kg Co and 2200 – 5500 mg/kg Cu; 120 – 260 mg/kg Co. In the absence of carbonate minerals (i.e., acid-soluble fraction), it remains unclear whether kaolinite or HFO host the metals. Therefore, to assess the role of kaolinite in hosting the metals, batch adsorption experiments were conducted (Chapter 5).

In F3 fraction, concentrations in bulk and clay-sized particles for each metal were in the ranges of 1300 – 2300 mg/kg Cu; 80 – 200 mg/kg Co and 2200 – 5500 mg/kg Cu ; 260 – 290 mg/kg Co. Cu concentration is equally distributed between F2 and F3. However, by default, metal concentrations

associated with F3 fraction are expected to be of a much greater proportion than F2 fraction due to the metal partitioning characteristics associated with the HFO surfaces (Lindsay et al., 2015). The high proportions of metals in F2 especially Cu is suggested to be a contribution from some loosely or weakly bound metals associated with the HFO coated bulk size grains (Fig. 6c) and clay-size particles. This observation is consistent with results of the previous study conducted by Essen and El Bassam (1981) which indicated that Fe oxides dissolve and release weakly adsorbed metals into solution at treatment conditions of pH < 6. Thus, acid-soluble fraction treatment at pH 5 (Table 7), some weakly adsorbed metals associated with HFO sites are desorbed. Other sequential extraction steps (i.e., F4, F5, F6, F7 and F8) revealed very low concentrations to the below detection limit.

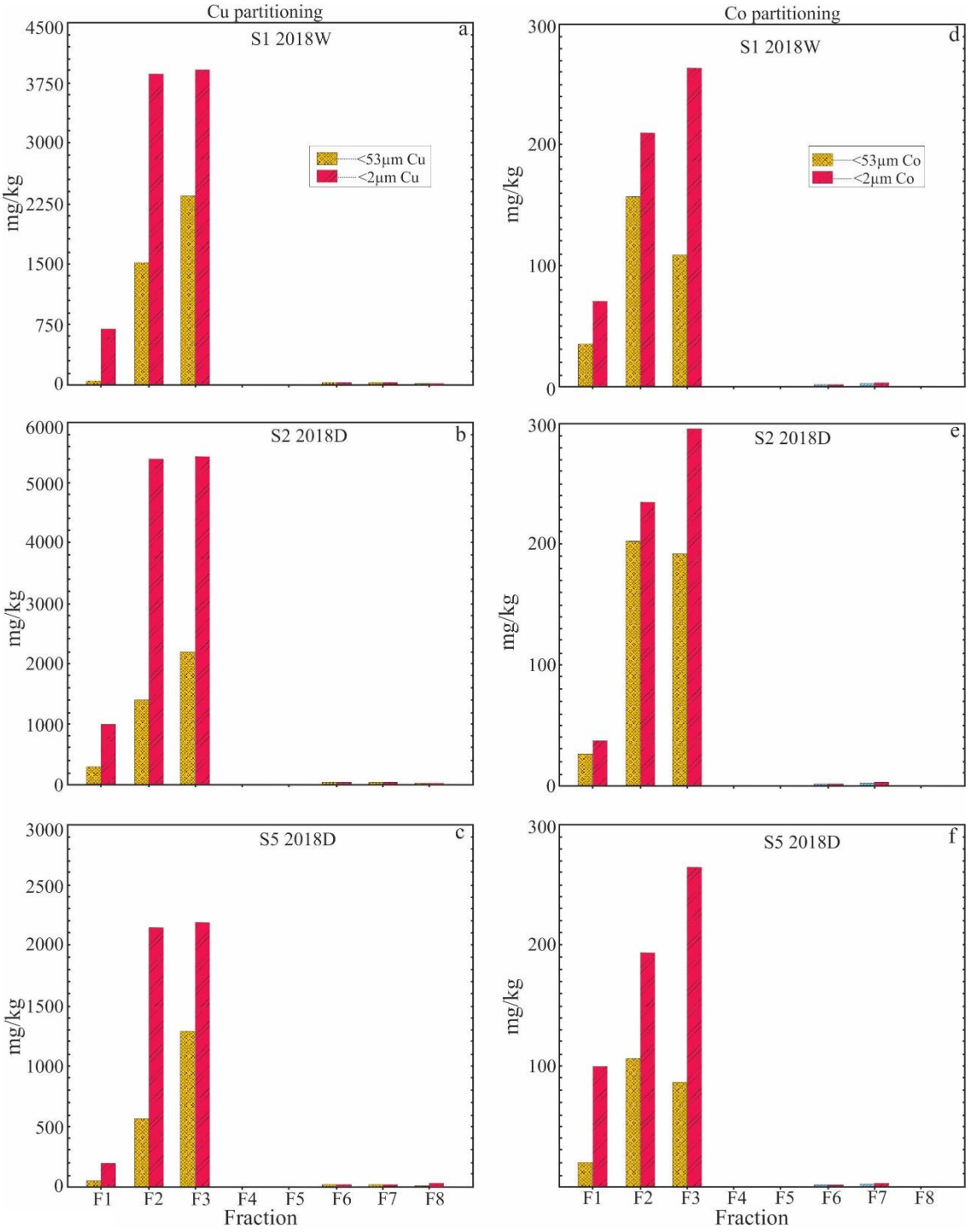

Figure 4. 9. Sequential extraction results of solid sludge. For individual fraction phases, refer to Table 7 and for sample location, refer to Fig. 3.3b and Table 8.

4.4 Chapter 4-Summary

- The dissolved Cu^{2+} and Co^{2+} concentration is low because of lime treatment which increases the pH conditions of the effluents. Despite the addition of lime to effluents, the metal carbonate solubility is low indicating that metal carbonate precipitation is not the major control of metal retention.
- Micas (i.e., biotite and muscovite), kaolinite, quartz and feldspar are the major component minerals with HFO existing as surface grain coating. The sources of HFO is the weathering of biotite which releases the Fe^{2+} and oxidises to Fe^{3+}.
- Kaolinite and HFO are the major mineral components in sludge solids whose surfaces generally control the fate and transport of metals in the studied sludge effluents and solids at solid-liquid interface through metal adsorption.
- The dominant metal partitioning phases are the exchangeable, acid soluble and weakly reducible fractions. On the basis of metal stability trends, the geochemical partitioning phases indicate that anthropogenic activities are the sources of metal contaminants, hence relatively labile.
- Both coarse and fine particle size adsorbs the metals partitioned in each individual fraction, though the high concentrations are a function of particle size distribution. In coarse particle sizes is dominated by quartz which sometimes is observed to be coated with HFO.

Chapter 5: Batch adsorption experiments and surface complexation modeling (SCM)

5.1 Overview

Heavy metal removal from solutions is one of the most significant studies in areas affected by anthropogenic activities. Adsorption is among the dominant process influencing the removal of heavy metal ions in such environments. Adsorption is mainly studied by batch experiments. Batch adsorption experiments are carried out by adding certain amount of solid into solution containing specific concentration of contaminants with a specific solid/liquid (S/L) ratio, vigorously stirred or shaken during the entire reaction time (Tsing-Hai Wang et al., 2009). The adsorption capacity obtained from a batch experiment is useful in providing information on the effectiveness of metal-sorbent system. Previous studies (Shiqing Gu et al., 2019) reviewed clay mineral adsorbents for heavy metal removal from wastewater through batch adsorption experiments. Their studies revealed that heavy metal adsorption by clay and clay composites consists of a series of complicated adsorption mechanisms, including ion exchange, surface complexation, and direct bonding of heavy metal cations to the surface of clays. Most clay minerals produce a small amount of net negative surface charge due to isomorphic substitution (Sposito, 1984; Stumm and Morgan, 1995). Furthermore, particle edges of clay minerals may produce charges according to the suspension pH as a result of broken primary bonds (Sposito, 1984). Clays have small particle sizes and high specific surface areas as a result of their complex porous structures, which facilitates physical and chemical interactions with dissolved species. These interactions result from crystallinity, electrostatic repulsion, adsorption and some cation exchange reactions (Tsing-Hai Wang et al., 2009). Another potential adsorbent in the removal of heavy metal contaminants from wastewater studied by batch adsorption experiment is hydrous ferric oxide (HFO) (Dzombak and Morel, 1990; Spark et al. 1995). HFO is most known to be effective for removing heavy metals

from aqueous solution because of its high specific surface area and potentially higher reactivity than bulk particles or natural minerals, which should confer greater sorption capacity. The mechanism by which HFO remove trace metals from solution has been postulated by various workers to be coprecipitation, adsorption and surface complexation (Smith, 1992; Jenne, 1998). Of potential significance in the role of heavy metal oxides on metal ion transport is the fact that the degree of interaction between the heavy metals and HFO is likely to be dependent on whether the heavy metal was present at the time of formation of the hydrous metal oxide precipitate or coating (Lee, 1975). It has been known for some time that much greater incorporation of chemicals into ferric hydroxide precipitates occurs when the precipitation takes place in the presence of the contaminant (Lee, 1975; Jenne, 1998). Clay minerals and HFO can coexists and is reportedly common is tropical soils in tropical climates (Carroll, 1960). Often times, HFO adhere to the surfaces of clay minerals in form of surface coating. As earlier alluded, clay minerals can adsorb metal at ion exchange sites. However, it is doubtful that the ion exchange of clay minerals such as kaolinite can play a significant role in heavy metal transport for several reasons. First, the cation exchange capacity represents a small part of the adsorption capacity of the particulate matter for cations. Another factor to consider is that competing for the cation exchange sites with the heavy metals of interest are the bulk metal species such as calcium, magnesium, and sodium which occur at concentrations many-fold over the heavy metals (Carroll, 1960; Jenne, 1998). Therefore, when considering the adsorption capacity of mineral fragments (i.e. clay minerals and HFO) for heavy metal species, consideration must be given to the possibility of hydrous metal oxide coatings on the surface of these particles which would in turn play a dominant role in the chemistry of heavy metals. For example, studies by Plumb and Lee, 1973 indicated that taconite sludge tailings derived from iron ore mining in the Mesabi Range in northern Minnesota showed significant adsorption

capacity for Cu on its surface. This adsorption capacity was manifested even though the sludge tailings were composed primarily of quartz and of an iron-magnesium silicate (cummingtonite). In order to investigate the adsorption performance of the adsorbent towards heavy metals at various pH conditions, SCM can predict the behaviours of metals with the host surfaces through chemical reaction between surface sites and metal ions in solution for which the equilibrium constants are modified by the surface charge. The DDL model of Dzombak and Morel (1990) is employed in this chapter to determine the metal behaviours to each of the dominant adsorbent (kaolinite and HFO) in sludge.

5.2 Materials and methods

5.2.1 Batch experiment

Two types of sludge materials were prepared and used in batch experiments. Sludge; (i) with HFO coating and (ii) without HFO coating. For sludge without HFO coating, the removal of HFO coating followed chemical extraction protocols and procedures outlined by Chao and Zhou (1983) using acidified ammonium oxalate (NH_4Ox). To ensure the total removal of HFO coating, additional chemical treatment steps outlined by Mehra (2013) were conducted. The batch adsorption experiments were performed in single and binary metal systems as shown in Figure 5.1 and as described below:

5.2.1.1 Sludges with and without HFO coating

Sodium nitrate ($NaNO_3$) from FUJIFILM Wako Pure analytical grade was used to prepare 100 ml of 0.05 M electrolyte in a 250 ml volume of polyethylene plastic bottles. Each of the 1g solid of < 2µm clay-size particles (i.e., sludge with and without HFO) was added to each of the separately prepared electrolytes and the initial pH adjusted to pH 3 by HNO_3. The solution was equilibrated by end-over-end shaking at speed of 200 rpm for 24 hours. In single metal system experiments,

1.10 mM copper (II) nitrate trihydrate (Cu $(NO_3)_2.3H_2O$ from FUJIFILM Wako Pure analytical grade) and 0.11 mM cobalt nitrate hexahydrate (Co $(NO_3)_2$. $6H_2O$ from FUJIFILM Wako Pure analytical grade) were added to each of the prepared electrolytes. In binary metal system experiments, 1.10 mM Cu and 0.11 mM Co were simultaneously added to each of the prepared electrolytes. The aliquots were equilibrated for 24 hours by an end-over-end shaker at a shaking speed of 100 rpm. Batch adsorption experiment involved titrating aliquot volume with 0.05 M HNO_3 and 0.05 M sodium hydroxide (NaOH; FUJIFILM Wako Pure analytical grade) to desired pH 3 - 9 under the magnetic stirring bar. After equilibration to the desired pH conditions, the mixture was again placed on an end-over-end shaker at 100 rpm for 24 hours after which pH re-measured, centrifuged and filtered with 0.2µm membranes. The filtrates were acidified by pure grade HNO_3 and analysed by ICP-AES.

5.2.1.2 Reference kaolinite

Reference kaolinite sample (JCSS-1101) was obtained from the Clay Science Society of Japan. The sample was acid washed in 0.1 M HCl solution, and oven-dried at 90^o for 24 hours and analysed by XRD. XRD results showed characteristic peaks of kaolinite with no other mineral components detected. The surface area was measured by the Brunauer-Emmett-Teller (BET) method by protocols outline by Brame and Griggs (2016) using a Quantachrome analyser (NOVA touch LX^3 NT3LX-1). The measured value was 18.34 m^2/g. Two sets of adsorption experiments were conducted by adding 1g kaolinite to 100 ml of 0.05 M $NaNO_3$ electrolyte in a single metal system. A 0.25 mM Cu and 0.0163 mM Co were each prepared and added to each of the prepared 100 ml volumes of electrolytes. The aliquot solutions were varied from pH 3 - 9 through titration with 0.1 M HNO_3 and 0.1 M NaOH solutions at 0.25-pH unit increment and equilibrated for 24

hours. The aliquot pH-re-measured, centrifuged, filtered through 0.2 µm filters and analysed by ICP-AES.

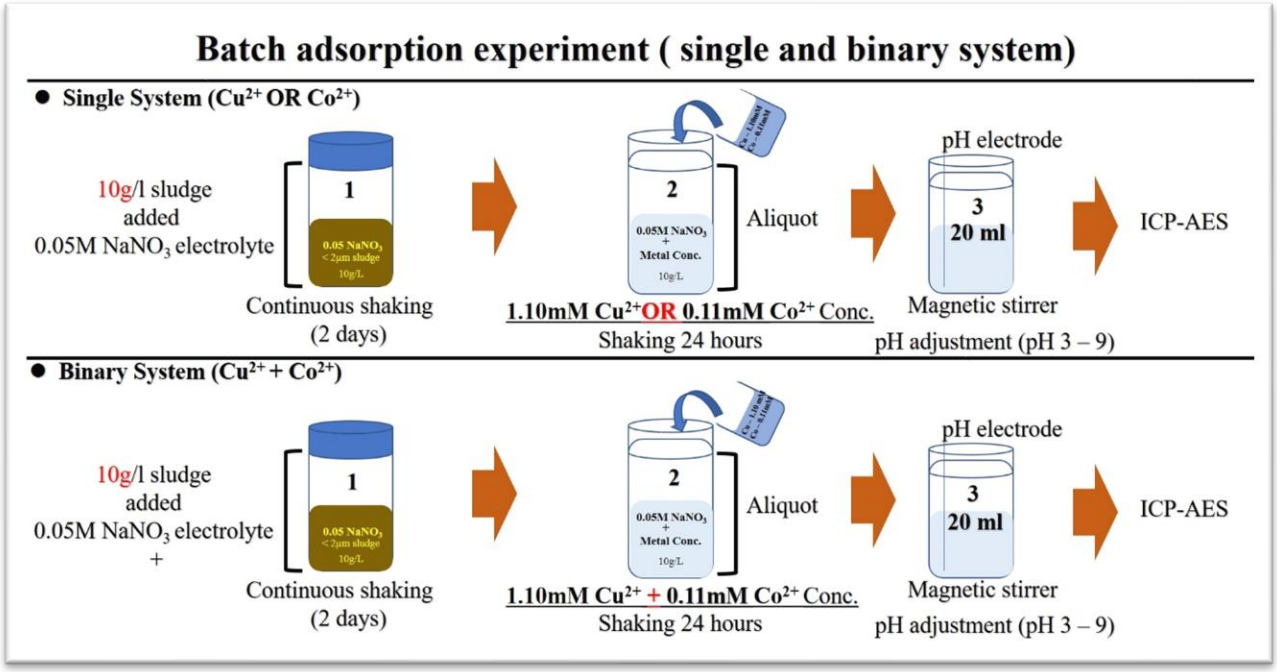

Fig. 5.1. Batch adsorption experiment

5.2.2 Surface complexation modeling (SCM)

The component additivity (CA) approach of SCM prediction was adopted. HFO sites were modeled with the FeOH+.sdat dataset in GWB package from the diffuse double layer (DDL) of Dzombak and Morel (1990) database by assuming strong sites >(s)FeOMe+ and weak sites >(w)FeOMe+ where Me^{2+} represents the metal adsorbed. The concentrations of Fe used in modeling were estimated from the chemical extraction treatment of HFO coating from sludge with NH_4Ox following sequential extraction protocols outlined in Table 7. Kaolinite modeling was made possible through SCM constants and equilibria obtained from the previously published papers cited in Table 10. SCM constants and equilibria from previous papers were used due to the lack of a thermodynamic database of micas. Therefore, kaolinite was assumed to be the dominant

host surface. For kaolinite adsorption, two sites, $>X_2Me$ and $>(KaO)_2Me$ were selected based on their reasonably better model fit to the experimental data. Both model simulations were constructed using the REACT module of GWB package software.

Table 11: Input parameters for the surface complexation modeling of kaolinite

Surface reactions	log K		
Surface reactions	H	Cu	Co
$>KaOH + H^+ = >KaOH_2^+$	3.24[a]		
$>KaOH = >KaO^- + H^+$	-7.15[a]		
$>X^-.Na^+ + H^+ = >X^-.H + Na^+$	-2.88[a]		
$>KaOH + Me^{2+} = >(KaO)_2Me^+ + H^+$		-4.58[b]	-6.87[a]
$2>X^-.Na^+ + Me^{2+} = >X^-_2.Me^{2+} + 2Na^+$		3.31[b]	3.02[b]
$>KaOH + Me^{2+} = >KaOMeOH + H^+$		-8.9	
Other parameters			
Surface area (m^2/g)	25.7[c]		
Site density X^- (mol/kg)	0.05[d]		
Site density SOH (mol/kg)	0.05[d]		

[a]Angove et al. (1997); [b]Ikhsan et al. (1999); [c]Landry et al. (2009); [d]Fan et al. (2019)

5.3 Results and discussion

5.3.1 Sludge without HFO: Single system-Cu^{2+}

The adsorption edges of single system for total Cu adsorption are given in Fig. 5.1a. The adsorption edges for both standard kaolinite and kaolinite in sludge is identical. This result reveals that in the absence of HFO, kaolinite in sludge is the main adsorbent of Cu^{2+} ions. Cu^{2+} showed two (2) initial stages of adsorption from pH 3 – 5 and from pH 5.5 - 6.5 representing the maximum adsorption boundaries for the exchange sites and variable charge sites (Schindler et al., 1987). In 0.05M electrolyte typical of our field condition, < 10% Cu is adsorbed. This result shows that at low pH conditions, metal adsorption is independent of pH conditions (Goldberg 2002). However, with

increasing pH, adsorption is mainly pH dependent and mostly concentrated at variable charge sites (Lutzenkirchen, 2006).

SCM predictions (Fig. 5.2b) reveals that low pH adsorption at exchange sites is dominated by X_2Cu species and with <10% Cu adsorbed. This low % adsorption is typical of metal adsorption onto kaolinite surfaces at permanent negative charge sites (Gu and Evans, 2008). With increasing pH conditions (i.e., pH 5 – 6.5), the dominant surface species according to SCM prediction is >KaOCuOH+ consistent with results suggested by Srivastava et al., 2005 of Cu adsorption onto kaolinite surfaces.

From the results of batch adsorption experiment (Fig. 5.2a) and SCM predictions (Fig. 5.2b), kaolinite shows the ability to adsorb Cu^{2+} ions at both low and high pH conditions. However, the low % adsorption at low pH is due to low CEC associated with kaolinite (Bergaya et al., 2006). With increased pH of adsorption, SCM predicts that >KaOCuOH+ commands significant adsorption onto kaolinite surfaces. This observation therefore, suggests that kaolinite has potential to host metals associated with the acid soluble fractions of the sequential extraction in the absence of carbonate minerals. Although, kaolinite has low surface area (Bergaya et al., 2006) to display high metal adsorption capacity, its high volume (>60%) in sludge shows the high potential to adsorb high metal concentrations.

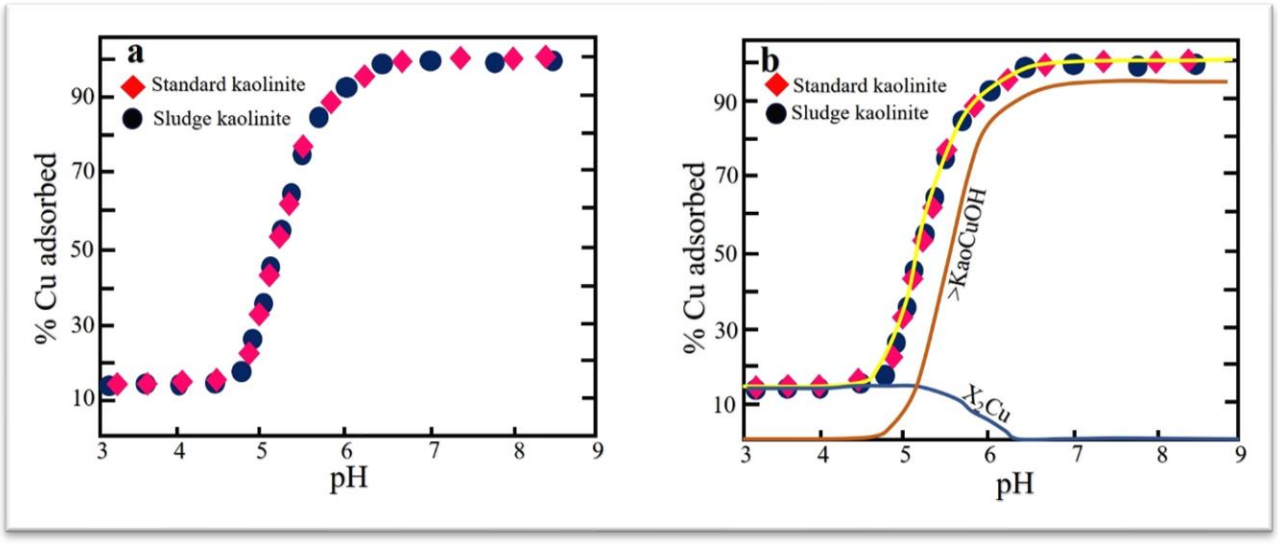

Fig. 5.2. a) Batch adsorption behavior of Cu^{2+} ion onto kaolinite: b) SCM predictions of the dominant Cu^{2+} surface species onto kaolinite surface.

5.3.2 Sludge without HFO: Single system-Co^{2+}

According to results of Co adsorption shown in Fig. 5.3a, Co exhibits a slightly different behaviour from that observed with Cu. Co adsorption at the initial stage occur from pH 3 – 6.5 and later stage pH 6.5 – 8 with an overall percentage adsorbed of < 10% Co. Co seem to show much longer retention at ion-exchange sites up to pH 6.5 (Fig. 5.3a). This behavior is possibly related to the metal electronegativity character suggested in the Irving-Williams series order (Irving and Williams 1948) and nature of the mineral surface relative to the metal affinity characteristics (Spark et al., 1995). At variable charge site, metal adsorption is pH dependent supporting the appropriateness of inner sphere complexation.

Figure 5.3b shows the SCM predictions of surfaces species onto kaolinite. Model predicted that low pH adsorption is largely dominated by ion exchange by X_2Co with <10% Co asorbed. The low % Co adsorption is consistent with the low CEC values of kaolinite (Bergaya et al., 2006). With increasing pH, the dominant surface species is $>(KaO)_2Co$ based on SCM predictions. In both cases (i.e., Cu^{2+} and Co^{2+}), the high adsorption capacity of kaolinite is pH-dependent and

therefore, kaolinite exhibits the high potential to host the metals associated with the acid soluble fraction of sequential extraction (See chapter 4).

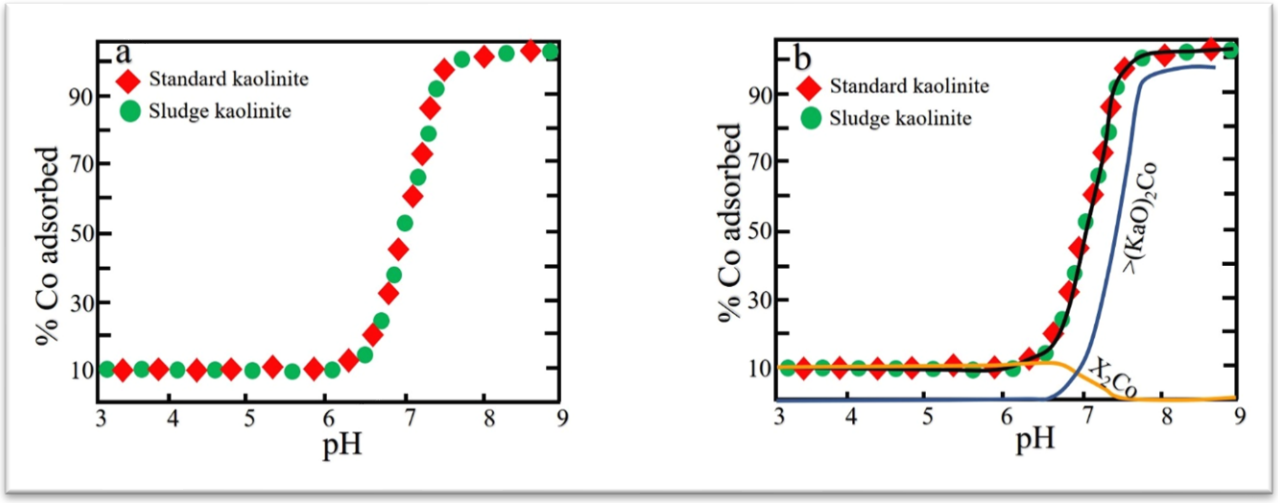

Fig. 5.3. a) Batch adsorption experiment of Cu^{2+} onto standard kaolinite and kaolinite in sludge: b) SCM predictions of Co^{2+} adsorption species onto kaolinite

5.3.3 Sludge with HFO: Single system-Cu^{2+}

Results of Cu^{2+} adsorption onto sludge with HFO is shown in Fig. 5.4a. Two distinct adsorption phases are revealed from pH 3 – 4.5 and pH 5 - 6.5. Approximately < 30% Cu is adsorbed below pH 4.5. Above pH 5, pH-dependent adsorption controls metal adsorption. The pH_{50} (i.e.50% adsorption) is observed at pH 5, slightly lower than that of Cu onto kaolinite (i.e. pH 5.3) suggested by Srivastava et al. (2005). The pH_{50} of HFO measured by Sposito (1984) is pH 5. Therefore, from the value of pH_{50}, it becomes clear that HFO coating influences metal adsorption when present. The maximum pH of Cu adsorption occurs at pH 6.5 indicating that at this pH condition most of the adsorbed Cu^{2+} is stable from release.

Figure 5.4b reveals the Cu^{2+} adsorption surface species onto the mixture of kaolinite and HFO (i.e., sludge with HFO). The model predicts that Cu is distributed mainly on ion exchange sites at pH < 4.5 through $>X_2Cu$ consistent with outer sphere adsorption (Lund et al., 2008). The model predicts

< 15% of the adsorbed Cu at ion exchange sites. The model prediction however, exhibited some misfits to the experimental data at pH < 4.5. Lund et al (2008) observed similar discrepancies in model fitting metal adsorption to the pure phases in the multicomponent system using the CA-SCM approach due to the potential experimental uncertainties during modeling simulations.

Above pH 4.5, adsorption on ion exchange sites decrease, and the pH-dependent bidentate sites of kaolinite >$(SO)_2$Cu and strong sites of HFO >(s)FeOCu+ and >(w)FeOCu+ species show significant adsorption with increases in pH conditions. However, for kaolinite, the bidentate sites of >$(KaO)_2$Cu species shows < 20% adsorption below pH 6. The low adsorption capacity of >$(KaO)_2$Cu onto kaolinite is consistent with low surface area associated with the edge surface (variable charge sites) of kaolinite (Angove et al., 1997; Ikhsan et al., 1999).

Cu^{2+} adsorption by HFO >(s)FeOCu+ is rapid between pH 3.5 – 4.5, after which adsorption decreases due to site saturation consistent with the results by Dzombak and Morel (1990) which indicated that the >(s)FeOMe+ specie of HFO exhibits high affinity for cations but with low site concentrations. In most cases where the sorbate concentration is low, the >(s)FeOMe+ of HFO show greater cation adsorption (Dzombak and Morel, 1990). The weak sites of >(w)FeOCu+ rapidly adsorbs at pH > 4.5. The increase in adsorption by >(w)FeOCu+ sites correlate with the sites characteristic of high site concentration with high sorbate concentration (Dzombak and Morel, 1990). This result suggests that the amount of sorbate (i.e., Cu concentrations) in the studied sludge is high, hence the >(w)FeOMe+ surface of HFO will dominate adsorption. The excellent model fit to experimental data showed by Cu^{2+} suggest that the HFO sites describes the Cu^{2+} adsorption very well at solid-liquid interface

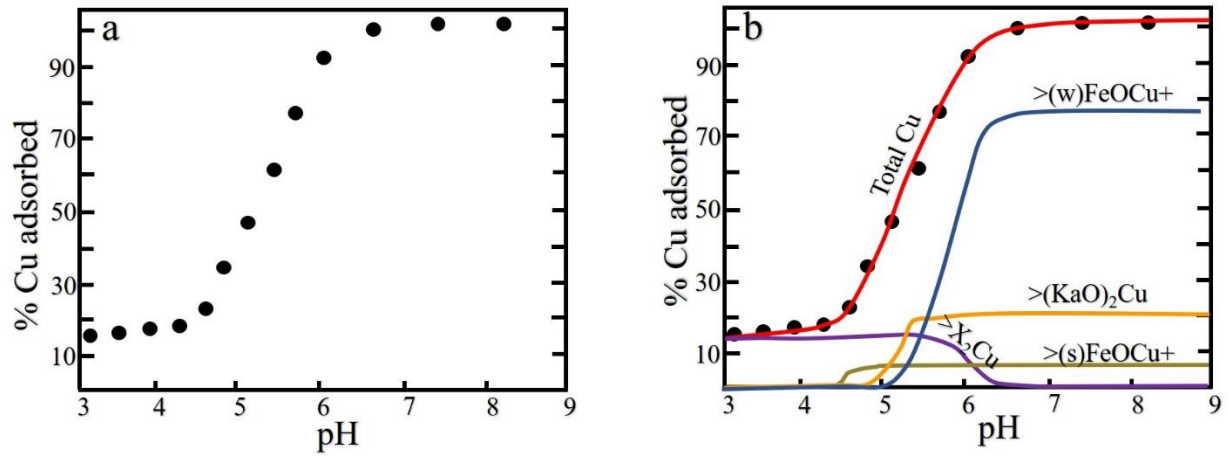

Fig. 5.4. Single system Cu^{2+} adsorption onto mixture of kaolinite + HFO in sludge: a) Batch Cu^{2+} adsorption behaviour; b) SCM prediction of surface species of Cu^{2+} adsorption onto sludge mixture

5.3.4 Sludge with HFO: Single system-Co^{2+}

In figure 5.5a, Co^{2+} show a slightly different behavior to that of Cu^{2+} (Fig. 5.4). The initial stage of Co^{2+} adsorption occurs from pH 3 – 5.5 and later stage from pH 5.5 – 8 (Fig. 5.1 d). At the initial stage, Co^{2+} exhibits a much longer retention at ion exchange sites. The most probable reasons are attributed to the; (i) electronegativity characteristic described by Irving and William (1948) and (ii) low hydrolysis behavior of the metal (Hizal et al., 2009; Loganathan et al., 2012). As pH increases, the extent of Co adsorption also increases associated with inner sphere complex (Landry et al., 2009). Thus, overall, our results of single metal system indicate that both metals adsorb at low pH, but much significant adsorption occur with increasing pH.

According to SCM, the model predicts that < 15% Co is adsorbed at ion exchange site by $>X_2Co$ from pH 3 - 5.5 (Fig. 5.5b). However, the model fit to experimental data at ion exchange site is poor. We attributed this result to one or several of the following: (i) artifact caused by the differences in experimental conditions and SCM constant and equilibria from literatures and (ii) Fe-oxide coating on sludge surfaces. The second reason is probably the most likely because it has

been observed that Co adsorption onto HFO surface >(s)FeOCo+ takes place at pH 5.5. Furthermore, HFO precipitation has been reported to occur from pH > 3.5 (Jenne, 1998). According to Lee (1975); Lee et al. (2002), HFO precipitation in the presence of contaminant tend to incorporates the metal cations. With increasing pH, the kaolinite bidentate site $>(KaO)_2Co$ show 20% adsorb at pH 7.5. From the SCM observations, Cu^{2+} (Fig. 5.4) and Co^{2+} (Fig. 5.5) adsorbs similar percentages at pH-dependent sites of kaolinite suggesting that without metal competition for available pH dependent adsorption sites, both metals adsorbs equally by kaolinite surfaces. It however, not clear as to whether the kaolinite adsorption sites are variable for each cation but going by the percentage metal adsorption, it is possible to suggests that both metals are adsorbing at different sites onto kaolinite consistent with previous literatures indicating that equal metal adsorption can be expected where adsorption occurs at different adsorption sites (O'Day et al., 1994; Lutzenkirchen, 2006).

Co^{2+} adsorption at HFO site is dominated by the >(s)FeOCo+ species from between pH 5.5 – 7 with approximately less 40% Co^{2+} adsorbed. The adsorption by >(s)FeOCo+ and >(w)FeOCo+shows significant differences in terms of the percentage of metal adsorption. Based on the individual metal concentrations and the sites characteristics of >(s)FeOCo+ and >(w)FeOCo+, it can be deduced that at high Co concentrations, this site adsorbs lesser amount of cation consistent with low site concentrations suggested by Dzomak and Morel (1990). At low Co concentrations, however, the same site can adsorb considerable number of metals consistent with the presence of high site concentrations associated with adsorption site (Dzombak and Morel, 1990). At pH > 7, the HFO surface site >(w)FeOCo+ dominates adsorption suggesting that when the high affinity and low concentrations sites >(s)FeOCo+ are saturated, the low affinity and high

concentration sites >(w)FeOCo+ also starts to dominate. The results are well comparable to those obtained by Landry et al. (2009) for pure mineral system.

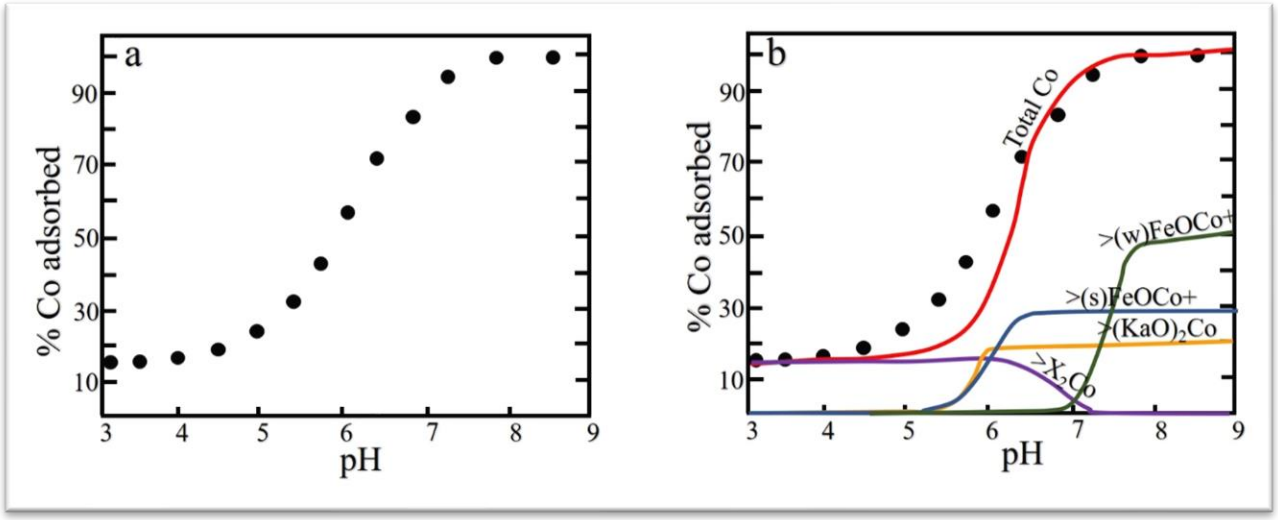

Fig. 5.5. Single system Co^{2+} adsorption onto mixture of kaolinite + HFO in sludge: a) Batch Co^{2+} adsorption behaviour; b) SCM prediction of surface species of Co^{2+} adsorption onto sludge mixture

5.3.5 Sludge without HFO: Binary system-Cu^{2+} - Co^{2+}

The binary system sorption behaviors investigated on sludge without HFO (i.e. kaolinite) is shown in Fig. 5.1 f. Generally, both metals show similar adsorption behavior observed in single (Fig. 5.1 a) and binary (Fig. 5.1 e) systems as confirmed by their relative positions of the adsorption edges. Both metals revealed <10% adsorption at ion exchange site from pH 3 – 6.5. At variable charge sites, Cu and Co adsorb from pH5.5 to 6.5 and 6.5 to 8 respectively. This behavior is slightly different to that observed with HFO. This observation demonstrates that in sludge with HFO, coprecipitation of HFO in the presence of the metal contaminant at low pH tend to also incorporate with the metals.

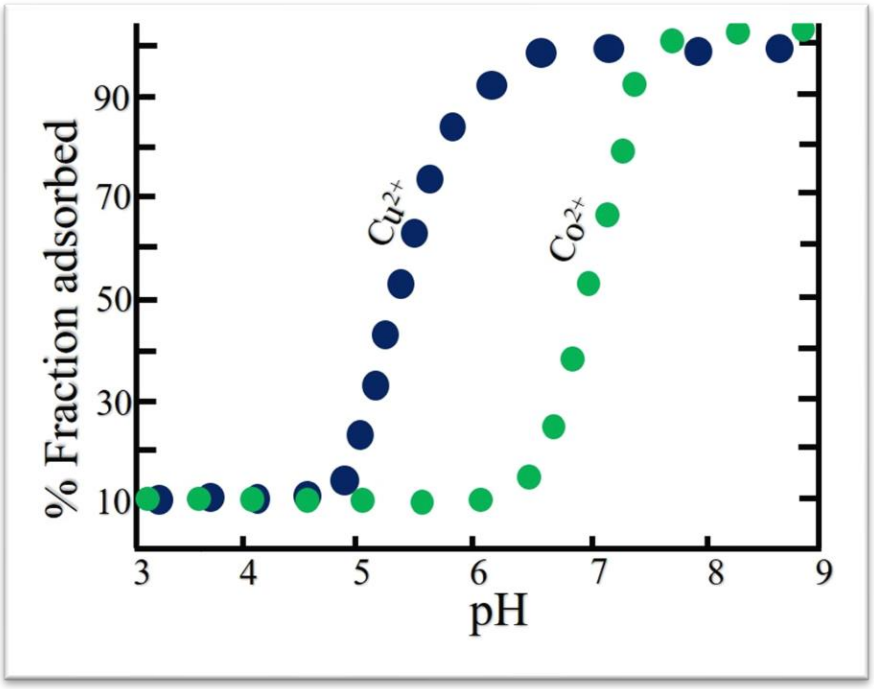

Fig. 5.6. Batch adsorption experiment results of binary system of Cu^{2+} and Co^{2+} onto kaolinite in sludge

5.3.6 Sludge with HFO: Binary system-Cu^{2+} - Co^{2+}

Figure 5.7a shows the adsorption edges of Cu and Co on sludge with HFO with seemingly identical behaviours to that observed in single metal systems (Fig. 5.4; 5.5). The adsorption of Cu^{2+} and Co^{2+} in binary system are shown in Fig. 5.7b. From the model, the ion exchange site by $>X_2Cu$ showed a percentage adsorption of 15% than that of $>X_2Co$ sites at 10%, indicating clearly that metal competition for sites was quite significant for Co than that of Cu. The high Cu concentration displaced much of Co concentrations at ion exchange sites, consistent with the previous studies by Atanassaova (1995). At increasing pH, adsorption at kaolinite site shows little to no discernible variation for both metals. As earlier alluded to in the preceding section, there exists some high possibilities of both metals to be adsorbing at different adsorption sites onto kaolinite surface. Based on simple electrostatic valence concepts suggested by O'Day et al., 1994, the >Al-OH and >Al-O-Si sites exposed on particle edges have excess non-bonded electron density on oxygen atoms and are potential sites for cation binding.

Cu adsorption to HFO sites show little to no significant difference between single and binary system indicating that Cu is specifically adsorbed consistent with its electronegativity characteristics described by Irving and Williams (1948). In the case of Co, adsorption was however, the most affected in the presence of Cu. The percentages of Co adsorption by >(s)FeOCo+ and >(w)FeOCo+ showed some remarkable decrease. For instance, Co adsorption at >(s)FeOCo+ decreased from 50% in single system to 25% in binary system at pH 6.5 whereas at >(w)FeOCo+ decreased from 35% in single system to 15% in binary system at pH 8. This result suggests that, apart from high affinity of Cu for HFO surfaces, the two metals likely adsorb to the similar HFO sites. The selectivity of Cu over Co is in agreement with the result by Sposito (1984) suggesting that metals with rapid/fast hydrolysis behaviour tend to have high affinities for surfaces. This behaviour of Cu has been shown in Fig. 3 with Cu hydrolysing at lower pH than Co. The little or negligible adsorption differences between single and binary system on kaolinite sites is unclear. But it appears to suggest the low affinities for both metals to the kaolinite sites.

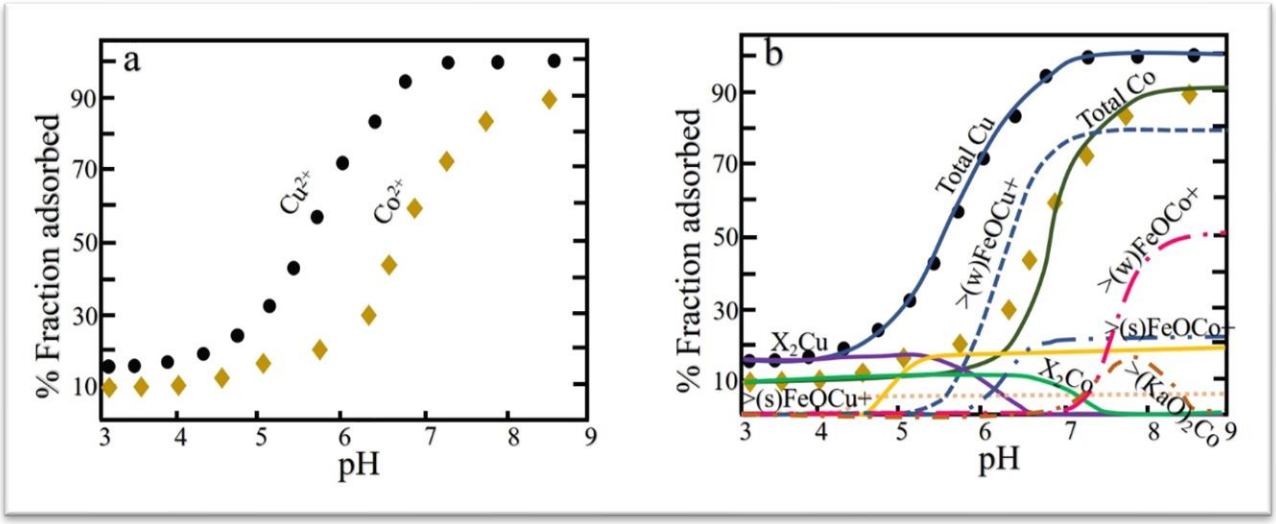

Figure 5.7. a) Batch adsorption results of binary system of Cu^{2+} and Co^{2+} onto sludge containing kaolinite and HFO; b) SCM prediction of surfaces species Model parameters for kaolinite are listed in Table 10 and HFO from Dzombak and Morel (1990). Experimental data (dots) and solid line and dotted lines are kaolinite and HFO predictions. Experiment conducted at 0.05M ionic strength.

5.4 Interpretation of sequential extraction results by SCM predictions

From the results of SCM predictions (Fig. 5.7), sequential extraction results (Fig. 4.11) are interpreted. From the results of sequential extraction, metal partitioning in F1 fraction translates to between 4-13 % Cu and 7 – 13 % Co. In a binary system (Fig. 5.7), modeling predicts 15 % Cu (i.e., $>X_2Cu$) and 10 % Co (i.e., $>X_2Co$) at pH 3 - 5 and pH 3 - 6 respectively. The decrease in Co percentages is consistent with the high Cu concentrations at the exchange sites due to competition. Besides, our sludge has the high Ca concentrations due to the addition of lime. This condition according to Harter (1992) is reported that high Ca concentrations compete favorably for exchange sites more than Co. Therefore, the presence of high Ca concentrations from the dissolution of lime is expected to affect Co adsorption in sludge rendering Co metal highly mobile into the environment. Our results between sequential extraction and modeling predictions are well comparable, though the small difference in percentage concentrations could be due to the use of modeling parameters extracted from previous literature data.

In F2 fraction, results of sequential extraction of metal partitioning at pH-dependent kaolinite site translates to between 46 – 47 % Cu and 35 – 48 % Co respectively. SCM predicts 20 % Cu^{2+} (i.e., $>(KaO)_2Cu$) and Co^{2+} (i.e., $>(KaO)_2Co$) adsorption for both metals at pH 5.5 and pH 7.5. Model predictions are consistent with kaolinite low adsorption characteristics due to the low surface area and low affinity sites (O'Day et al., 1994; Gu and Evans, 2008). The difference in percentage concentrations between the two experimental results is suggested to be as a result of metal desorption from loosely or weakly bound HFO sites as earlier reported in sequential extraction results and supported by the results of previous study by Essen and El Bassam (1981).

In F3 fraction, results of sequential extraction of metal partitioning at HFO sites translates to between 46 – 47 % Cu and 35 – 53 % Co. The model predicts 70 % Cu and 40 % Co at pH 7.5.

The difference in percentages of model prediction with sequential extraction is that the model assumes that no desorption of metals occurred during the F2 leaching stage. Comparing the results of sequential extraction and model predictions, most metals are loosely or weakly bound to kaolinite and HFO sites, and that they tend to desorb at the acid-soluble leaching stage. Therefore, the reported metal release by sludge on the Zambian Copperbelt is as a result of the dominance in metals concentrations associated with the labile fractions and weakly adsorbed metals onto HFO surfaces.

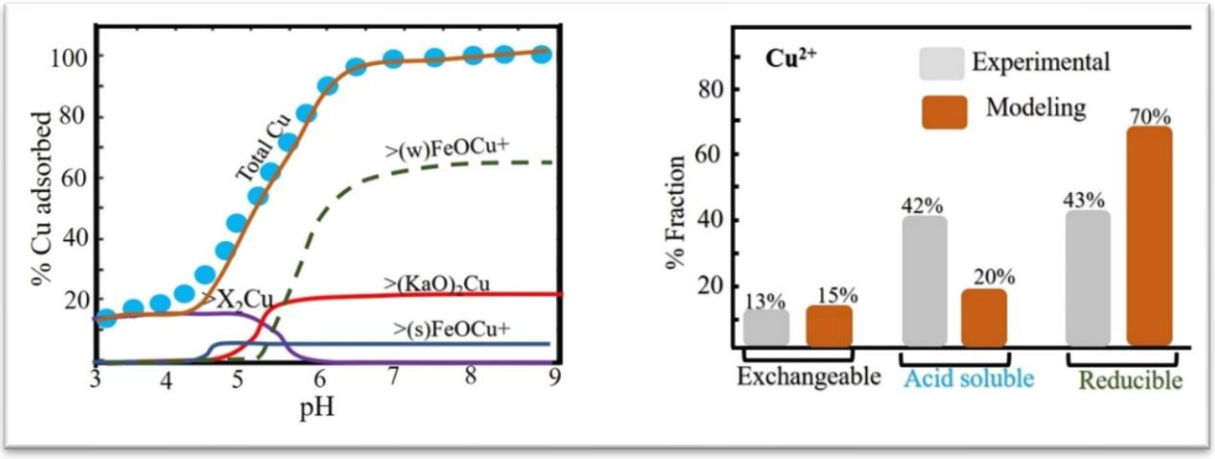

Fig. 5.8. Interpretation of sequential extraction from SCM predictions of Cu^{2+} species onto sludge with HFO (i.e., kaolinite + HFO)

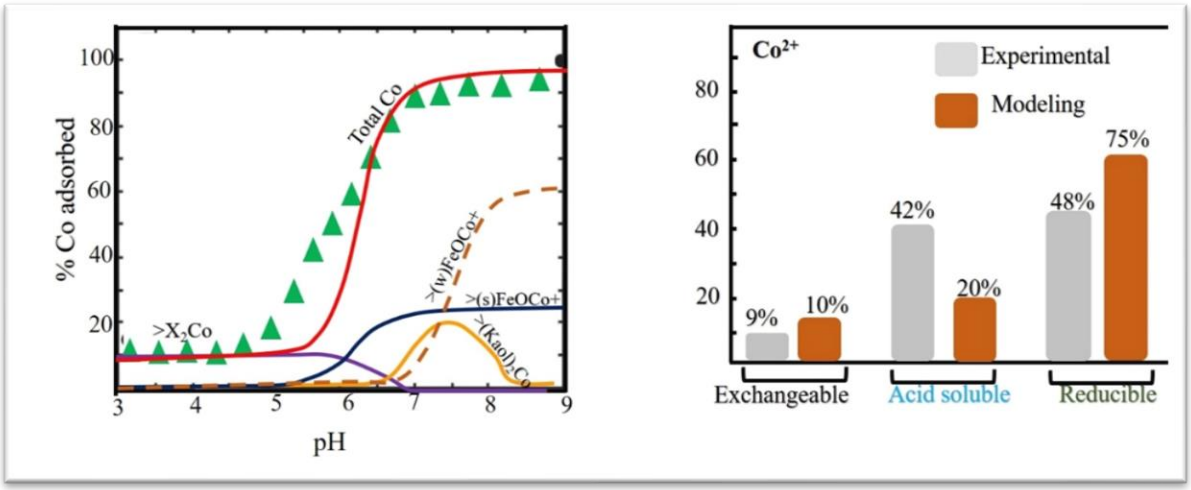

Fig. 5.9. Interpretation of sequential extraction from SCM predictions of Co^{2+} species onto sludge with HFO (i.e., kaolinite + HFO)

5.5 Chapter 5-Summary

- Cu^{2+} and Co^{2+} adsorption onto kaolinite and HFO sites are responsible for controlling their mobility in sludge effluents and solid deposits. This finding is very important because it means that the metal retention mechanisms by sludge is largely dependent on the availability and concentrations of kaolinite and HFO adsorption sites. However, for the most part, Cu^{2+} and Co^{2+} adsorption is less stable and can be highly mobile under variable geochemical conditions and thus be of some environmental concerns.
- The adsorption capacity of Cu^{2+} and Co^{2+} onto kaolinite and HFO has well been described by the CA-SCM approach. This approach has revealed that Co adsorbs and binds onto kaolinite sites that might not have been dominated by Cu metal ions. With HFO sites, both Cu^{2+} and Co^{2+} ions show greater affinity for adsorption sites, however, Cu^{2+} is highly and specifically adsorbed due to its electronegativity characteristics, thus is more preferentially retained on HFO sites more than that of Co^{2+} ion. This result, therefore, suggests that high metal concentrations in binary or multi-elemental systems will in some way affects the adsorption behavior of the other metals present depending on the individual metal characteristic been sort. Through the CA-SCM approach, useful predictions of metal partitioning from sequential extraction were produced. Therefore, the CA-SCM approach represents a powerful tool to predict metal adsorption in single and binary system and metal partitioning from sequential extraction.

Chapter 6: Implications for Green Mining

6.1 Overview

Green mining is defined as technologies, best practices and mine processes that are implemented as a means to reduce the environmental impacts associated with the extraction and processing of metals and minerals (Ghose, 2009; Kachan, 2013). Currently, the mining industry holds the key to sustaining the current economic growth and global developments for many countries throughout the world. The demand for metals has greatly contributed to extensive exploration and exploitation of mineral deposits. However, in the recent past few decades, mining has had the potential to affect its environment which include ecosystem destruction, negative effects on biodiversity, release of heavy metals, toxic substances and particulate matter through both mining and the beneficiation processes, and significant use of water resources. Mine wastewater can potentially damage the ecosystem through acid mine drainage, lowering pH value and causing the leaching of heavy metals and other toxic contaminates into the water table, making water unusable for drinking and agriculture and affecting aquatic life. To make mining a sustainable undertaking, adopting strategies to promote green mining to reduce the footprint on the environment caused by mining activities is quite significant. One of the approaches is to deploy minimum(zero)-discharge waste processes (Song et al., 2015; Tong et al., 2016) that re-use existing waste materials and to recover valuable minerals and metals. This process involves minimising the generation of wastes from the sources resulting into low discharges.

Another approach of reclaiming the existing waste material at the deposition sites is by acid treatment to recover the metals. Heap or dump leaching has widely been used in reprocessing of mine waste for residual metals through application of chemical solutions to the solid material after extracting it and placing it on a lined surface, which largely prevents solutions from penetrating

into the ground and ground water thereby improving efficiency in mining with reduced environmental impacts (Blengini et al., 2019).

Therefore, the objective of this chapter is to use surface complexation modeling to assess:

- Optimisation of wastewater (effluent) treatment conditions by lime
- Metal stability conditions in sludge
- Metal recoveries from solid sludges

6.2 Materials and methods

Table 12 show the hydrogeochemical parameters of rainwater and drainage effluents used as input parameters in geochemical modeling (surface complexation modeling) simulation to predict the optimal pH of wastewater treatment condition as well as ascertaining the minimum pH at which Cu^{2+} and Co^{2+} can be leached out of sludge after rainwater percolations. Dzombak and Morel (1990) database for HFO and kaolinite database from previous published datasets were used in the modeling simulation

Table 12: Hydrogeochemical parameters of Copperbelt rainwater and source drainage

	Rainwater	**Drainage effluent**
pH	5.2	5.14
EC (uS/cm)	145	1088
Ca^{2+} (mg/l)	23.21	122.2
Mg^{2+}	9.81	52.67
Na^{+}	12.12	bdl
K^{+}	80.94	29
SO_4^{2-}	123.4	966
HCO_3^{-}	bdl	1.80
Cl^{-}	17.04	10.57
Cu^{2+}	1.87	14.52
Co^{2+}	bdl	0.95

Abbreviation: bdl-below detection limit

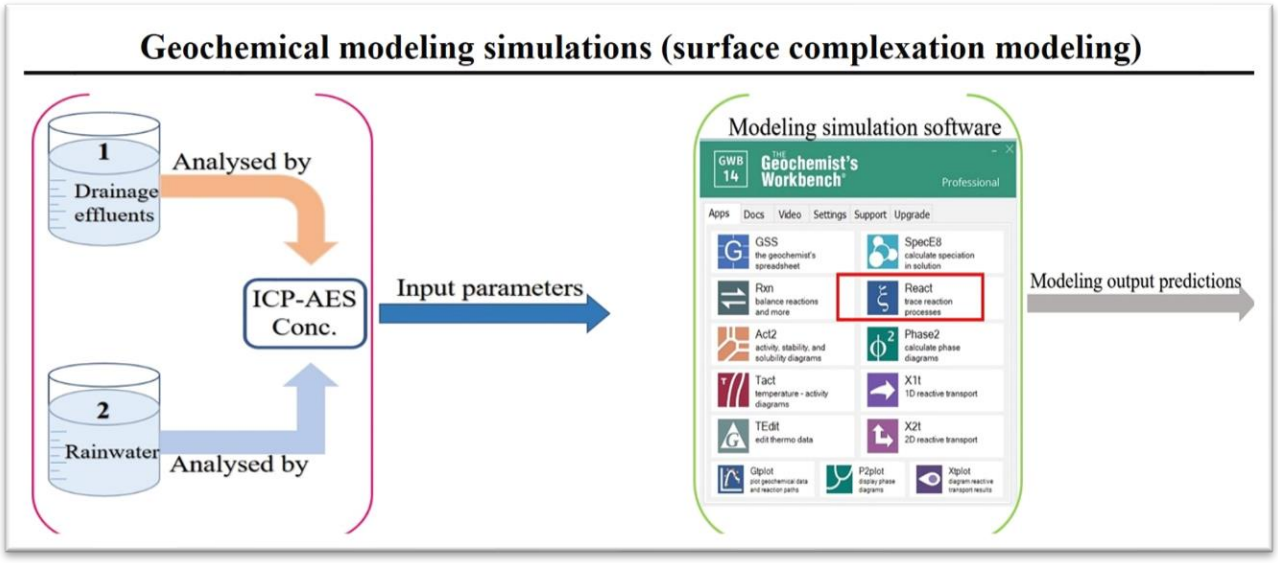

Fig. 6.1: Surface complexation model simulation for predicting optimal pH of wastewater treatment and metal stability conditions by rainwater percolations

6.3 Results and Discussions

6.3.1 Optimisation of wastewater treatment by lime

Determination of optimal pH conditions plays an important role in the wastewater treatment process. As a chemical component of the wastewater, pH has direct influence on wastewater treatability – regardless of whether treatment is physical or chemical process. The current wastewater treatment at studied site involves un-mechanised type system which lacks pH monitoring and control (Fig. 6.2), thus treatment optimisation is generally a source of major concerns.

Fig. 6.2. Un-mechanised wastewater treatment without pH monitoring and control

Based on results of geochemical modeling simulations; below are the results that:

- The addition of lime to drainage upto pH 6.3 (Fig. 6.2a) is sufficient to decrease significantly the Cu^{2+} concentrations to below regulation standard of 1.5 mg/l (EPA, 2017)
- Similarly, addition of lime to drainage upto pH 7.2 (Fig. 6.2b) is sufficient to decrease the Co2+ concentrations to below the regulation standard set by the WHO of 50 µg/l (WHO, 2005).

Therefore, in a binary system consisting of both Cu^{2+} and Co^{2+} ions as in the case of the drainage effluents at the studied site, the overall optimal pH 7.5 is sufficient to decrease the dissolved concentrations to below the regulated standards. The advantages of this optimal pH 7.5 are that; a) low amount of lime dosage is required; and b) less generation of voluminous amount of sludge that might require vast storage spaces of land.

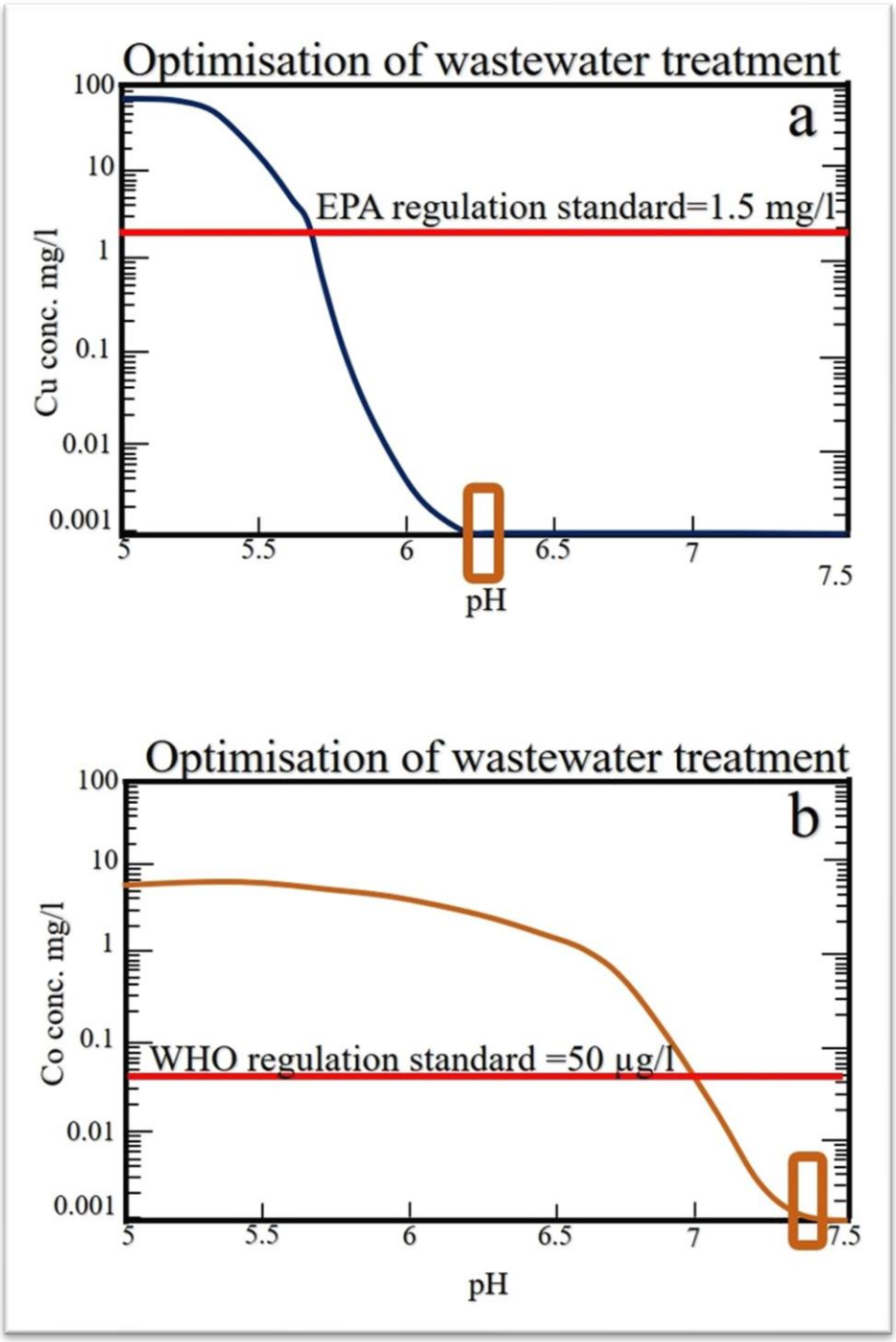

Fig. 6.3. SCM prediction of wastewater treatment optimisation; a) Cu^{2+} ions and b) Co^{2+} ions

6.3.2 Proposed optimisation treatment of effluents at mine site

The current wastewater treatment is of high cost associated with electricity charges and increased labour work for force due to the pumping back of sludge from the storage ponds to the treatment site that are 2.5 km distant apart. As a countermeasure to the existing lime treatment of effluents along the drainages, this study suggests the following measures;

- Construct an internal wastewater treatment facility that would replace the current system of pumping back sludge from storage sites to the treatment plant. Figure 6.3 illustrates how this process can be achievable at a minimum cost of operations. The advantages of this process are that:
  - Volumes of wastewater can be harvested in form of by-product during effluent treatment. This water can be used for domestic consumption or re-used for agricultural purposes
  - Minimal disposal of sludge solid to the storage ponds, thus minimizing the usage of vast spaces of land than can productively be used for human habitation and agriculture.

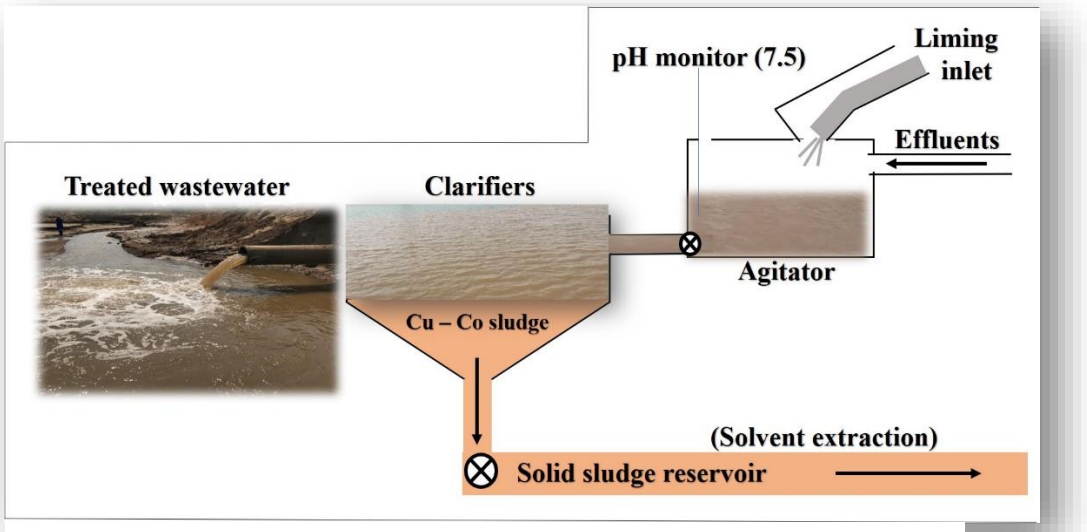

Fig. 6.4. Proposed wastewater treatment optimisation at the mine site

6.3.3 Metal stability

When rainwater fall onto the sludge at sludge storage ponds, it gets absorbed and becomes wet (capture and percolation). If wetting continues, the sludge gets progressively saturated with water (storage) and some of which might not be retained and overflows. Given the hydrogeochemical results and the mineralogical composition results obtained in chapter 4, and of adsorption onto kaolinite and HFO in chapter 5, it is evident that metal adsorption onto kaolinite and HFO is main retention mechanism in sludge. Overall, sludge physical and chemical properties and pH conditions play direct and preponderant roles in the metal retention mechanisms in sludge. The pH of rainwater recorded in wet seasons were pH 5.2 and 7.1 respectively whilst in the dry season was pH 7.3. The degree at which pH affects metal stability in sludge has been envisaged in this study through surface complexation modeling simulations.

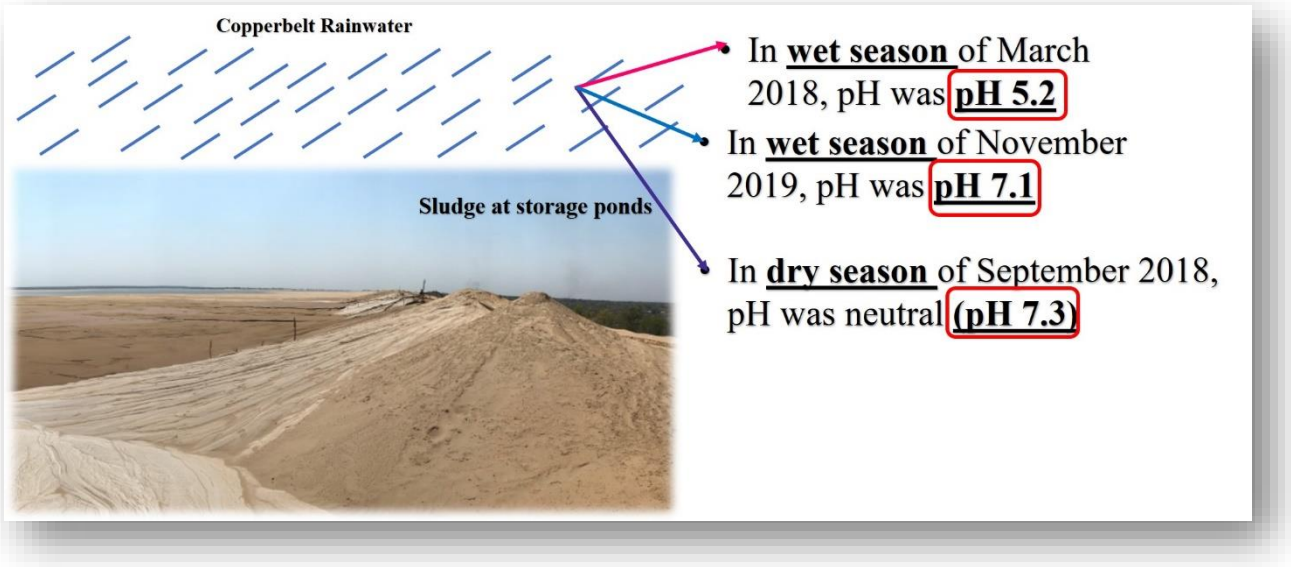

Fig. 6.5. Assessment of metal stability conditions through rainwater percolation onto sludges

6.3.3.1 Metal stability onto kaolinite surface

The adsorption of metals onto surfaces of natural and modified clays was previously reviewed by Liu and Zhang (2007) who suggested that the adsorption of trace metals on clay surfaces is mostly controlled by both surface reaction and surface binding sites provided the appropriate geochemical conditions are existing which allows for the ion exchange and complexation of metal cations with the functional groups on the uncovered surface (Liu and Zhang (2007). In chapter 5 (here-in), Cu^{2+} and Co^{2+} adsorption onto kaolinite surfaces was described and suggested that ion exchange and inner sphere complexation are the dominant retention mechanisms despite their weak binding strength compared to their contemporaneous HFO surfaces. The binding strength of kaolinite surfaces in sludge were assessed by surface complexation modeling and results are shown in Figure 6.6. According to the modeling predictions, pH > 5.5 is sufficient to retain Cu^{2+} and Co^{2+} ions on surfaces of kaolinite. It is therefore evident that labile fractions will begin to desorb from kaolinite as pH decreases below pH 5.5. As earlier indicated in Fig. 6.5 that pH 5.2 was once recorded in rainwater during the wet season (March 2018) suggesting that this low pH had some potential to cause desorption of Cu^{2+} and Co^{2+} from sludge. This result is consistent with results of sequential extraction (See Chapter 4) indicating that the high metal desorption does occur associated with exchangeable and acid soluble fraction.

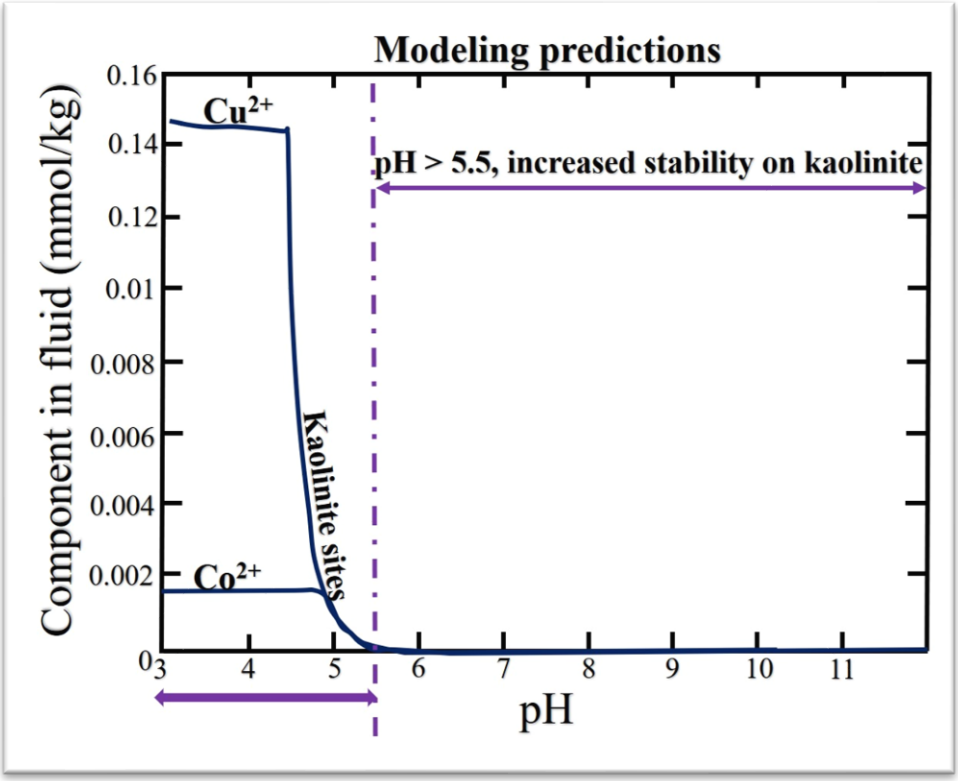

Fig. 6.6. Optimal pH of Cu^{2+} and Co^{2+} ion stability onto kaolinite surfaces

6.3.3.2 Metal stability onto HFO surface

Most previous studies have centred on metal adsorption and coprecipitation onto solid phases such HFO surfaces that are perceived to have enhanced metal retention ability as revealed by the behaviour of the adsorption edge through an observable shift to lower pH conditions (Crawford et al., 1993). During this adsorption process, the contaminants are not incorporated into the internal crystal structure of the solid surface, but rather remain adsorbed to the outer solid surface by chemisorption, resulting from the coordination between the contaminant and the hydroxyl surface or physisorption resulting from the electrostatic interactions, Van der Waals forces or dipole interactions (Peters, R W., Shem, L., 1993). This enhancement is mainly as a result of the greater binding to a single surface type or multiple surface site types due to an effective increase in surface

area for adsorption (Crawford et al, 1993). However, a few studies available in public domain have so far directly attempted to determine the pH conditions which affects the metal stability conditions in solid phase materials particularly using a well-defined model surface.

At high Cu concentrations, weak binding sites of HFO outcompetes the strong binding sites at high pH and the strong binding sites predominates only at low pH condition (See chapter 5). In addition, at low concentrations of Co, the strong binding sites outcompete the weak binding sites for Co over the low pH range. At high Co concentrations, the strong binding sites predominate only at low pH. Because all the strong binding sites become filled at higher pH, most of the Co resides at the more numerous weak binding sites at high pH and large Co concentrations (See chapter 5).

From our results of modeling simulations and predictions (Fig. 6.7), the ranges of pHs (i.e. pH > 5.1) for Cu and pH (i.e.., pH > 4.5) for Co are optimal to keep the metals stable from release by rainwater percolation. The results of the simulation are consistent with the results of Dzombak and Morel (1990) showing Cu and Co concentration to be more strongly adsorbed at high pH values than at low pH values. Therefore, at pH < 5.1 of rainwater, Cu^{2+} and Co^{2+} ions are likely to desorb from HFO surfaces, thereby posing an environmentally hazardous condition to the natural ecosystem.

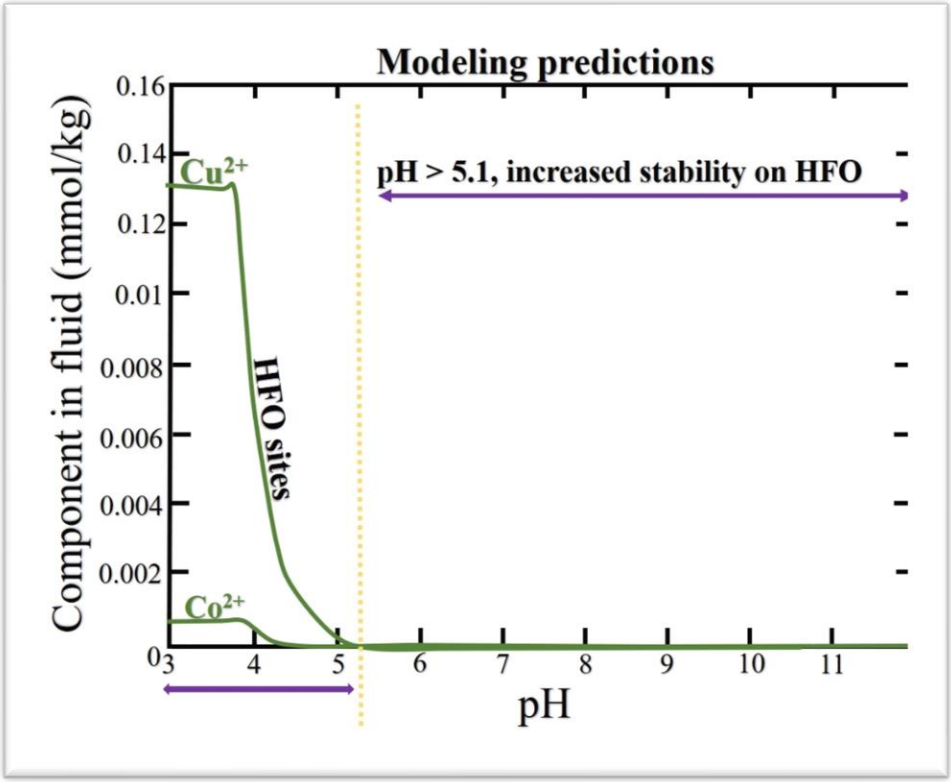

Fig. 6.7. Optimal pH of Cu^{2+} and Co^{2+} ions stability onto HFO surface

6.3.4 Metal recovery from sludge through acid treatment

Currently, the sludges are treated with high concentrated sulphuric acid (pH 1 – 1.5) to recover the adsorbed metals (Fig. 6.8). The major drawbacks of sludge treatment at concentrated low pH condition is as follows.

- High amount of SO_4^{2-} ions from $H_2SO_{4(aq)}$ are discharged together with sludge effluents into drainages. Such SO_4^{2-} ions tend to get involved in complexing and precipitation reactions such as gypsum and hexahydrite (See chapter 4) which affect solubility of dissolved metals and other substances.

- High amount of lime dosage is required to increase the pH to neutral conditions which is technically costly (quick lime) as far as mining operation costings is concerned.

However, based on our suggested results of sequential extraction (See chapter 4), weak or dilute acid treatment at pH 3 is enough to recover the metals from sludge. The advantages of this treatment is that:

- The concentrations of SO_4^{2-} ions in both drainages and sludge will be low, thus less complexation or precipitation of sulphate-rich salts (i.e., gypsum) that might impede the reuse of sludge as a construction material

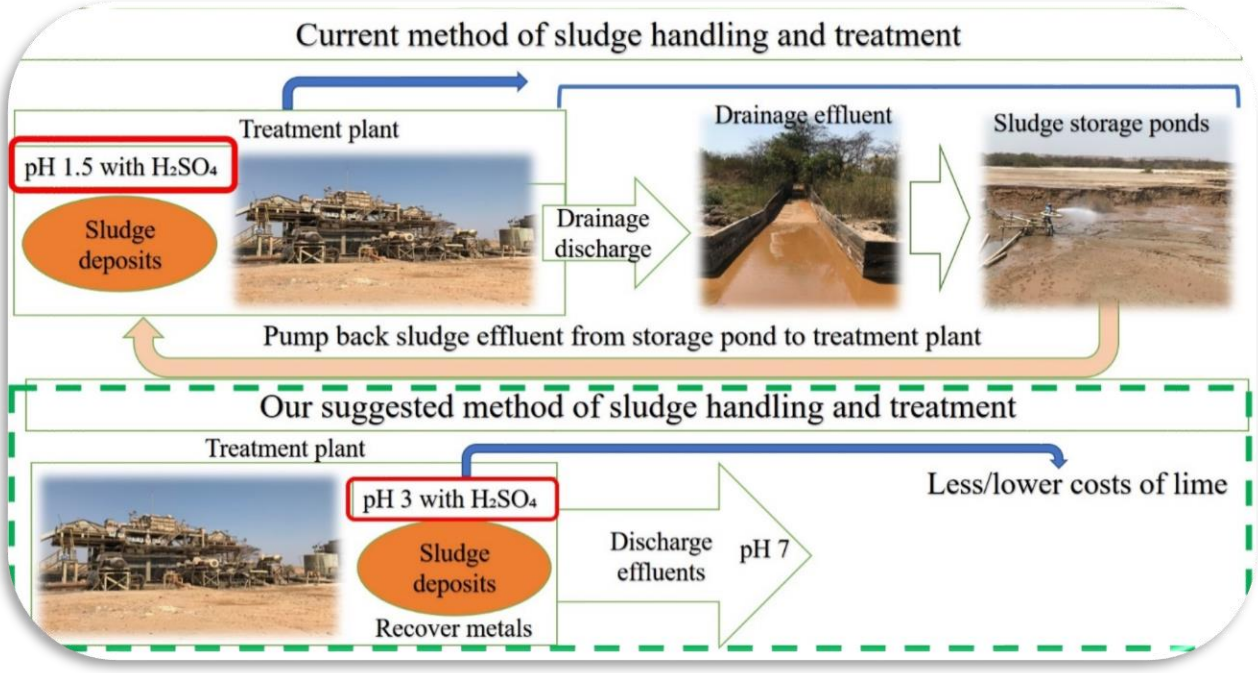

Fig. 6.8. Metal recovery from sludge through acid treatment

6.3.5 Heap and/or dump leaching

Heap leaching is a hydrometallurgical process whereby ore is stacked onto an impermeable base and 'irrigated' with a process solution that liberates the product from the ore and mobilises it into solution (Reichardt, 2008). It involves reprocessing of low-grade ores or mine waste for residual metals. A simplistic heap leach method is illustrated in Fig. 6.8. The lixiviating solution is irrigated on top of the metal-laden sludge and the discharged solution is collected at pregnant solution pond. This pond typically has several backup solution or storm ponds to handle temporary solution surges from weather events. The heap leach process is designed to contain all solutions from the environment and recover the dissolved metal or mineral values.

The advantages of the application of **heap leaching** to the currently studied solid waste materials are based on the following factors (refer to chapter 4):

- The absence in ***expansive clays*** that might significantly cause pore occlusions
- ***Easy agglomeration*** (i.e., sand (>53µm) + clay particles (<2µm)) to facilitate the leaching process
- ***Labile fractions*** dominating metal partitioning that easily desorb metals based sequential extraction results
- ***Availability of sulphuric acid (H_2SO_4)*** produced from smelter, thus low costs involved in the leaching process

Operational advantages of heap leaching at studied site

- High metals prices have prompted mining companies to consider treating previously uneconomic ore (i.e., metal-laden wastes such as sludges or tailings). From our results of sequential extraction the sludges contain Cu concentrations ranging between 0.5 – 2% and Co concentrations ranging between 0.02 – 0.07%. These metal concentrations economically feasibility at high metal prices
- Greater volumes of disposed waste material such as low-grade ore, metal-laden sludges or tailings can be reprocessed, thus minimizing unwarranted usage of productive land spaces.
- Heap leaching can result in more efficient reagent usage, as the process chemicals are retained within a closed circuit and recirculated for reuse (thus reducing the requirement for reagent 'top up' to maintain the leach solution at effective process concentrations) (Reichardt, 2008)

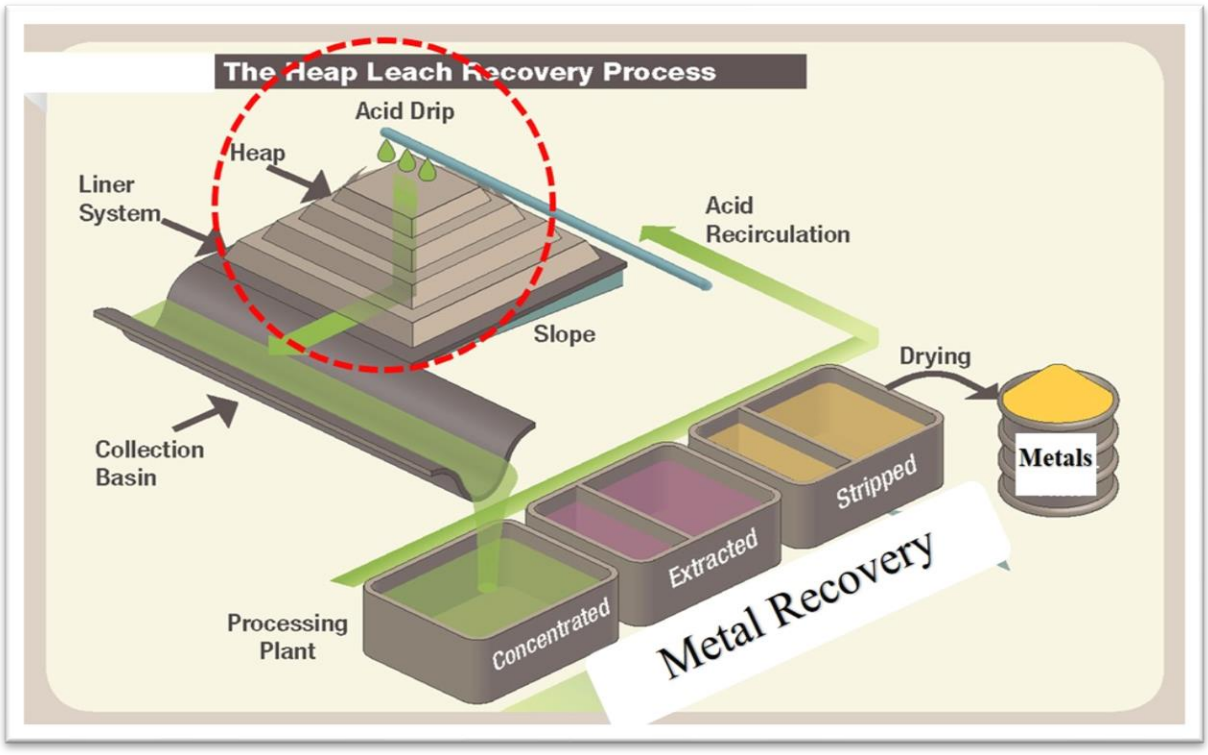

Fig. 6.8. Heap leaching methods. Courtesy of http://www.nrc.gov/reading-rm/doc-collections/nuregs/staff/sr1350/

6.4 Chapter 6-Summary

The study indicated that recycling and reuse are among the most efficient measures that can be taken to reduce the environmental impact of the mining generated wastes.

- The first option was by simple adsorption process treatment rather than installing expensive treatment systems that combine and increase the volume of the waste. The second option was metal recovery from waste through heap/dump leaching. These methods have potential of been of zero-discharge when successfully implemented. In practice this technology and its application go by many other names such as clean technology, waste minimization, pollution prevention, waste recycling, resource utilization, residue utilization, etc.
- Water reuse allows communities to become less dependent on groundwater and surface water sources and can decrease the diversion of water from sensitive ecosystems. Additionally, water reuse may reduce the nutrient loads from wastewater discharges into waterways, thereby reducing and preventing pollution. This ‘new’ water source may also be used to replenish overdrawn water sources and rejuvenate or reestablish those previously destroyed

Chapter 7: Conclusion, relevance and recommendations

7.1 Conclusions

This study discussed the geochemical behavior of heavy metals in sludge effluents on the Zambian Copperbelt. The major findings of the present study are summarized as follows:

Sludge effluent treatment with lime decreased the dissolved trace metals and influenced the precipitations of secondary minerals such as HFO. HFO exists as a coating on surfaces of component minerals such as micas (i.e. biotite and muscovite), kaolinite and quartz. The oxidations of Fe^{2+} to Fe^{3+} ions from biotite weathering and dissolution are the ultimate source of HFO precipitates.

Trace metal distribution and partitioning are concentrated in the exchangeable, acid-soluble and reducible fraction. The host mineral in the exchangeable and acid-soluble fraction is kaolinite whereas in reducible is HFO. In the absence of carbonates, this study has revealed that kaolinite show potential to host the metals associated with the acid-soluble fraction through batch experimental results. Cu and Co are partitioned mostly in the exchangeable and acid-soluble fraction that are commonly labile due to the loose or weak binding to kaolinite and HFO sites through adsorption mechanisms. Model predicted that Cu shows preferential and selective adsorption behavior onto the adsorption sites more than Co and because of metal competition for limited adsorption sites, most Co is relatively mobile into the environment.

Sludge treatment with lime is efficient in decreasing the trace metal concentrations at optimal pH 7.5. This optimal pH of treatment was derived from the observed maximum adsorption of metals in a binary system. At this pH condition, metals are stable and below the maximum contamination levels. The adsorbed metals are, however, easily leachable and recoverable after treatment with

acid at pH < 3. The resultant sludge can become a potential aggregate in the field of engineering after further treatment and purification.

7.2 Relevance to the scientific body of knowledge

The outcomes of this project have generated some important basic knowledge that have or will be useful in environmental remediation, specifically dealing with mechanism of heavy metal adsorption/desorption on mineral surfaces of sludges.

This research has revealed that metal partitioning is largely dominated by labile fractions bound by kaolinite and HFO through adsorption process as the main retention mechanism of the metals in sludge at solid-liquid interface. The metal binding onto kaolinite and HFO occurs at different sites (i.e. basal surface and edge surface sites). Heavy metals held on basal surfaces were exchangeable with other cations and at edge sites were weakly and/or loosely bound onto kaolinite and HFO sites. Following the metal binding behaviour envisaged with kaolinite and HFO surfaces, it means that slight changes in the geochemical conditions such as low pH increases the mobility of the metals. Thus, knowledge revealed by this study provides insights in to predicting the fate and transport of some heavy metals in sludge and its significance in designing technologies for cost effective remediation mechanism.

Wastewater treatment optimisation has been found to largely be influenced by the adsorption process. The study established that treatment of sludge effluents containing Cu and Co metals can efficiently be treated at optimal pH 7.5. At this pH condition, both metals are stable from release onto solid surfaces of the adsorbed minerals. The advantages of this optimal pH of treatment is that it generates relatively low voluminous gelatinous sludge as a result of low lime dosage, thereby reducing the operation costs and preserving land spaces that could have been taken up by sludge volumes.

Adsorption is reportedly a fast process that can occur within minutes, and the adsorbed metals tend to be loosely bound onto surfaces of the adsorbents. This condition is good in terms of metal recovery processes during the material leaching process. The removal of the adsorbed metals involves the use of less concentrated lixiviate solutions such as dilute sulphuric acid and acetate. This new knowledge has so far shown to nullify the use of some of the more costly and ineffective technologies currently employed.

7.3 Recommendations for future research

Technology and innovation: The current un-mechanised type of sludge effluent treatment onsite is highly inefficient and lacks optimisation. It is recommended that a well-designed circuit of effluent treatment be considered in the future undertaking that will allow less amount of lime treatment dosage and at the time allow enough resident time during treatment to yield meaningful results.

Results of SCM revealed that there exists competition for adsorption sites between Cu and Co metals in sludge effluents, and that Co inability to effectively compete with Cu renders it highly mobile into the environment. It is therefore recommended that when designing the effluents treatment between the metals, the effects of metal competition in multi-element wastewater be given strict considerations.

Reference

Angove, M.J., Johnson B.B., Wells, J.D., 1999. The influence of temperature on the adsorption of cadmium (II) and cobalt (II) on kaolinite. Journal of Colloid Interface, 204 93-103. https://doi.org/10.1006/jcis.1998.6010

Appel, C., Ma, L., 2002. Concentration, pH and surface charge effects on Cadmium and Lead sorption in three tropical soils. Journal of Environmental Quality 31, 581 - 589. https://doi.org/10.2134/jeq2002.5810

Arroyo, L.J., Li, H., Teppen, B.J., Boyd, S.A., 2005. A simple method for partial purification of reference clays. Clays and Clay Minerals 53, (5), 512 - 520. https://doi.org/10.1346/CCMN.2005.0530507

Atannasova, I.D., 1995. Adsorption and desoption of Cu at high pH equilibrium concentrations by soils and clay samples from Bulgaria. Environmental Pollution 87, 17 - 21. https://doi.org/10.1016/S0269-7491(99)80003-7

Bacon, J.R., Davidson, C.M., 2008. Is there a future for sequential chemical extraction? Analyst 133 (1), 25 - 46. https://doi.org/10.1039/B711896A

Balek, J., Perry, J.E., 1973. Hydrology of seasonally inundated African headwater swamps. Journal of Hydrology 19 (3), 227–249.

Bethke, C.M., 2008. Geochemical and biogeochemical reaction modeling, second ed. Cambridge University Press, New York.

Binda, P.L., 1994. Stratigraphy of Zambian Copperbelt orebodies. Journal of AfricanEarth Sciences 19, 251–264

Bisdom, E.B.A., Stoops, G., Delvigne, J., Curmi, P., Altemuller, H.J. 1982. Micromorphology of weathering biotite and its secondary products. Pedologie 32, (2), 225 – 252

Blengini, G.A.; Mathieux, F., Mancini, L.; Nyberg, M.; Viegas, H.M. (Editors); Salminen, J.; Garbarino, E.; Orveillon, G.; Saveyn, H.; Mateos Aquilino, V.; Llorens González, T.; García Polonio, F.; Horckmans, L.; D'Hugues, P.; Balomenos, E.; Dino, G.; de la Feld, M.; Mádai, F.; Földessy, J.; Mucsi, G.; Gombkötő, I.; Calleja,I., 2019. Recovery of critical and other raw materials from mining waste and landfills: State of play on existing practices, EUR 29744 EN, Publications Office of the European Union, Luxembourg, 2019, ISBN 978-92-76-08568-3, doi:10.2760/600775, JRC116131

Blowes, D.W., Ptacek, C.J., Jambor, J.L., Weisener, C.G., 2003. The geochemistry of acid mine drainage. In: Lollar, B.S., Holland, H.D., Turekian, K.K. (eds.), Environmental Geochemistry. Treatise on Geochemistry 9,149–204

Bourg, A.C.M., 1988. Metal in aquatic and terrestrial systems: Sorption, speciation and mobilisation, in Solomons, W., and Forstner, U., (eds)., Chemistry and biology of solid waste: Berlin, Springer-Verlag, 3 - 32

Bradl, H.B., 2004. Adsorption of metal ions on soils and soil constituents. Journal of colloidal and interface science, 277, 1-18.

Brame, J. A., Griggs, C., 2016. Surface Area Analysis Using the Brunauer-Emmett-Teller (BET) Method: Scientific Operation Procedure Series : SOP-C. Engineer Research and Development Center: 1–23.

Bullock, A., 1992. Dambo hydrology in southern Africa-review and reassessment. Journal of Hydrology 134 (1–4), 373–396.

Carroll, D., 1959. Ion exchange in clays and other minerals. Geological society of America Bulletin 70, (6), 749-779. https://doi.org/10.1130/0016-7606(19859)70[749:IEICAO]2.0.CO;2

Chakraborty, S., Bardelli, F., Mullet, M., Greneche, Jean-Marc., Varma, S., Ehrhardt, Jean-Jacques., Banerjee, D., Charlet, L., 2011. Spectroscopic studies of arsenic retention onto biotite. Chemical geology 281, 83 - 92. doi:10.1016/j.chemgeo.2010.11.030

Chang, J.E., Lin,T.T., Lo, M.S., Liaw, D.S., 1999. Stabilization/Solidification of Sludges Containing Heavy Metals by Using Cement and Waste Pozzolans. Journal of Environmental Science and Health A34 (5), 1143-1160

Chao, T. T., Zhou, L., 1983. Extraction Techniques for Selective Dissolution of Amorphous Iron Oxides from Soils and Sediments. Soil Science Society of America Journal 47(2), 225–32. https://doi.org/10.2136/sssaj1983.03615995004700020010x

Crawford, R.J., Harding, I.H., Mainwaring, D.E., 1993. Adsorption and Coprecipitation of Single Heavy Metal Ions onto the Hydrated Oxides of Iron and Chromium. Langmuir, 9, 3050-3056

Crawford, J., 1999. Geochemical Modelling – A Review of Current Capabilities and Future Directions. Natur Vards Verket (Swedish Environmental Protection Agency). Retrieved from http://www.swedishepa.se/Documents/publikationer/afr-r-262-se.pdf

Davis J.A., Coston J.A., Kent D.B. and Fuller C.C. (1998), "Application of the surface complexation concept to complex mineral assemblages", Environ. Sci. Technol. 32, 2820-2828.

Davis J.A., Payne, T.E. and Waite, T.D. (2002), "Simulating the pH and pCO2 dependence of uranium(VI) adsorption by a weathered schist with surface complexation models", in Geochemistry of Soil Radionuclides, Special publication No. 59, Zhang PC, Brady PV (ed.), Soil Science Society of America, Madison, WI.

Davis, J. A.,. Hayes, K.F., 1986. Geochemical Processes at Mineral Surfaces : An Overview Water Resources Division. https//doi.org/10.1021/bk-1987-0323.ch001

Davis, J. A.; Meece, D. E.; Kohler, M.; Curtis, G. P., 2004. Approaches to surface complexation modeling of uranium (VI) adsorption on aquifer sediments. Geochim. Cosmochim. Acta 2004, 68 (18), 3621− 3641.

Davis, J.A., Coston, J.A., Kent, D.B., Fuller, C.C., 1998. Application of the surface complexation concept to complex mineral assemblages. Environmental Science and Technology 32, 2820–2828. https://doi.org/10.1021/es980312q

Diederix, D., 1977. The geology of Nchanga Mining Licence Area. Unpublished Company Report, Nchanga Consolidated Copper Mines Limited Chingola Division, pp. 59

Dong Wenming., Wan, Jianmin., 2014. Additive surface complexation modeling of uranium (VI) adsorption onto quartz-sand dominated sediments. Environmental Science and Technology 48, 6569 - 6577. https//dx.doi.org/10.1021/es501782g

Dzombak, D.A., Morel, F.M.M., 1990. Surface Complexation Modeling: Hydrous Ferric Oxide. John Wiley and Sons, New York

EPA., 2017. National primary drinking water regulations. http://water.epa.gov/drink/contaminants/index.cfm.

Essen, J., El Bassam, N., 1981. On the mobility of cadmium under aerobic soil conditions. Environmental Pollution Series A, Ecological and Biological 26 (1) 15-31. https://doi.org/10.1016/0143-1471(81)90095-7

Esteoule-Choux, J., Esteoule, J., Hallalouche, D., 1995. Congruent dissolution of microcline and epitaxial growth and skeletal quartz during weathering of a granite the Central Hoggar (Algeria). In Clays: Controlling the Environment edited by GJ Churchman, RW Fitzpatrick, RA Eggleton

Ettler, Vojtěch 1, Martina Vítková, Martin Mihaljevič, Ondřej Šebek, Mariana Klementová, František Veselovský, Pavel Vybíral, Bohdan Kříbek., 2014. Dust from Zambian smelters: mineralogy and contaminant bioaccessibility. Environ Geochem Health 36(5):919-33. doi: 10.1007/s10653-014-9609-4

Evans,L.J., 1989. Chemistry of metal retention by soils. Environ Sci. Technol, 23 (1989), pp. 1046-1056

Everett, P.A., Lister, T.R., Fordyce, F.M., Ferreira, A.M.P.J., Donald, A.W., Gowing, C.J.B., Lawley, R.S., 2019. Stream sediment geochemical atlas of the United Kingdom. Geoanalytical and modeling program. Open report OR/18/048. British Geological Survey, pp. 94

Fan, Q., Li, P., Pan, D., 2019. Radionuclides sorption on typical clay minerals: Modeling and spectroscopies. Interface Science and Technology 29, 1-38. https://doi.org/10.1016/B978-0-08-102727-1.00001-7

Fanning, D.S., Keramidas, V.Z., El-Desoky, M.A., 1989. Minerals in Soil Environments, Volume 1, Second Edition. Soil Science Society of America, Madison, Wisconsin

Filgueiras, A.V., Lavilla, I., Bendicho, C., 2002. Chemical sequential extraction for metal partitioning in environmental solid samples. Journal of Environmental Monitoring, 4, 823-857. https://doi.org/10.1039/B207574C

Ghabru, S.K., Mermut, A.R., St.Arnaud, R.J., 1987. The nature of weathered biotite in sand-sized fractions of Gray Luvisols (Boralfs) in Saskatchewan, Canada. Geoderma 40, 1–2, 65-82. https://doi.org/10.1016/0016-7061(87)90014-0

Ghose, A. K., 2009. Technology vision 2050 for sustainable mining. The 6th International Conference on Mining Science & Technology. Procedia Earth and Planetary Science 1, 2–6. http//doi.org/10.1016/j.pro .2009.09.003

Gilbert, S.E., Cooke, D.R., Hollings, P., 2003. The effects of hardpan layers on the water chemistry from the leaching of pyrrhotite-rich tailings material. Environmental Geology 44, 687–697. https://doi.org/10.1007/s00254-003-0810-5

Gilkes, R.J., Suddhiprakarn, A., 1979. Biotite alteration in deeply weathered granite. i. morphological, mineralogical, and chemical properties. Clays and Clay Minerals 27,5, 349-360, 1979.

Girvin, D.C., L.L. Ames, A.P. Schwab, and J.E. McGarrah. 1991. Neptunium adsorption on synthetic amorphous iron oxyhydroxide. Journal of Colloid and Interface Science 141: 67-78

Glaydson Simoes dos Reisa., Bogdan Grigore Cazacliu, Catalina Rodriguez Correa, Ekaterina Ovsyannikova ,Andrea Kruse , Carlos Hoffmann Sampaioa, Eder Claudio Lima , Guillherme Luiz Dotto., 2020. Adsorption and recovery of phosphate from aqueous solution by the construction and demolition wastes sludge and its potential use as phosphate-based fertiliser. Journal of Environmental Chemical Engineering 8, 1, 103605. https://doi.org/10.1016/j.jece.2019.103605

Goldberg, S., Criscenti, L.J. 2008. Modeling adsorption of metals and metalloids by soil components. In: A. Violante et al., editors, Biophysico-chemical processes of heavy metals and metalloids in soil environments. John Wiley & Sons, New York. p. 215– 264.

Graupner, T., Kassahun, A., Rammlmair, D., Meima, J.A., Kock, D., Furche, M., Fiege, A., Schippers, A., Melcher, F., 2007. Formation of sequences of cemented layers and hardpans within sulfide-bearing mine tailings (mine district Freiberg, Germany). Applied Geochemistry 22, 2486–2508. https://doi.org/10.1016/j.apgeochem.2007.07.002

Grim, R.E., 1968. Clay Mineralogy, 2nd edition. McGraw-Hill, New York.

Gu, Xueyuan., Evans, Les J., 2008. Surface complexation modeling of Cd(II), Cu(II), Ni(II), Pb(II) and Zn(II) adsorption onto kaolinite. Geochimica et Cosmochimica Acta 72, 267–276. http://dx.doi.org/10.1016/j.gca.2007.09.032.

Gustafsson, J.P., Pechova, P., 2003. Modeling Metal Binding to Soils: The Role of Natural Organic Matter. Environmental Science and Technology 37, 2767-2774. https//doi.org/10.1021/es026249t

Hansen, B.O., Kwan, P., Benjamin, M.M., Li, Chi-Wang., Korshin, G.V., 2001. Use of iron oxide-coated sand to remove strontium from simulated Hanford tank wastes. Environmental Science and Technology 35, 4905 - 4909. https://doi.org/10.1021/es0108990

Harter, R. D. 1992. Competitive Sorption of Cobalt, Copper, and Nickel Ions by a Calcium-Saturated Soil. Soil Science Society of America Journal 56 (2), 444–49. https://doi.org/10.2136/sssaj1992.03615995005600020017x

Hass,A., Fine, P., 2010. Sequential Selective Extraction Procedures for the Study of Heavy Metals in Soils, Sediments, and Waste Materialsa Critical Review. Critical Reviews in Environmental Science and Technology 40 (5), 365–99. https://doi.org/10.1080/10643380802377992

Hayes, K. F., and Katz, L. E. (1996). "Application of X-ray absorption spectroscopy for surface complexation modeling of metal ion adsorption." Physics and Chemistry of Mineral Surfaces, P. V. Brady, ed., CRC Press, Boca Raton, Fla, 147-223.

Hayesm K.F., 1987. Equilibrium, spectroscopic and kinetic studies of ion adsorption at the oxide/aqueous interface. PhD. Thesis, Stanford University, Stanford, CA.

Hayes, K. F., and Leckie, J. O. (1986). "Mechanism of Lead-Ion Adsorption at the Goethite-Water Interface." Acs Symposium Series, 323, 114-141.

Heiri, O., Lotter, A.F. & Lemcke, G. Loss on ignition as a method for estimating organic and carbonate content in sediments: reproducibility and comparability of results. Journal of Paleolimnology 25, 101–110 (2001). https://doi.org/10.1023/A:1008119611481

Horowitz, A.J., 1985. A Primer on Trace Metal Sediment Chemistry. United States Geological Survey Water-Supply Paper 84 - 2277

Hughes J. C., Brown G., 1979. A crystallinity index for soil kaolins and its relation to parent rock, climate and soil maturity. Journal of soil science 30, 557 – 563. https://doi.org/10.1111/j.1365-2389.1979.tb01009.x

Huthnance, J. M., Allen, J., Davies, I. A. M., Hydes, D. J., James, 1. D., Jones, J. E., Millward, G. E., Prandle, D., Proctor, R., Purdie, D. A., Statham, P. J., Tett, P. B., Thomson, S. & Wood, R. G. (1994). Towards water quality models. In Understanding the North Sea System (H. Charnock, K. R. Dyer, J. M. Huthnance, P. S. Liss, J. H. Simpson & P. B. Tett, eds), pp. 191-206. Chapman and Hall, Cambridge, UK.

Ikhsan, J., Johnson, B.B., Well, J.D., 1999. A comparative study of the adsorption of transition metals on kaolinite. Journal of colloid and Interface Science 217, 403-410. https://doi.org/10.1006/jcis.1999.6377

Irving J. P., H., Williams, H., 1948. Order of Stability of Metal Complexes. Nature 162, 746–47. https://doi.org/10.1038/162746a0

Ito, A., Otake, T., Ki-Cheol Shin, Kamar Shah Ariffin, Fei-Yee Yeoh, Sato, T., 2017. Geochemical Signatures and Processes in a Stream Contaminated by Heavy Mineral Processing near Ipoh City, Malaysia. Applied Geochemistry 82, 89–101. https://doi.org/10.1016/j.apgeochem.2017.05.007

Jenne, E. A., 1968. Controls on Mn, Fe, Co, Ni, Cu, and Zn concentrations in soils and water: the significant role of hydrous Mn and Fe oxides, Advances in Chemistry Series, Vol. 73, Trace Inorganics in Water, pp. 337-387

Jenne, E.A., 1998. Adsorption of Metals by Geomedia Variables, Mechanisms, and Model Applications. Academic press, USA

Jung J, Cho Y-H, Hahn P: Comparative study of Cu2+ adsorption on goethite, hematite and kaolinite: mechanistic modeling approach. Bulletin Korean Chemical Society 1998, 19:324-327.

Kachan D., 2013. Emerging Green Mining Innovation: Managing risk and profiting from new 15 mining technology breakthroughs. Canada; Kachan & Co.

Kampunzu, A.B., and Cailteux, J.L.H., 1999, Tectonic evolution of the Lufilian arc (Central Africa Copper Belt) during Neoproterozoic Pan African orogenesis: Gondwana Research, v. 2, no. 3, p. 401–421 (Modified stratigraphic map)

Kent, D.B., Abrams, R.H., Davis, J.A., Coston, J.A. and LeBlanc, D.R. (2000), "Modelling the influence of variable pH on the transport of zinc in a containated aquifer using semiempirical surface complexation models", Water Res. Research 36, 3411-3425.

Kinniburgh, D.G. and Jackson, M.L. 1981. Cation adsorption by hydrous metal oxides and clay. In: M.A.Anderson and A.J.Rubin (eds) Adsorption of Inorganics at Solid-Liquid Interfaces. Ann Arbor Science, Michigan

Kinoshita, T., Akita, S., Kobayashi, N., Nii, S., Kawaizumi, F., Takahashi, K., 2003. Metal recovery from non-mounted printed wiring boards via hydrometallurgic processing. Hydrometallurgy 69 (1–3), 73–79

Kirkey, J., 2014. Eco Friendly Mining Trends for 2014. Available online at: https:// www.mining-technology.com/features/featureenvironment-friendly-miningtrends-for-2014-4168903/. https://doi.org/10.3389/fenrg.2020.00018

Koretsky, C., 2000. The significance of surface complexation reactions in hydrologic systems: a geochemist's perspective. Journal of Hydrology 230, 127–171

Landry, C., Koretsky, C.M., Tracy J. Lund, T.J.,Schaller, M.,Das, S., 2009. Surface Complexation Modeling of Co(II) Adsorption on Mixtures of Hydrous Ferric Oxide, Quartz and Kaolinite. Geochimica et Cosmochimica Acta 73 (13), 3723–37. https://doi.org/10.1016/j.gca.2009.03.028

Lee, G., Bigham, J.M., Faure, G., 2002. Removal of trace metals by coprecipitation with Fe, Al and Mn from natural waters contaminated with acid mine drainage in the Ducktown Mining District, Tennessee. Applied Geochemistry 17, 569–581

Leermakers, M., Mbachou, B.E., Husson, A., Lagneau, V., Descostes, M., 2019. An alternative sequential extraction scheme for the determination of trace elements in ferrihydrite rich sediments. Talanta 199, 80–88

Levlin, E., 1998. Sustainable Sludge Handling – Metal and Phosphorus Removal Proceedings of a Polish-Swedish seminar. In Advanced Wastewater Treatment, B. Hultman, J. Kurbiel, ISBN 91-7170-324-1, 73-82.

Lim, C.H., Jackson, M.I., Koons, R.D., Helmke, P.A., 1980. Kaolins: sources of differences in cation-exchange capacities and cesium retention. Clays and Clay Minerals, 28, 3, 223-229, 1980.

Lindsay, M.B.J., Moncur, M.C., Bain, J.G., Jambor, J.L., Ptacek, C.J., Blowes, D.W., 2015. Geochemical and mineralogical aspects of sulfide mine tailings. Applied Geochemistry 57, 157 - 177. http://dx.doi.org/10.1016/j.apgeochem.2015.01.009

Liu, P., Zhang, L.X., 2007. Adsorption of dyes from aqueous solutions or suspensions with clay nano-adsorbents. Separation and Purification Technology 58 (1), 32-39. https://doi.org/10.1016/j.seppur.2007.07.007

Loganathan, P., Vigneswaran, J.K., Naidu, R., 2012. Cadmium sorption and desorption in soils: A review. Critical reviews in environmental science and technology, 42(5), 489 - 533. https://doi.org/10.1080/10643389.2010.520234

Lottermoser, B.G., 2010. Mine Wastes Characterization, Treatment and Environmental Impacts. 3rd edition, Springer Heidelberg Dordrecht London New York

Lund, T.J., Koretsky, C.M., Landry, C.J., Schaller, M.S., Das, S., 2008. Surface complexation modeling of Cu(II) adsorption on mixtures of hydrous ferric oxide and kaolinite. Geochemical Transaction 9 (9), 1 - 16. https//doi.org/10.1186/1467-4866-9-9

María Jesús Belzunce., Oihana Solaun., José Antonio González Oreja., Esmeralda Millán., Víctor Pérez., 2004. Chapter 12 - Contaminants in sediments. Elsevier Oceanography Series 70, Pages 283-315

McBride, M.B., 1989. Reactions controlling heavy metal solubility in soil. Adv Soil Sci, 10 (1989), pp. 1-56

McGowan, R.R., Roberts, S., Boyce, A.J., 2006. Origin of the Nchanga copper–cobalt deposits of the Zambian Copperbelt. Mineralium Deposita 40, 617–638. https//doi.org/ 10.1007/s00126-005-0032-8

McGowan, R.R., Roberts, S., Boyce, A.J., 2006. Origin of the Nchanga copper-cobalt deposits of the Zambian Copperblt. Mineral Deposita 40, 617-638

McGregor, R.G., Blowes, D.W., 2002. The physical, chemical and mineralogical properties of three cemented layers within sulfide-bearing mine tailings. Journal of Geochemical Exploration 76, 195–207. https://doi.org/10.1016/S0375-6742(02)00255-8

McLean, J.E., Bledsoe, B.E., 1992. Behavior of Metals in Soils. Ground Water Issue. EPA/540/S-92/018

Mehra, O. P., 2013. Iron Oxide Removal from Soils and Clays by a Dithionite-Citrate System Buffered with Sodium Bicarbonate. Clays and Clay Minerals 7(1), 317–27. https://doi.org/10.1016/B978-0-08-009235-5.50026-7

Mendelsohn, F., 1961. The Geology of the Northern Rhodesian Copperbelt. Macdonald and Co., London. 523 pp

Nordstrom, D.K., Alpers, C.N., 1999. Geochemistry of acid mine waters. In: Plumlee, G.S., Logsdon, M.J. (eds.), The Environmental Geochemistry of Mineral Deposits, Reviews in Economic Geology 6A. Society of Economic Geologists Inc.,Littleton, Colorado, USA, 133–160. http://dx.doi.org/10.1016/j.apgeochem.2015.01.0090

Nordstrom, D.K., 2011. Mine Waters: Acidic to Circumneutral. Elements 7, 393–398. http://dx.doi.org/10.2113/gselements.7.6.393

Nowak, O., 2006. Optimizing the Use of Sludge Treatment Facilities at Municipal WWTPs. Journal of Environmental Science and Health, Part A Toxic/Hazardous Substances and Environmental Engineering 41 (9), 1807-1817. https://doi.org/10.1080/10934520600778986

O'Day, P.A., Parks, G.A., Brown, G.E., 1994. Molecular Structure and Binding Sites of Cobalt(II) Surface Complexes on Kaolinite from X-Ray Absorption Spectroscopy. Clays Clay Mineral. 42, 337–355. https://doi.org/10.1346/CCMN.1994.0420312

Oakley, S.M., Nelson, P.O., Williamson, K.J., 1981. Model of Trace-Metal Partitioning in Marine Sediments. Environmental Science and Technology 15 (4), 474-480. https//doi.org/ 10.1021/es00086a015

O'Connor, D.J., 1988. Models of sorptive toxic substances in freshwater systems. I. Basic equations. J Environ Engrg, 114 (1988), pp. 507-532

O'Day, P.A., Parks, G.A., Brown, G.E., 1994. Molecular Structure and Binding Sites of Cobalt(II) Surface Complexes on Kaolinite from X-ray Absorption Spectroscopy. Clays and Clay Minerals 42, 3, 337-355. http//doi.org/10.1346/CCMN.1994.0420312

Ogasawara, M., Mikoshiba , M., Geshi, N., Shimoda, G., Ishizuka, Y., 2018. Optimization of analytical conditions for major element analysis of geological samples with XRF using glass beads. Bulletin of the Geological Survey of Japan, vol. 69 (2), p. 91–103, 2018

Pan, Z., Li, W., Fortner, J.D., Giammar, D.E., 2017. Measurement and surface complexation modeling of U(VI) adsorption to engineered iron oxide nanoparticles. Environmental Science and Technology 51, 9219 - 9226. https//doi.org/10.1021/acs.est.7b01649

Payne, T.E., K. Sekine, J.A. Davis, and T.D. Waite. 1992. Modeling of radionuclide sorption processes in the weathered zone of the Koongarra ore body. Alligator Rivers Analogue Project

Annual Report, 1990-1991. P. Duerden, ed. Australian Nuclear Science and Technology Organization: 57-85

Peacock C. L, Sherman D. M: Surface complexation model for multisite adsorption of copper (II) on kaolinite. Geochimica et Cosmo chimica Acta 2005, 69:3733-3745.

Peters, R W., Shem, L. Separation of heavy metals: Removal from industrial wastewaters and contaminated soil. United States: Web.

Peterson,R.C., Hammarstrom, J.M., Seal, R.R., 2006. Alpersite (Mg,Cu)SO4·7H2O, a new mineral of the melanterite group, and cuprian pentahydrite: Their occurrence within mine waste. American Mineralogist 91, 261–269. https://doi.org/10.2138/am.2006.1911

Petterson, U.T., Ingri, J., Anderson, P.S., 2000. Hydrogeochemical processes in the Kafue River upstream from the Copperbelt Mining Area. Aqua Geochemistry 6,385–411

Pettersson, U.T., Johan Ingri, J.,2001. The Geochemistry of Co and Cu in the Kafue River as It Drains the Copperbelt Mining Area, Zambia. Chemical Geology 177 (3–4), 399–414. https://doi.org/10.1016/S0009-2541(00)00422-8

Porada, H., Berhorst, V., 2000. Toward a new understanding of the Neoproterozoic-Early Palaeozoic Lufilian and northern Zambezi Belts in Zambia and the Democratic Republic of Congo. Journal of African Earth Sciences 30, 727–771.

Prusty, B.G., Sahu, K.C., Godgul, G., 1994. Metal contamination due to mining and milling activitites at the Zawar zinc mine, Rajasthan, India. Contamination of stream sediments: Chemical Geology 112, 275 - 292. https://doi.org/10.1016/0009-2541(94)90029-9

Qin, Hai-Bo., Yang, S., Tanaka, M., Sanematsu, K., Arcilla, C., Takahashi, Y., 2020. Chemical speciation of scandium and yttrium in laterites: New insights into the control of their partitioning behaviors. Chemical Geology 552, 119771. https://doi.org/10.1016/j.chemgeo.2020.119771

Quispe, D, Pérez-López, R, Acero, P., Ayora, C., Miguel Nieto, J., Tucoulou, R., 2013. Formation of a hardpan in the co-disposal offly ash and sulfide mine tailings and its influence on the generation of acid mine drainage. Chemical Geology 35, 45 - 55. https://doi.org/10.1016/j.chemgeo.2013.07.005

Rainaud,S., Armstrong, M.R.A., Robb, L.J., 2005. Geochronology and Nature of the Palaeoproterozoic Basement in the Central African Copperbelt (Zam bia and the Democratic Republic of Congo), with Regional Implications. Journal of African Earth Sciences 42 (1-5), 1–31. https://doi.org/10.1016/j.jafrearsci.2005.08.006

Rauret, G., López-Sánchez, J.F., Sahuquillo, A., Rubio, R., Davidson, C., Ure, A., Quevauviller, P., 1999. Improvement of the BCR three step sequential extraction procedure prior to the certification of new sediment and soil reference materials. Journal of environmental monitoring 1, 57 - 67. https://doi.org/10.1039/A807854H

Reichardt, C., 2008. Heap Leaching and the Water Environment – Does Low Cost Recovery Come at a High Environmental Cost?. https://www.IMWA CONGRESS 2008_f.doc

Rounds, S.S.,2015. Alkalinity and acid neutralizing capacity. In: Wilde, F.D.(eds.) National Field manual for the collection of water-quality Data. Handbook for water-Resources investigations. USGS, Reston, VA.

Salomons, W. & Fösrtner, U. (1984). Metals in the hydrocycle. 3. Sediments and the transport of metals. Berlin: Springer.

Sanchez Espana, J., 2008. Acid Mine Drainage in the Iberian Pyrite Belt: an Overview with special emphasis on generation mechanisms, aqueous composition and associated mineral phases. Macia 10, 34 - 43

Sanchez, A.L., J.W. Murray, and T.H. Sibley. 1985. The adsorption of plutonium IV and V on goethite. Geochimica et Cosmochimica Acta 49: 2,297-2,307

Santhanama, M., Cohen, M.D., Olek, J., 2003. Effects of gypsum formation on the performance of cement mortars during external sulfate attack. Cement and Concrete Research 33, 325 – 332. https://doi.org/10.1016/S0008-8846(02)00955-9

Schindler, P.W., Liechti, P.; Westall, J.C.., 1987. Adsorption of copper, cadmium and lead from aqueous solution to the kaolinite/water interface. Netherlands Journal of Agriculture Science 35, 219

Serrano, S., Peggy, A. O'Day , P.A., Vlassopoulos, D., Garcı´a-Gonza´lez, M.T., Garrido, F., 2009. A surface complexation and ion exchange model of Pb and Cd competitive sorption on natural soils. Geochimica et Cosmochimica Acta 73, 543–558. https//doi.org/10.1016/j.gca.2008.11.018

Sghaier, N., Prat, M. Effect of Efflorescence Formation on Drying Kinetics of Porous Media. Transp Porous Med 80, 441 (2009). https://doi.org/10.1007/s11242-009-9373-6

SGS MINERALS SERVICES REPORT – T3 SGS 853, 10-2013

Shin-Min Shih, Ch'un-Sung Ho, Yuen-Sheng Song, and Jyh-Ping Lin., 1999. Kinetics of the Reaction of Ca(OH)2 with CO2 at Low Temperature. Industrial and Engineering Chemistry Research 38 (4), 1316-1322. https://doi.org/10.1021/ie980508z

Shiqing Gu, Xiaonan Kang, Lan Wang, Eric Lichtfouse, Chuanyi Wang., 2019. Clay mineral adsorbents for heavy metal removal from wastewater: a review. Environmental Chemistry Letters, Springer Verlag 17 (2), pp.629-654. ff10.1007/s10311-018-0813-9f

Shuman, L. M. 1991. Chemical forms of micronutrients in soils. In J. J. Mortvedt (ed.). Micronutrients in agriculture. Soil Soc. Soc. Amer. Book Series #4. Soil Sci. Soc. Amer., Inc., Madison, WI

Singh, K., Subramanian, V., Gibbs, R.J., 1984. Hydrous Fe and Mn oxides - Scavengers of heavy metals in the aquatic environment. Critical Reviews in Environmental Control 14, 33-90. https://doi.org/10.1080/10643388409381713

Smith, K.S. 1999. Metal sorption on mineral surfaces: An overview with examples relating to mineral deposits. In The Environmental Geochemistry of Mineral Deposits. Part B: Case Studies and Research Topics. 6B, Chapter 7. Filipek, L., Plumlee, G. (eds). Reviews in Economic Geology. Society of Economic Geologists, Inc., Chelsea, MI, 161-182.

Solomons, W., 1995. Environmental impact of metals derived from the mining activities: Processes, predictions, prevention: Journal of Geochemical Exploration 52, 5 - 23. https://doi.org/10.1016/0375-6742(94)00039-E

Song, Qingbin., Li, Jinhui., Zeng, Xianlai., 2015. Minimizing the increasing solid waste through zero waste strategy. Journal of Cleaner Production 104, 199 – 210. http://dx.doi.org/10.1016/j.jclepro.2014.08.027 0959-6526

Spark, K. M., Johnson, B.B., Wells, J.D., 1995. Characterizing Heavy-metal Adsorption on Oxides and Oxyhydroxides. European Journal of Soil Science 46 (4): 621–31

Sposito, G. 1984. The surface chemistry of soils. Oxford University Press, New York.

Sracek, O, Veselovsky, F., Kribek, B., Malec, J., Jehlicka, J., 2010. Geochemistry and Mineralogy of Cu and Co in Mine Tailings at the Copperbelt, Zambia. Journal of African Earth Sciences 57(1–2), 14–30. https://doi.org/10.1016/j.jafrearsci.2009.07.008

Sracek, O., 2015. Formation of secondary hematite and its role in attenuation of contaminants at mine tailings: review and comparison of sites in Zambia and Namibia. Frontiers in Environmental Science. https//doi.org/ 10.3389/fenvs.2014.00064

Sracek, O., Kribek,B., Mihaljevic, M., Majer, V., Veselovsky., Vencelides, Z., Nyambe, I. 2012. Mining-Related Contamination of Surface Water and Sediments of the Kafue River Drainage System in the Copperbelt District, Zambia: An Example of a High Neutralization Capacity System. Journal of Geochemical Exploration 112, 174–88. https://doi.org/10.1016/j.gexplo.2011.08.007

Sracek, O., Mihaljevič, M., Kříbek, B., Majer, V., Veselovský, F., 2010. Geochemistry and mineralogy of Cu and Co in mine tailings at the copperbelt, Zambia. Journal of African Earth Sciences 57 (i-2), 14-30.

Srivastava, P., Singh, B., Angove, M., 2005. Competitive adsorption behavior of heavy metals on kaolinite. Journal of Colloid Interface Science 290, 28 - 38. https://doi.org/10.1016/j.jcis.2005.04.036

Stumm, W., Morgan, J.J., 1995. Aquatic Chemistry: Chemical Equilibria and Rates in Natural Waters, 3rd (eds). A Wiley-interscience publication John Wiley & Sons, Inc. New York

Stumm, W., Morgan, J.J., 1996. Aquatic chemistry: chemical equilibria and rates in natural waters, 3rd ed., John Wiley & Sons, New York, NY.

Sverjensky D. A., Sahai N., 1996. Theoretical prediction of single-site surface-protonation equilibrium constant for oxides and silicates in water. Geochim. Cosmochim. Acta 60, 3773– 3797

Sverjensky, D.A., 1994. Zero-point-of-charge prediction from crystal chemistry and solvation theory. Geochimica et Cosmochimica Acta 58, 3123–3129.

Tack,F.M.G., Verloo, M.G., 1995. Chemical speciation and fractionation in soils and sediment heavy metal analysis: a review. International Journal of Environmental Analytical Chemistry. https://doi.org/10.1080/03067319508041330

Tessier, A., Campbell, P.G.C., Bisson, M., 1979. Sequential Extraction Procedure for the Speciation of Particulate Trace Metals. Analytical Chemistry 51(7), 844–51. https://doi.org/10.1021/ac50043a017

Thomas, G.W., 1982. Exchangeable cations. In A.L.Page, R.H. Miller, D.R. Keeney (eds), Methods of soil analysis Part 2, 159 - 165. https://doi.org/10.2134/agronmonogr9.2.2ed.c9

Tong, T., Elimelech, M., 2016. The Global Rise of Zero Liquid Discharge for Wastewater Management: Drivers, Technologies, and Future Directions.Environmental Science and Technology 50, 6846−6855. http//doi.org/10.1021/acs.est.6b01000

Tsing-Hai Wang., Ming-Hsu Li., Shi-Ping Teng., 2009. Bridging the gap between batch and column experiments: A case study of Cs adsorption on granite. Journal of Hazardous Materials 161 409–415. http//doi.org/10.1016/j.jhazmat.2008.03.112

Tuncuk, A., Stazi, V., Akcil, A., Yazici, E.Y., Deveci, H., 2012. Aqueous metal recovery techniques from e-scrap: Hydrometallurgy in recycling. Minerals Engineering 25, 28–37. https//doi.org/10.1016/j.mineng.2011.09.019

Turner, D.R. 1993. Mechanistic Approaches to Radionuclide Sorption Modeling. CNWRA 93-019.San Antonio, TX: Center for Nuclear Waste Regulatory Analyses. UN report, 2014. Safety guidelines and good practices for tailings management facilities. United Nations Economic Commission for Europe

Van Benschoten, J.E., Young, W.H., Matsumoto, M.R. and Reed, B.E. (1998), "A nonelectrostatic surface complexation model for lead sorption on soils and mineral surfaces", J. Environ. Qual. 27, 24-30.

Van der Sloot, H. A., Van Zomeren, A., 2012. Characterisation Leaching Tests and Associated Geochemical Speciation Modelling to Assess Long Term Release Behaviour from Extractive Wastes. Mine Water Environ, 31, 92-103.

VAN Wilderode, J., EL Desouky, H.A., Elburg, M.A., Vanhaecke, F., Muchez, P., 2014. Metal sources for the Katanga Copperbelt deposits (DRC): insights from Sr and Nd isotope ratios. Geologica Belgica (2014) 17/2: 137-147

Waegele, M.M., Gunathunge, C.M., Li, Jingyi., Li, Xiang., 2019. How cations affect the electric double layer and the rates and selectivity of electrocatalytic processes. J. Chem. Phys. 151, 160902 (2019); doi: 10.1063/1.5124878.

Wang, Shaobin., Peng, Yuelian., 2010. Natural zeolites as effective adsorbents in water and wastewater treatment. Chemical Engineering Journal 156, 11–24. https//doi.org/10.1016/j.cej.2009.10.029

Wang, Zimeng., Giammar, D. E., 2013. Mass Action Expressions for Bidentate Adsorption in Surface Complexation Modeling: Theory and Practice. Environ. Sci. Technol. 2013, 47, 3982−3996.

Weng, L., Temminghoff, E.J.M., Van Riemsdijk., W.H., 2001. Contribution of individual sorbents to the control of heavy metal activity in sandy soil. Environmental Science and Technology 35, 4436 - 4443. https://doi.org/10.1021/es010085j

Westall, J.C., Cernik, M. and Borkovec, M. (1998), "Modeling metal speciation in aquatic systems", Metals in Surface Waters, Ann Arbor Press, Ann Arbor, MI, pp. 191–216.

White, G.N., Dixon, J.B., 2002. Kaolin–Serpentine Minerals. Soil science society, SSSA book series. https://doi.org/10.2136/sssabookser7.c12

WHO, 2006. Cobalt and inorganic cobalt compounds. Concise International Chemical Assessment 69, 93, WHO Press, 1211 Geneva 27, Switzerland.

Whyte, R. M.,Schoeman,N.,Bowes, K.G., 2001. Processing of Konkola Copper Concentrates and Chingola Refractory Ore in a Fully Integrated Hydrometallurgical Pilot Plant Circuit. Journal of The South African Institute of Mining and Metallurgy 101(8), 427–36

Wilson, M. J. Weathering of the primary rock-forming minerals: processes, products and rates. Clay Minerals 39, 233–266. DOI: 10.1180/0009855043930133

Wilson, M.J., 2004. Weathering of the primary rock-formingminerals: processes, products and rates. Clay Minerals 39, 233–266

Windom, H.L., Byrd, T., Smith, R.G., Huan, F., 1991. Inadequacy of NASQUAN data for assessing metal trends in the nation's rivers. Environmental Science Technology 25, 1137-1142

Zhang Chang., Yu, Zhi-gang., Zeng, Guang-ming., Jiang, Min., Yang, Zhong-zhu., Cui, Fang., Zhu, Meng-ying., Shen,Liu-qing., Hu Liang., 2014. Effects of sediment geochemical properties on heavy metal bioavailability. Environment International 73, 270 - 281. https://doi.org/10.1016/j.envint.2014.08.010

Zhu, C., Anderson, G., 2002. Environmental Applications of Geochemical Modeling. Cambridge, United Kingdom: The Press Syndicate of the University of Cambridge.

Zinck, J. 2005. Review of Disposal, Reprocessing and Reuse Options for Acidic Drainage Treatment Sludge. CANMET Report 04-007 CR prepared for MEND (Report 3.42.3)